PREDICTION OF STRENGTH LIMITS OF THIN WALL, BEAM PANELS USING THE FINITE ELEMENT METHOD

Nihat M. Taner

A Thesis

in

The Department

of

Civil Engineering

Presented in partial fulfillment of the requirement
for the degree of Doctor of Engineering at
Concordia University
Montreal, Quebec, Canada

April 1976

ABSTRACT

PREDICTION OF STRENGTH LIMITS OF THIN WALL, BEAM PANELS USING THE FINITE ELEMENT METHOD

by

Nihat M. Taner

ABSTRACT

A finite element model is developed for the analysis of planar reinforced concrete members - beam panels in particular - under short-time, static, in-plane loads. The model describes the behaviour of structural members at any load stage, from the initial elastic state up to failure. Nonlinearities due to cracking, plasticity and crushing of concrete, and yielding of the reinforcement are taken into account.

A series of tests on full-scale beam panels were conducted. The accuracy of the finite element model is verified by results of these tests and comparable test results of other investigators. This verification shows that the finite element model can predict the behaviour of reinforced concrete members quite accurately.

Relevant simplified formulae used to define strength of deep beams are briefly reviewed and their applicability to beam panels is checked using experimental results.

ACKNOWLEDGEMENTS

ACKNOWLEDGEMENTS

The author expresses his sincere appreciation to Professors Z.A. Zielinski and P.P.Fazio for their guidance, advice and critical supervision in the course of the investigation and in the preparation of this thesis. He is also indebted to Dr. S. Mirza for his helpful comments and valuable suggestions in the early stages of the theoretical study.

The research reported herein was supported by the National Research Council (NRC). The experimental work was carried out using the facilities of the Building Research Centre, Concordia University. The author thanks his fellow graduate students, the Structures Laboratory personnel and the Academic Support Group, Concordia University Computer Centre, for their generous help during the various stages of the research program, and to Miss M. Stredder for her concerned work in typing the thesis.

A very special thanks goes to Bahar, for her encouragement, understanding and assistance in preparing the draft copy and proofreading.

TABLE OF CONTENTS

TABLE OF CONTENTS

LIST OF TABLES

LIST OF TABLES

LIST OF FIGURES

LIST OF FIGURES

NOTATIONS

NOTATIONS

The following symbols have been adopted for use in the text.

a	Shear span (measured from center of support to center of load area)
A_s, A_s'	Area of tension and compression reinforcement, respectively
$[B]$	Displacement transformation matrix
b	Width of structural element
$[D], [D]_{ur}$	Stress-strain matrix in general and local coordinates, respectively
$[D]_{ep}$	Elasto-plastic matrix
d	Effective depth of structural element
E	Modulus of elasticity
E_c, E_s	Modulus of elasticity for concrete and steel, respectively
f_c'	Compressive strength of concrete
f_{ct}	Compressive stress in concrete subject to biaxial tension-compression
f_t	Tensile strength of concrete
f_{tc}	Tensile stress in concrete subject to biaxial tension-compression
f_{ti}	Indirect tensile (splitting) strength of concrete (determined from cylindrical samples)
f_y	Yield strength of the reinforcement
G	Shear modulus
H	Tensile force developed in the main longitudinal reinforcement and carried over the support
h	Total depth of structural element
$[J]$	Jacobian matrix
$[k]$	Element stiffness matrix

$[K]$	Structural (system) stiffness matrix
ℓ	Total length of structural element
$[N]$	Matrix of shape functions
P	Concentrated load in general
$\{P\}$	Vector of nodal forces
p	Reinforcement ratio
$\{P\}_{eq}$	Vector of equivalent nodal forces
P_{ult}	Ultimate load
$[T]_{\varepsilon}$	Strain transformation matrix
$[T]_{\sigma}$	Stress transformation matrix
t	Thickness of finite element
ν	Poisson's ratio
V	Shear force
V_s	Shear force at diagonal splitting
V_{ult}	Ultimate shear at failure
β	Shear retention factor
$\{\delta\}$	Vector of nodal displacements
$\{\varepsilon\}, \{\varepsilon\}_u$	Strain vector in general and local coordinates, respectively
ε_{eq}	Equivalent strain (von Mises' criterion)
ε_{ℓ}	Limit compressive strain in concrete
$\{\sigma\}, \{\sigma\}_u$	Stress vector in general and local coordinates, respectively
$\{\sigma\}_{ex}$	Excess stress vector

The following notations for coordinates are used throughout the text.

u,v	Local rectangular coordinates for cracked concrete or reinforcement, u - axis is oriented among the crack or reinforcement direction
x,y	General (Cartesian) coordinates
ξ,η	Local curvilinear coordinates for stiffness matrix formulation

CHAPTER 1

INTRODUCTION

CHAPTER I

INTRODUCTION

1.1 GENERAL

Deep beams and shear walls are examples of planar reinforced concrete elements designed to carry in-plane loads. The methods generally used for the analysis and design of these elements can be classified and summarized as follows :

(i) The planar element is assumed to behave as an ordinary beam. The stresses and required reinforcement are computed using either the working stress or ultimate strength method. Although the analysis is greatly simplified with the above assumption, the validity of the results obtained are questionable since the formulae used are developed for ordinary beams assuming a linear strain variation, and they cannot be extended to "deep" sections.

(ii) The planar element is considered to be in the plane stress state. An elastic analysis is performed and a solution is obtained either in closed form or using numerical methods. The amount of steel to be provided is determined based on the computed tensile stresses (39). The main deficiency of such an approach is the fact that the redistribution of stresses and internal forces following cracking is ignored.

(iii) Based on experimental investigations, an equation relating the applied loads or limiting stresses to some selected parameters is developed. The equation is derived either by assuming a certain collapse mode or by conducting a parametric study. Unfortunately, the applicability of such equations is usually limited to elements comparable to those studied experimentally and cannot be generalized.

A point common to the methods described above is that the influence of crack formation and propagation, plasticity and crushing of concrete and yielding of the reinforcement are either neglected or grossly approximated. A method that can incorporate nonlinear material properties and describe the load-deformation relationship at any work stage, from the initial elastic state up to failure is desirable in order to obtain more accurate results and reduce the need for extensive experimental verifications which at times can be very costly and time consuming. The finite element method has been found to be most suitable for this purpose.

1.2 PREVIOUS RESEARCH

In 1967, Ngo and Scordelis (32) published first the application of the finite element method to reinforced concrete

beams. Simply supported concrete beams containing tensile flexural reinforcement, with predefined crack patterns were analyzed on the basis of linear elastic theory. The concrete and the steel were represented by constant strain triangular finite elements and bond was simulated by linkage elements which consisted of two orthogonal linear springs.

Nilson (33) recognized nonlinear material behaviour and used a nonlinear bond-slip relationship in his study of concentrically and eccentrically reinforced tension members loaded through the reinforcing bars. The uncracked structure was loaded incrementally. When the average value of the principal tensile stress in two adjacent elements exceeded the tensile strength (taken equal to the modulus of rupture) a crack was assumed to form between those two elements along their common edge. After cracking the structure was unloaded, the elements on each side of the crack were disconnected at the nodes along the crack, and the structure was reloaded incrementally. As concluded by the author, this may not be a realistic representation of the actual loading. Also, the dictation of the crack direction by element boundaries may lead to erroneous results if the direction of the principal tension stresses are not perpendicular to the element boundaries. For cracks not starting at the boundary, the disconnection of nodes common to the elements on each side of the crack results in the overestimation of the initial crack length.

Valliappan et al (41,42) used the "initial stress" approach (49,50,51) to study cracking and plasticity problems. According to this approach, if the principal stress in an element exceeds the prescribed tensile strength of concrete, the element is assumed to have cracked in a direction normal to the principal tension. The excess stresses are converted to equivalent nodal forces which are applied to the structure as to distribute the excess stresses to adjacent elements (the approach was initially referred to as the "stress transfer" method.) The process is repeated until equilibrium is reached, i.e., the transfer forces become negligible. The initial stiffness matrix is used throughout the analysis. The stresses are adjusted by an iterative process to reproduce the actual stresses which would have been obtained by using a variable stiffness matrix. With the initial stress approach, unloading and reloading of the structure, redefinition of the topology are eliminated; crack directions can be accurately determined and the response of the structure from the initial loading to failure can be traced in a single computer analysis.

Franklin (15) studied analytical reinforced concrete frames under lateral loads. The frames were single bay, one or two storey, with or without infill panels. Special flexural elements were used to represent the reinforced concrete frames. The elements were rectangular with four corner nodes each having two degrees of freedom. The con-

crete was considered to be composed of ten slices and a maximum of four discrete reinforcement areas at arbitrary distances along the depth could be accommodated. The unreinforced panels were represented by quadrilaterals derived from two linear edge strain triangular elements. The initial twelve degrees of freedom of each triangle were first reduced to eight by imposing a linear displacement variation along two edges. The triangles were connected to form a quadrilateral with an internal node which was then eliminated by static condensation. Tie-links (similar to bond links of previous investigators) were used to connect the shear panels to frame members. Reinforcing bars were represented by line elements. Nonlinear stress-strain relationships were approximated by linear increments.

Cervenka (6) analyzed reinforced concrete shear panels under monotonically increasing and cyclic loads. Constant strain triangular elements with composite concrete-steel properties were used. The analysis was found to be less accurate in the case of cyclic loading. Yuzugullu (45) studied the inelastic behaviour of a shear wall-frame system subject to monotonically increasing loads. The composite material properties developed by Cervenka were used. A constant shear retention factor was used for cracked concrete to simulate aggregate interlock and dowel action. Flexural elements similar to Franklin's, but with a single slice, were used to represent the frame members. Quadrilateral ele-

ments composed of four constant strain triangles were used to represent frame or wall sections. The quadrilateral element was selected because it was found to be less stiff than the equivalent rectangular plane stress element. Wall and frame sections were connected by tie-links. The flexural element was found to be inadequate and a layering concept was suggested.

Mirza et al (29,30) used triangular and rectangular elements to represent both steel and concrete. Bond and dowel action at the steel-concrete interface, and shear resistance of cracked concrete were simulated by linkage elements. The stress transfer method was used and the stiffness matrix of the structure was modified by setting the stiffness of the cracked elements equal to zero.

A detailed review of the various aspects of the finite element method of analysis of reinforced concrete structures was made by Scordelis (38). The considerable lack of agreement among investigators, on the significance of the various parameters influencing the behaviour of reinforced concrete members was indicated and the need for a more accurate analytical method of study was recognized.

Recent studies indicate the superiority of higher order finite elements. For example, twenty-node isoparametric bricks were used by Suidan (40) in the study of flexural members. Nam (31) analyzed reinforced concrete beams using isoparametric quadrilaterals to represent the concrete and

line elements to represent the reinforcement. The inadequacy of the quadrilateral element in flexure was improved by adding incompatible modes, as suggested by Wilson (43). The various types of elements used in different studies are illustrated in Figure 1.1.

Most of the finite element models incorporated a uniaxial stress-strain relationship for concrete (35). However, even in ordinary beams critical biaxial stress conditions may exist. The most comprehensive experimental study on the biaxial strength of concrete is that reported by Kupfer et al (25). Several mathematical models have been proposed for the constitutive relationship of concrete, but further research is still necessary.

1.3 SCOPE OF THE STUDY

Precast, modular, thin-walled panels are used in the construction of various buildings to minimize construction time, labor and material consumption. These panels are used as floor or wall elements, and generally work as slabs or columns. In many cases, however, the loading and support conditions may be such that the panel has to work as a deep beam. The phrase "beam panel" is used to represent panels which are subject to high shear and flexural stresses.

The main objective of this study is to develop a finite element model that will describe the behaviour of planar, reinforced concrete members - beam panels in parti-

cular - subject to monotonically increasing, static, in-plane loading, from the initial elastic state up to failure. Non-linearities due to cracking, plasticity and crushing of concrete, and yielding of the reinforcement are taken into account. The influence of biaxial stress states on the behaviour of concrete is recognized and a biaxial failure envelope is incorporated in the model.

The quadratic edge displacement isoparametric rectangle is selected for the finite element study. This particular element produces exact results in flexure, and does not have the shape and loading limitations of the linear edge displacement isoparametric rectangle with incompatible modes. The element is curvilinear in general coordinates, thus permits a better description of curved structural boundaries.

A series of tests on full-scale beam panels was conducted as part of the research program in order to:

(i) Investigate the capabilities and limitations of the finite element model, and

(ii) Study the effect of varying amounts of tensile flexural reinforcement and of different shear span ratios on the overall response of the panels.

Relevant simplified formulae used to define strength of deep beams are briefly reviewed and their applicability to beam panels is verified.

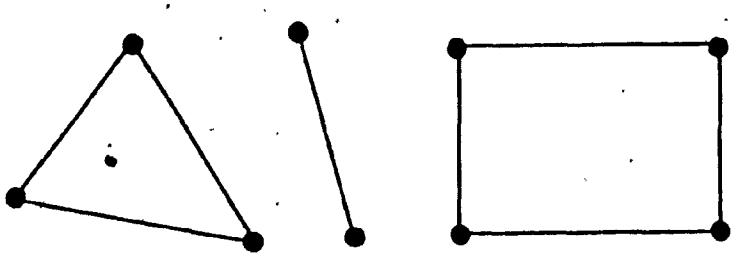

* (41) † (31,37,41) + (9)

+ (6,9) x (29) Linkage Element

x (29,30,32,33,37) (15,29,30,32,33,37,45)

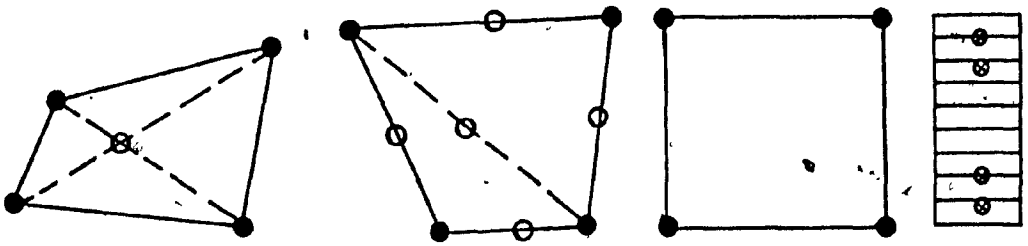

+ (45) * (15) Frame Element

(15,45)

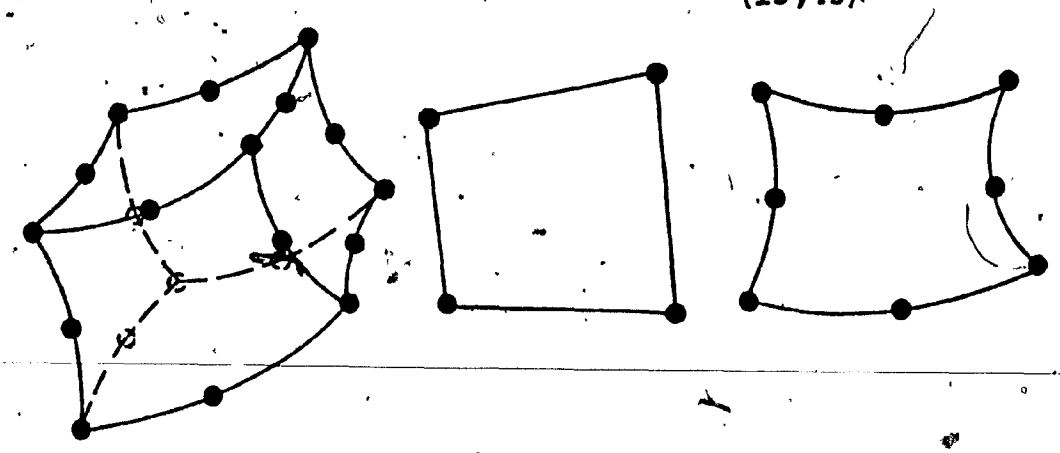

+ (40) * (31) + (Present Study)

● Node

○ Condensed Node

⊗ Reinforcement

Applications

* Concrete
† Reinforcement
+ Composite material
x Concrete and Reinforcement

FIG. 1.1 TYPES OF ELEMENTS USED IN DIFFERENT INVESTIGATIONS
(Numbers in parentheses indicate references)

CHAPTER 2

IDEALIZATION OF MATERIAL PROPERTIES

CHAPTER 2

IDEALIZATION OF MATERIAL PROPERTIES

2.1 INTRODUCTION

Behaviour of flexural reinforced concrete elements under increasing loads is characterized by cracking of the concrete, yielding of the steel, and plasticity and crushing of the concrete. Other variations are possible, as in compression members where macrocracking may not be visible until failure, or as in under-reinforced beams in which initiation of cracks immediately leads to the yielding of the reinforcement.

Cracking and plasticity are factors that result in nonlinear behaviour. Other phenomena such as creep and shrinkage of concrete, and bond-slip between the reinforcement and the surrounding concrete also lead to the nonlinear response of reinforced concrete members. This study is restricted to short-time loading, therefore time-dependent phenomena are not considered. The weakening of bond, and slip due to increasing loads can be simulated by linkage elements (15,29,30,32,33,37) as the one shown in Fig. 1.1. However, this type of modelling leads to a finite element mesh predefined by the location of the reinforcing bars which becomes uneconomical for sections reinforced with wire mesh, or with numerous, closely spaced bars.

It is well known that the bond strength along the reinforcement is increased if deformed bars are used. This is due to the mechanical bond produced by the lugs. For sections where the reinforcement is provided as welded wire mesh, bond-slip becomes a secondary phenomenon due to the high surface area-to-volume ratio of the wires, and more importantly, due to the effective anchorage provided by the welded junctions of the cross wires. In deep members, a relatively large portion of the reinforcing bars is affected by the compression at or near the supports, which also leads to a higher bond resistance.

Based on the above points, it is assumed that sufficient bond exists for the component materials, i.e., concrete and steel, to deform equally at all stages of loading. The reinforced concrete is treated as a composite material and its stiffness is derived by the superposition of the component material stiffnesses as illustrated in Fig. 2.1.

2.2 CONCRETE

The assumed stress-strain relationship for concrete is linear elastic in tension and extends from linear elastic to perfect plastic in compression, as illustrated in Fig.2.2. In tension, the actual stress-strain curve is linear up to about 90% of the ultimate load, thus the assumption of linearity does not lead to any serious loss of accuracy. In compression, the actual stress-strain curve is linear up to about 30% of the ultimate load, and then deviates gradually

from a straight line. Near the ultimate load the stress-strain curve begins to bend more sharply to the horizontal and then, having reached a peak, it ends in a descending tail (which may or may not be observed.) The variation in the concrete modulus of elasticity necessitates the use of an anisotropic elasticity matrix when biaxial stresses are being considered:

$$[D] = \frac{1}{1-\nu_1\nu_2}\begin{bmatrix} E_1 & \nu_2 E_1 & 0 \\ \nu_1 E_2 & E_2 & 0 \\ 0 & 0 & G_{12}(1-\nu_1\nu_2) \end{bmatrix}$$

where E_1, E_2 represent the concrete modulus of elasticity in orthogonal directions. Symmetry of the matrix requires that

$$\nu_1 E_2 = \nu_2 E_1$$

indicating that ν_1 and ν_2 have to differ proportionately to E_1 and E_2, i.e., if ν_1 is kept constant, ν_2 has to vary according to the ratio E_2/E_1, which means that at higher loads Poisson's ratio decreases. Physical evidence, however, indicates that the opposite is true and due to the rapid increase in transverse strain near collapse, apparent Poisson's ratio increases. Consequently, it would be appropriate to assume $\nu_1 = \nu_2$ and constant at all stages of loading. This in turn, requires that $E_1 = E_2$, and thus an isotropic stress state is defined. This poses the analyst with another problem; which value to select as the concrete modulus of elasticity if the biaxial stresses are not of similar magnitudes? Franklin (15)

discussed the case where both stresses are compressive. If σ_1 is much larger compared to σ_2 and close to the ultimate compressive strength of concrete, E_1 will be smaller than E_2 indicating the increasing damage in the material. But this damage means that the higher stiffness E_2 cannot exist and in fact may be a value much closer to E_1. Therefore, instead of a mean value, the smaller of E_1,E_2 was used. However, if cracking is a predominant factor, it is more appropriate to investigate the case of biaxial compression-tension. In this case, the stiffness E_1 along the tensile stress component σ_1 will be equal to or greater than E_2, and if E_2 is used in the elasticity matrix this will lead to an overestimation of the crack load. Thus the initial tangent stiffness was used both in compression and tension.

A computational advantage of using a constant value for the modulus of elasticity of concrete is observed here. If a nonlinear stress-strain relationship was used, the stiffness matrices would have to be regenerated at each load stage, even if no cracking or plasticity occurred.

An important point to keep in mind is that the distribution of forces, among other factors depends mainly on the geometry of the structure, thus a constant value for the modulus of elasticity is not a gross approximation. For example, in a determinate truss the bar stresses may be determined from joint forces by static equilibrium and moduli of elasticity of the materials need not be considered. Similarly,

Sample computer runs for the first crack load using E_c versus $0.5E_c$ as the modulus of elasticity of concrete gave results differing by less than 8% (20.5 kips versus 19 kips for a 4 ft x 9 ft, simply supported panel reinforced with a wire mesh, under midspan load.)

Behaviour of concrete under uniaxial and biaxial stresses differs significantly. Concrete subject to biaxial compression exhibits higher strength than the uniaxial compression strength. Under combined compression and tension stresses, concrete reaches the cracking limit before the tension stress component reaches the uniaxial tensile strength, thus it is in a more critical state than that expressed by uniaxial relations. Ignoring the biaxial stress state, especially for sections subject to combined flexural and high shear stresses, may lead to erroneous results. Some of the formulae used to express the biaxial failure envelope of concrete are given below and illustrated in Fig. 2.3.

(i) Biaxial Compression

Kupfer et al (25):

$$(\sigma_1 + \sigma_2)^2 + (\sigma_1 + 3.65\sigma_2)f'_c = 0 \qquad (2.1)$$

Liu et al (27)

$$\left.\begin{aligned} \sigma_1 - \frac{1}{1.2}\sigma_2 &= -f'_c \quad \text{for } \frac{\sigma_2}{\sigma_1} < 0.2 \\ \sigma_1 &= -1.2\, f'_c \text{ for } 0.2 \leq \frac{\sigma_2}{\sigma_1} \leq 1.0 \end{aligned}\right\} \quad (2.2)$$

von Mises

$$\sigma_1^2 + \sigma_2^2 - \sigma_1\sigma_2 = (f'_c)^2 \quad (2.3)$$

Suwalski and Zalewski (46):

$$\sigma_1 - 0.2\sigma_2 = -f'_c \quad (2.4)$$

(ii) Tension-Compression

Kupfer et al:

$$\sigma_2 - \frac{0.8\, f_t}{f'_c}\sigma_1 = f_t \quad (2.5)$$

Suwalski and Zalewski:

$$\sigma_2 - \frac{f_t}{f'_c}\sigma_1 = f_t \quad (2.6)$$

(iii) Biaxial Tension

Kupfer et al:

$$\sigma_2 = f_t \quad (2.7)$$

Suwalski and Zalewski:

$$\sigma_1 + \sigma_2 = f_t \qquad (2.8)$$

In the above formulae

f_c' = uniaxial compressive strength

f_t = uniaxial tensile strength

σ_1, σ_2 = principal stresses

Although the validity of von Mises' criterion in case of concrete may be questionable, it is included for comparison purposes since it has been used in several finite element analyses (6,40,41,45,51).

In this study the maximum normal stress theory is adopted for biaxial tension (as verified by Kupfer et al.) von Mises' yield criterion is used for biaxial compression and a linear variation is assumed in the tension-compression zone.

2.2.1 Uncracked Concrete

Uncracked concrete is assumed to be isotropic and homogeneous. The stresses are related to the strains according to Hooke's law as

$$\begin{Bmatrix} \sigma_x \\ \sigma_y \\ \tau_{xy} \end{Bmatrix} = [D] \begin{Bmatrix} \varepsilon_x \\ \varepsilon_y \\ \gamma_{xy} \end{Bmatrix} \text{ where } [D] = \frac{E_c}{1-\nu^2} \begin{bmatrix} 1 & \nu & 0 \\ \nu & 1 & 0 \\ 0 & 0 & \frac{1-\nu}{2} \end{bmatrix} \quad (2.9)$$

2.2.2 Cracked Concrete

Cracked concrete is assumed to be capable of carrying stresses along the crack direction which is taken to be orthogonal to the principal tension direction in the concrete just prior to crack formation. In local coordinates, the stress-strain relation for cracked concrete is

$$\{\sigma\}_u = [D]_u \{\varepsilon\}_u$$

where

$$[D]_u = \begin{bmatrix} E_c & 0 & 0 \\ 0 & 0 & 0 \\ 0 & 0 & \frac{\beta E_c}{2(1+\nu)} \end{bmatrix} \quad (2.10)$$

β is referred to as the shear retention factor and represents the shear capacity of cracked concrete, relative to uncracked concrete. $\beta = 0$ implies that cracked concrete consists of uniaxial fibers capable of carrying normal stresses along the crack direction only. Such a link is unstable with respect to any other stress state. Geometrically, the

lattice must be formed by three links in different directions in order to be stable in the general stress state. Thus, cracked concrete is stable only if it contains bi-directional reinforcement and if cracks are not parallel to either reinforcement direction.

Shear resistance of cracked concrete (due to aggregate interlock and any dowel action that may be present) is a function of the crack width, thus β should have an upper and lower bound of one and zero, respectively. It is, however, reported that, - excluding the mathematically unacceptable value of zero - the value of β used has very little influence on the numerical solution (16,45). This indicates that, rather than as a shear retention factor, β must be looked upon as a factor which causes the mathematical model to remain stable. Stresses and strains in local and general coordinates can be related using the appropriate transformation matrices. That is

$$\{\sigma\}_u = [T]_\sigma \{\sigma\}_x \quad \text{and} \quad \{\varepsilon\}_u = [T]_\varepsilon \{\varepsilon\}_x$$

where the stress transformation matrix is

$$[T]_\sigma = \begin{bmatrix} c^2 & s^2 & 2cs \\ s^2 & c^2 & -2cs \\ -cs & cs & c^2-s^2 \end{bmatrix} \qquad (2.11)$$

and the strain transformation matrix is

$$[T]_\varepsilon = \begin{bmatrix} c^2 & s^2 & cs \\ s^2 & c^2 & -cs \\ -2cs & 2cs & c^2-s^2 \end{bmatrix} \qquad (2.12)$$

where $c = \cos\theta$, $s = \sin\theta$ and θ is the angle between the x axis and the crack direction, measured counterclockwise.

Using the above relations

$$\{\sigma\}_x = [T]_\sigma^{-1} [D]_u [T]_\varepsilon \{\varepsilon\}_x$$

The stress-strain matrix in general coordinates is then

$$[D] = [T]_\sigma^{-1} [D]_u [T]_\varepsilon$$

Since $[T]_\sigma^{-1} = [T]_\varepsilon^T$, we can write

$$[D] = [T]_\varepsilon^T [D]_u [T]_\varepsilon \qquad (2.13)$$

2.2.3. Plasticity of Concrete

Plasticity of concrete is to be considered separately for cracked and uncracked concrete. Cracked concrete is in a uniaxial state of stress. Since perfect plasticity is assumed, the modulus of elasticity of concrete $E_c = 0$, thus $[D] = [0]$.

Uncracked concrete is assumed to yield when the stresses satisfy von Mises' criterion:

$$F(\sigma) = (\sigma_x^2 - \sigma_x\sigma_y + \sigma_y^2 + 3\tau_{xy}^2)^{\frac{1}{2}} - \sigma_0 = 0 \qquad (2.14)$$

where σ_0 represents the uniaxial strength of the material (f'_c in the case of concrete.) Incremental strains and stresses are related as

$$\{\Delta\sigma\} = [D]_{ep}\{\Delta\varepsilon\} \qquad (2.15)$$

In the above equation

$[D]_{ep}$ = elastoplastic matrix = $[D]([I] - [\Omega])$

where

$[D]$ = elasticity matrix for uncracked concrete

$[I]$ = identity matrix

$$\{\Omega\} = \frac{\{q\}\{q\}^T[D]}{\{q\}^T[D]\{q\}}$$

$$\{q\} = \frac{\partial F(\sigma)}{\partial\{\sigma\}}$$

$[D]_{ep}$ represents the instantaneous stiffness of concrete in the plastic range as a function of the existing stresses.

2.2.4 Crushed Concrete and Concrete With Two Cracks

Cracked concrete in compression is assumed to have crushed when it reaches the limiting compression strain, ε_ℓ. For uncracked concrete under biaxial compression, crushing is assumed to occur when the equivalent strain ε_{eq} reaches

ε_ℓ where

$$\varepsilon_{eq} = (\varepsilon_x^2 - \varepsilon_x\varepsilon_y + \varepsilon_y^2 + \frac{3}{2}\gamma_{xy}^2)^{\frac{1}{2}} \qquad (2.16)$$

Cracked concrete in tension is assumed to crack again, along a direction perpendicular to the first crack when the tensile stress reaches the uniaxial tensile strength. Both crushed concrete and concrete with two cracks are assumed to be incapable of carrying any load, thus [D] = [0].

2.3 REINFORCEMENT

Reinforcement properties can be described similarly to that of cracked concrete. Prior to yielding, the stress-strain matrix in local co-ordinates is

$$[D]_u = \begin{bmatrix} P_u E_s & 0 & 0 \\ 0 & 0 & 0 \\ 0 & 0 & 0 \end{bmatrix} \qquad (2.17)$$

where P_u = ratio of reinforcement volume to element volume

Transformation from local to general coordinates is identical to that of cracked concrete.

Following yielding

$$E_s = 0$$

thus

$$[D] = [0]$$

The stress-strain relationship for the reinforcing steel is illustrated in Fig. 2.4.

2.4 COMPOSITE MATERIAL

The stress-strain matrix for the concrete-reinforcement composite is formed by the superposition of the stress-strain matrices of the component materials.

$$[D]_{composite} = [D]_{concrete} + \Sigma[D]_{reinforcement} \quad (2.18)$$

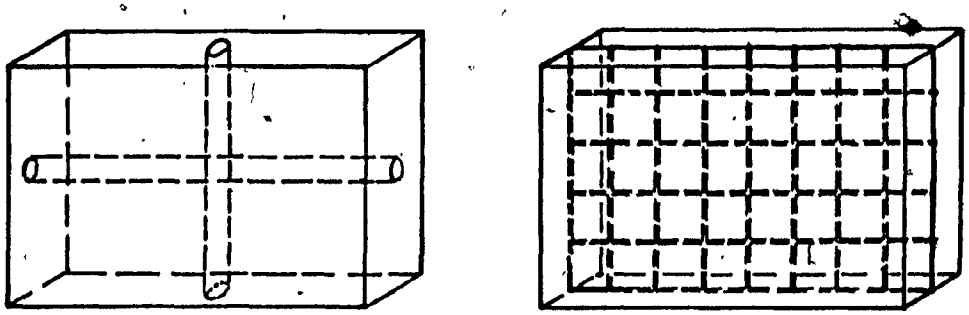

(a) Uncracked - real

(b) Uncracked - assumed

FIG. 2.1 IDEALIZATION OF THE CONCRETE-REINFORCEMENT COMPOSITE

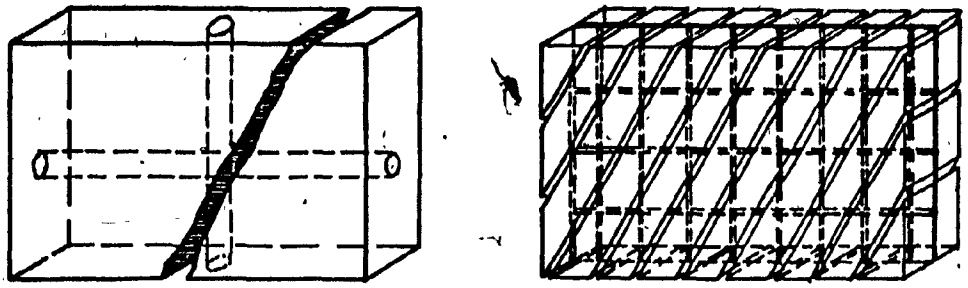

(c) Cracked - real

(d) Cracked - assumed

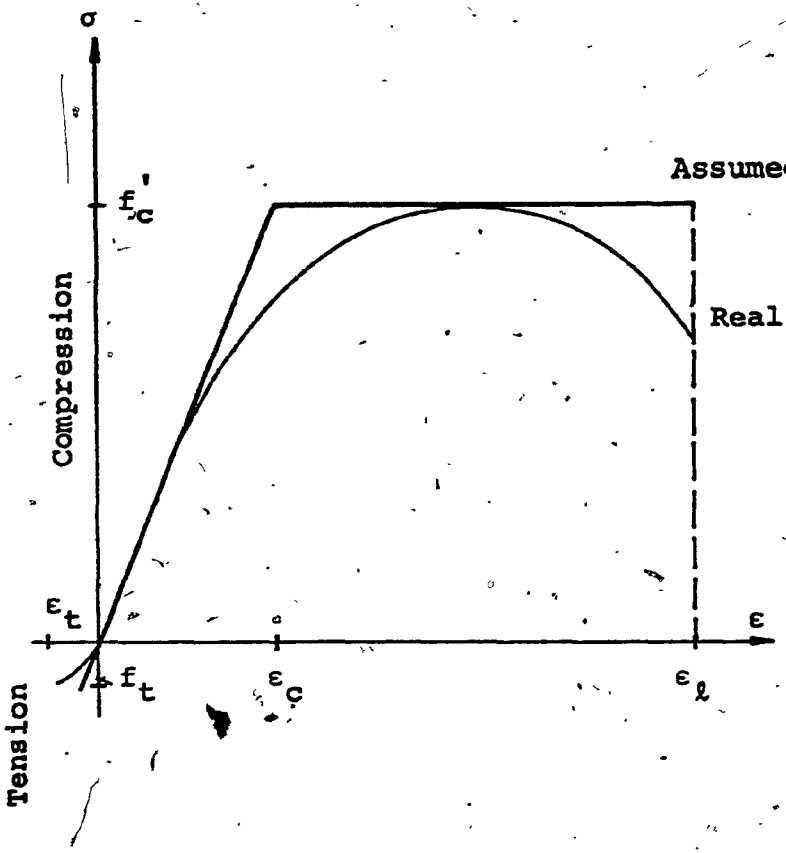

FIG. 2.2 UNIAXIAL STRESS-STRAIN RELATIONSHIP FOR CONCRETE

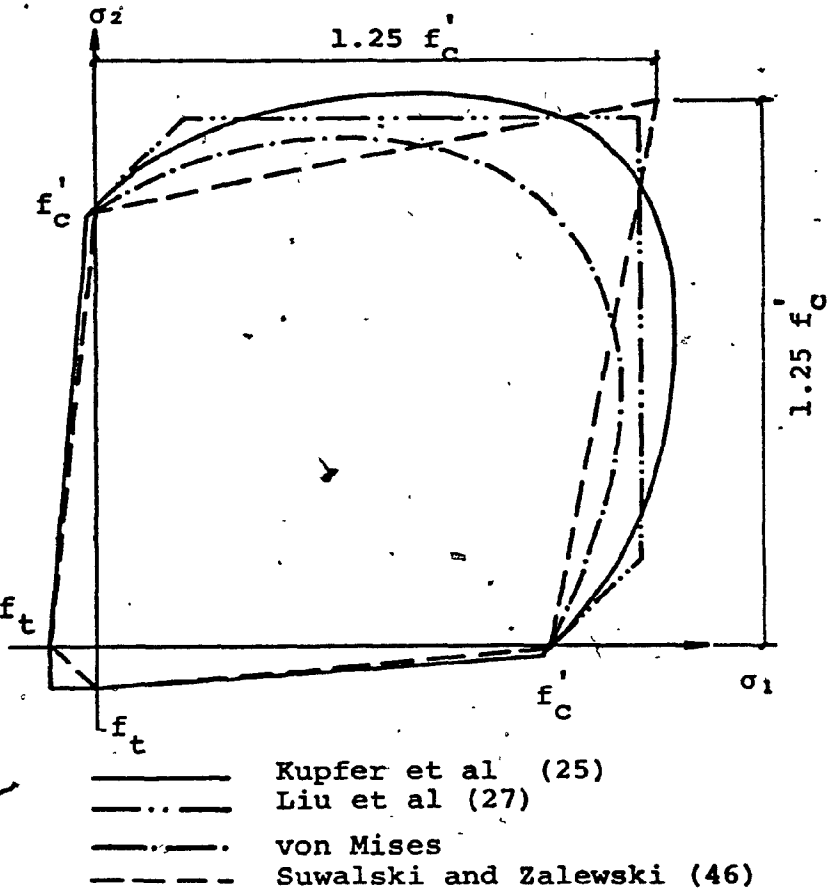

FIG. 2.3 BIAXIAL FAILURE ENVELOPE OF CONCRETE

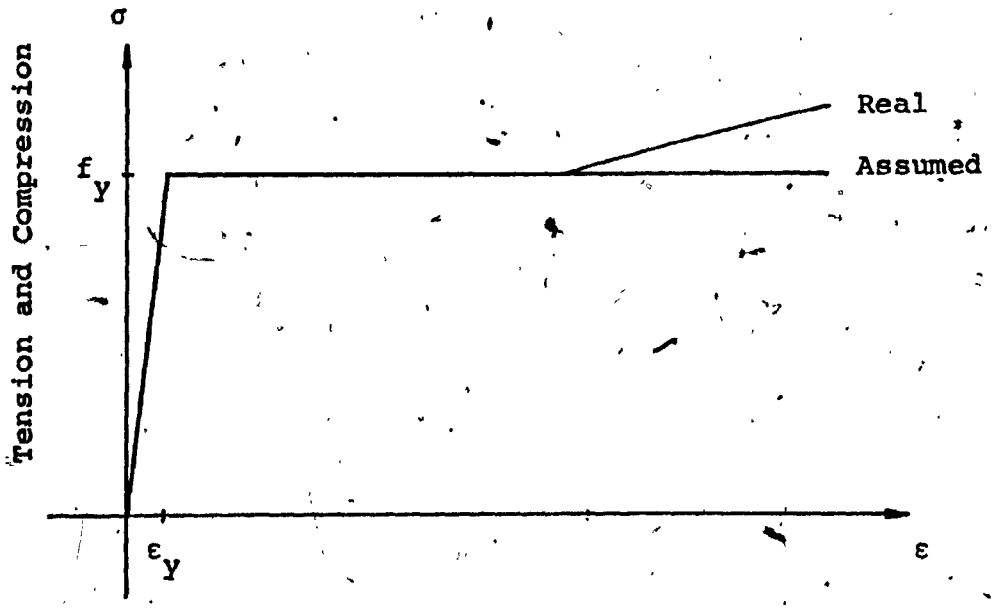

FIG. 2.4 STRESS-STRAIN RELATIONSHIP FOR THE REINFORCEMENT

CHAPTER 3

FINITE ELEMENT ANALYSIS

CHAPTER 3

FINITE ELEMENT ANALYSIS

3.1 GENERAL DESCRIPTION

The finite element method requires some structural idealizations, the most important one being the replacement of the continuum with a discrete system so that a finite number of degrees of freedom are defined.

The system is composed of elements interconnected at nodal points. The nodal displacements are treated as the unknowns and the finite element formulation leads to a system of equations relating the displacements and the applied loads. The method is described in detail in the literature (12,49), therefore only the basic relationships relevant to our particular case will be reviewed here.

The displacements at any point within an element $\{\delta(x,y)\}$ are related to the nodal displacements $\{\delta\}$ as follows:

$$\{\delta(x,y)\} = [N]\{\delta\} \qquad (3.1)$$

where $[N]$ represents the matrix of the "shape functions". For the plane stress problem the relevant strains are those occurring in the plane. The strain vector as a function of displacements is defined as

$$\{\varepsilon\} = \begin{Bmatrix} \varepsilon_x \\ \varepsilon_y \\ \gamma_{xy} \end{Bmatrix} = \begin{Bmatrix} \frac{\partial u}{\partial x} \\ \frac{\partial v}{\partial y} \\ \frac{\partial u}{\partial y} + \frac{\partial v}{\partial x} \end{Bmatrix} \qquad (3.2)$$

where u and v represent the displacements in the x and y directions, respectively, of a typical point in Cartesian coordinates. Thus, strains can be related to the nodal displacements

$$\{\varepsilon\} = [B]\{\delta\} \qquad (3.3)$$

from which stresses can be determined by means of a stress-strain matrix [D]

$$\{\sigma\} = [D]\{\varepsilon\} \qquad (3.4)$$

The element stiffness matrix is derived using energy theorems and the above relations and is given as

$$[k] = \int_V [B]^T[D][B]dV \qquad (3.5)$$

The element stiffness matrices are superposed to form [K], the stiffness matrix of the system and the load-displacement relation for the structure is given by

$$[K]\{\delta\} = \{P\} \qquad (3.6)$$

where {P} and {δ} represent the nodal forces and displacements respectively. It should be noted that before a solu-

tion of the system of equations above is attempted, prescribed displacements should be introduced to avoid rigid body motion. Once the nodal displacements have been determined, stresses in the elements can be found using the relations described above.

3.2 ELEMENT SELECTION

A significant improvement in accuracy has been achieved by using higher order finite elements (such as those with more degrees of freedom) instead of the basic triangular and rectangular elements (49). A smaller number of higher order elements is required to get a definition as good as or better than that which would be achieved by lower order ones. Although more computer time will be required due to the larger bandwidth that may be encountered and the additional complexity of the formulation, considerable economy can still occur. Since fewer elements are needed when using complex elements, data preparation may also be reduced to some extent.

Isoparametric elements (the same shape functions are used to define the geometry and the displacements) have been used successfully in finite element analysis. The linear edge displacement rectangle with four corner nodes, although more economical than the higher order isoparametric elements, cannot represent flexure realistically. Modifications such as evaluating some of the stiffness terms at locations different from the sampling points, introducing internal degrees of freedom, or adding incompatible modes (10,43) improved

the accuracy considerably. However, some of these modified elements fail the patch test unless the element is rectangular. Some are not invariant, and different orientation of the element yields different results. Activation of incompatible modes due to an axial state of stress may also lead to erroneous results for non-rectangular elements (10,11).

In the present work, the quadratic edge displacement rectangle is used. The element is curvilinear with 4 corner and 4 midside nodes and yields exact results in flexure. The element is illustrated in Fig. 3.1.

3.3 STIFFNESS MATRIX FORMULATION

The element which is distorted in global coordinates has to be transformed to curvilinear local coordinates for the evaluation of the stiffness terms. A very convenient method of establishing the coordinate transformations is by using the shape functions relating nodal displacements to displacements within the element itself (49). Thus

$$x = \sum_{i=1}^{8} N_i x_i \quad \text{and} \quad y = \sum_{i=1}^{8} N_i y_i \qquad (3.7)$$

The shape functions for the quadratic edge displacement element are given as

$$N_i = \tfrac{1}{4}(1 + \xi_0)(1 + \eta_0)(\xi_0 + \eta_0 - 1) \qquad (3.8a)$$

for corner nodes

$$N_i = \tfrac{1}{2}(1 - \xi^2)(1 + \eta_0) \text{ where } \xi_i = 0 \qquad (3.8b)$$

$$N_i = \tfrac{1}{2}(1 + \xi_0)(1 - \eta^2) \text{ where } \eta_i = 0 \qquad (3.8c)$$

for midside nodes

In the above equations

$$\xi_0 = \xi\ \xi_i \quad \text{and} \quad \eta_0 = \eta\ \eta_i$$

The portion of the stiffness matrix for any i,j combination is given as

$$[k_{ij}] = \int_V [B_i]^T[D][B_j]\, dV = t \int_A [B_i]^T[D][B_j]\, dxdy \qquad (3.9)$$

[D] is determined for different modes of material behavior and $[B_i]$ is expressed in terms of the shape functions as

$$[B_i] = \begin{bmatrix} \frac{\partial N_i}{\partial x} & 0 \\ 0 & \frac{\partial N_i}{\partial y} \\ \frac{\partial N_i}{\partial y} & \frac{\partial N_i}{\partial x} \end{bmatrix} \qquad (3.10)$$

In matrix notation, using the chain rule, the partial derivatives of N_i with respect to ξ and η are given as

$$\begin{bmatrix} \frac{\partial N_i}{\partial \xi} \\ \frac{\partial N_i}{\partial \eta} \end{bmatrix} = \begin{bmatrix} \frac{\partial x}{\partial \xi} & \frac{\partial y}{\partial \xi} \\ \frac{\partial x}{\partial \eta} & \frac{\partial y}{\partial \eta} \end{bmatrix} \begin{bmatrix} \frac{\partial N_i}{\partial x} \\ \frac{\partial N_i}{\partial y} \end{bmatrix} = [J] \begin{bmatrix} \frac{\partial N_i}{\partial x} \\ \frac{\partial N_i}{\partial y} \end{bmatrix} \qquad (3.11)$$

where [J] is the Jacobian matrix.

Substituting $x = \Sigma N_i x_i$ and $y = \Sigma N_i y_i$, the Jacobian matrix becomes

$$[J] = \begin{bmatrix} \Sigma \frac{\partial N_i}{\partial \xi} x_i & \Sigma \frac{\partial N_i}{\partial \xi} y_i \\ \Sigma \frac{\partial N_i}{\partial \eta} x_i & \Sigma \frac{\partial N_i}{\partial \eta} y_i \end{bmatrix} \tag{3.12}$$

Thus

$$\begin{bmatrix} \frac{\partial N_i}{\partial x} \\ \frac{\partial N_i}{\partial y} \end{bmatrix} = [J]^{-1} \begin{bmatrix} \frac{\partial N_i}{\partial \xi} \\ \frac{\partial N_i}{\partial \eta} \end{bmatrix} \tag{3.13}$$

which means that $[B_i]$ is determined using the partial derivatives of the shape functions in local coordinates, and the global coordinates of the nodal points.

Substituting $d\xi d\eta |J| = dxdy$ where $|J|$ = the determinant of $[J]$ and specifying the limits of integration in terms of local coordinates

$$[k_{ij}] = t \int_{-1}^{1}\int_{-1}^{1} [B_i]^T [D][B_j] |J| d\xi d\eta = \int_{-1}^{1}\int_{-1}^{1} f(\xi,\eta)\, d\xi d\eta$$

Due to the complexity of the explicit form of $[f(\xi,\eta)]$, numerical integration is used. According to Gauss quadrature we can evaluate the integral

$$[k_{ij}] = \int_{-1}^{1}\int_{-1}^{1} f(\xi,\eta)\, d\xi d\eta$$

as

$$[k_{ij}] = \sum_{i=1}^{n} \sum_{j=1}^{n} H_i H_j f(\xi_j,\eta_i) \tag{3.14}$$

Element properties can be improved considerably by using the minimum integration order, because

(a) Reduced integration decreases the stiffness - the displacement elements are overstiff.

(b) Attention is focused on the integration point, regions where the displacements may be over-constrained to achieve inter-element compatibility are excluded from the formulation.

Abcissae and the weight coefficients for the quadratic element are given as

$$n = 2, \quad H_1 = H_2 = 1.0, \quad \varepsilon_1 = \eta_1 = -\frac{1}{\sqrt{3}}, \quad \varepsilon_2 = \eta_2 = \frac{1}{\sqrt{3}}$$

3.4 ANALYSIS OF NONLINEAR MATERIAL BEHAVIOUR

The procedure for linear elastic analysis described in Section 3.1, can be utilized along with an iterative process to study nonlinear material behavior. For reinforced concrete structures the solution is generally path-dependent. Therefore, an incremental loading technique is usually adopted.

The fundamental steps for a typical load increment can be summarized as

(1) Generation of the structural stiffness matrix

(2) Assembly of the incremental load vector

(3) Solution for nodal displacements

(4) Calculation of incremental strains

(5) Determination of element stresses by adding incremental stresses ($\{\Delta\sigma\} = [D]\{\Delta\varepsilon\}$) to existing stresses

(6) Check for cracking, plasticity and crushing

(7) Determination of nodal forces from unbalanced (excess) element stresses

(8) Check for convergence

(9) Re-analysis

Steps 1 through 5 represent the typical procedure for the displacement method of elastic analysis. Steps 6 through 9 are additional for nonlinear analysis and they are explained next.

3.4.1 Cracking of Concrete

3.4.1.1 Crack formation

Concrete subject to biaxial tension is assumed to have cracked when the larger of the principal stresses exceeds the uniaxial tensile strength, f_t. The validity of the maximum normal stress theory for the cracking of concrete in biaxial tension was verified experimentally by Kupfer et al (25).

Concrete under biaxial tension-compression cracks before the tension stress component reaches the uniaxial tensile strength. Suwalski and Zalewski (46) used a simplified linear relationship to define the cracking strength of

concrete under biaxial tension-compression. According to this relationship, concrete is assumed to have cracked when

$$\sigma_1 > f_t\left(1 + \frac{\sigma_2}{f_c'}\right) \qquad (3.15)$$

where

σ_1 = principal tension stress

σ_2 = principal compression stress

f_c' = uniaxial compression strength of concrete

f_t = uniaxial tensile strength of concrete

The crack direction is assumed to be perpendicular to the (larger) principal tension. Due to the crack formation the tensile stress that existed just before cracking has to be removed and transferred elsewhere and the stress-strain matrix [D] has to be modified accordingly (see Section 2.2.2). The components of the tensile stress to be transferred are:

$$\begin{aligned} \sigma_x &= \sigma_1 \cdot \cos^2\theta \\ \sigma_y &= \sigma_1 \sin^2\theta \\ \tau_{xy} &= \sigma_1 \sin\theta \cos\theta \end{aligned} \qquad (3.16)$$

where θ is the angle between the x axis and σ_1. The cracked element is assumed to carry stresses along the crack direction.

3.4.1.2 Cross cracking

Cracked concrete is assumed to crack once again when the normal stress exceeds the uniaxial tensile strength. The direction of the crack is perpendicular to the first crack direction. Concrete stiffness is set to zero. Reinforcement in compression is assumed to be incapable of sustaining any load.

3.4.2 Plasticity of Concrete

3.4.2.1 Cracked concrete - uniaxial compression

In uniaxial compression, concrete is assumed to be linear elastic until the stress reaches f'_c. Perfect plasticity is assumed thereafter until the strain reaches ε_ℓ, the maximum uniaxial compressive strain, as shown in Fig. 2.2. If the strain exceeds ε_ℓ, concrete is assumed to have crushed. The stiffness is set to zero and the concrete stress is transferred to the rest of the structure.

3.4.2.2 Uncracked concrete - biaxial compression

Concrete is assumed to exhibit limited plasticity and von Mises' yield criterion is used in the analysis (see Section 2.2.3). The procedure for the elasto-plastic solution within a typical load increment (49,51) can be summarized as follows:

(1) Incremental stresses $\{\Delta\sigma\}$ are added to existing stresses $\{\sigma\}_0$ and the new stresses $\{\sigma\}_1$ are obtained.

(2) The yield condition is checked. If $F(\sigma) < 0$, the element is elastic and the process is terminated.

(3) If $F(\sigma) > 0$, and previously $F(\sigma) = 0$, (the element was plastic), the admissible stress increments satisfying the plasticity conditions are

$$\{\Delta\sigma\}_1 = [D]_{ep} \{\Delta\varepsilon\} \qquad (3.17)$$

The element stresses are updated as

$$\{\sigma\}_1^* = \{\sigma\}_0 + \{\Delta\sigma\}_1 \qquad (3.18)$$

$\{\sigma\}_1^*$ is beyond the yield surface, and must be scaled to the yield surface to obtain the final element stresses $\{\sigma\}_1^f$.

(4) If $F(\sigma) > 0$, but previously $F(\sigma) < 0$, (the element was elastic), the intermediate stresses $\{\sigma\}_i$ at which $F(\sigma) = 0$ must be determined. Thus

$$\{\Delta\varepsilon\} = \{\Delta\varepsilon\}_i + \{\Delta\varepsilon\}_1$$

$$\{\Delta\sigma\} = \{\Delta\sigma\}_i + \{\Delta\sigma\}_1 \qquad (3.19)$$

and $$\{\sigma\}_i = \{\sigma\}_0 + \{\Delta\sigma\}_i$$

where $\{\Delta\varepsilon\}_i$ and $\{\Delta\varepsilon\}_1$ represent the elastic and plastic strain increments, respectively. The element stresses are updated as in Step 3

$$\{\sigma\}_1^* = \{\sigma\}_i + [D]_{ep} \{\Delta\varepsilon\}_1 \qquad (3.20)$$

and scaled to the yield surface to obtain the final element stresses $\{\sigma\}_1^f$.

(5) The excess stresses are converted to equivalent nodal forces which are applied to the structure in the following iteration. Steps 1-5 are repeated until the equivalent forces become sufficiently small.

The equivalent strain associated with von Mises' criterion is given as

$$\varepsilon_{eq} = (\varepsilon_x^2 - \varepsilon_x\varepsilon_y + \varepsilon_y^2 + \frac{3}{2}\gamma_{xy}^2)^{\frac{1}{2}} \qquad (3.21)$$

When ε_{eq} exceeds ε_ℓ, the limiting compression strain, concrete is assumed to have crushed and all of the stresses have to be transferred elsewhere.

3.4.3 Yielding of the Reinforcement

Linear elasticity followed by perfect plasticity is assumed in both compression and tension, as shown in Fig.2.4. Yielding occurs when the steel stress σ^s reaches the yield

stress f_y. This may occur within a load increment, such that at the end of the incremental process

$$\sigma_0^s + \Delta\sigma^s = \sigma_1^s \geq f_y \tag{3.22}$$

The yield stress is exceeded by an amount

$$\sigma_{ex}^s = \sigma_1^s - f_y \tag{3.23}$$

The excess stress which has to be transferred is

$$\sigma_{ex}^s = p_u \, \sigma_{ex}^s \tag{3.24}$$

where p_u represents the reinforcement ratio.

3.4.4 The Stress Transfer Process

Following the application of a load increment, changes in material modes may occur resulting in unbalanced (excess) element stresses $\{\sigma\}_{ex}$. These stresses are converted to equivalent nodal forces

$$\{P\}_{eq} = \int_V [B]^T \{\sigma\}_{ex} \, dV \tag{3.25}$$

which are applied to the structure in the next iteration. Note that the externally applied loads are not changed during this process.

The deterioration of the structural stiffness due to cracking, plasticity and crushing under increasing loads can be treated using either the variable(modified) or the con-

stant stiffness method.

3.4.4.1 The variable stiffness method

The stress-strain matrix [D] is modified according to the material modes of the elements, and the system stiffness matrix [K] is regenerated. If we denote the structural stiffness prior to the load application by $[K]_0$, the nodal displacement vector will be $\{\delta\} = \{0\} = \{\delta\}_0$. The displacements after the load application are $\{\delta\}_1 = [K]_0^{-1}\{P\}$ and the iteration process will be repeated with $\{\delta\}_n = [K]_{n-1}^{-1}\{P\}$ until convergence is achieved.

3.4.4.2 The constant stiffness method

The initial stiffness matrix $[K]_0$ remains unchanged. If cracking, crushing or plasticity occurs $[K]_0$ does not represent the true stiffness and the equilibrium equations are re-established as $([K]_0 + [\Delta K])(\{\delta\}_0 + \{\Delta\delta\}) = \{P\}$ so that $[\Delta K]$ represents the change in the stiffness matrix and $[\Delta K](\{\delta\}_0 + \{\Delta\delta\}) = \{P\}_{eq}$ can be considered as an equivalent load. $\{\Delta\delta\} = [K]_0^{-1}\{P\}_{eq}$ and the process is terminated when $\{P\}_{eq}$ becomes sufficiently small.

Due to the high cost of repeated regeneration of the stiffness matrix, the constant stiffness method has been favored because $[K]_0$ is generated once and used throughout the analysis. The computing time difference between the two methods is balanced partially by the larger number of iterations required by the constant stiffness method. How-

ever, it is argued that the two methods may give different results for load path dependent materials and that the application of the constant stiffness approach to the concrete cracking problems may lead to erroneous predictions (31).

In this study, the stiffness matrix is modified whenever cracking occurs, whereas plasticity of component materials is dealt with using the constant stiffness method.

The structure is re-analyzed and this process is continued until convergence is achieved. Convergence is checked by comparing the final load vector with the load vector of the first iteration. After reaching a prescribed tolerance level such as

$$(P_{max})_{\text{last iteration}} \leq 0.01\,(P_{max})_{\text{first iteration}}$$

where (P_{max}) represents the component of the load vector largest in absolute value, the process is terminated and the next load increment is applied. However, upon reaching the collapse state unlimited plastic deformations occur and the iteration process does not converge. For this reason, a limit deformation is specified at the beginning of the analysis. The execution is terminated when the limit deformation is reached.

Other control criteria such as checking the convergence of nodal displacements rather than the convergence of

nodal forces, or setting an upper bound for the number of iterations within a specific load increment can also be used.

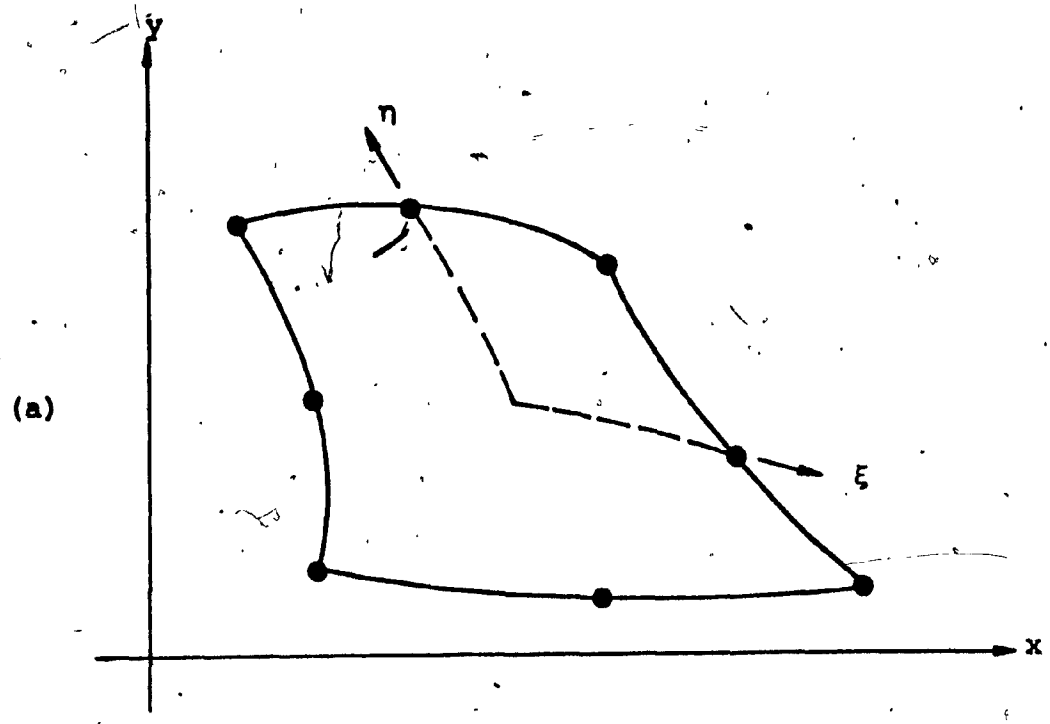

(a)

FIG. 3.1 QUADRATIC EDGE DISPLACEMENT ISOPARAMETRIC RECTANGLE

(a) In General Coordinates

(b) In Normalized, Local Coordinates

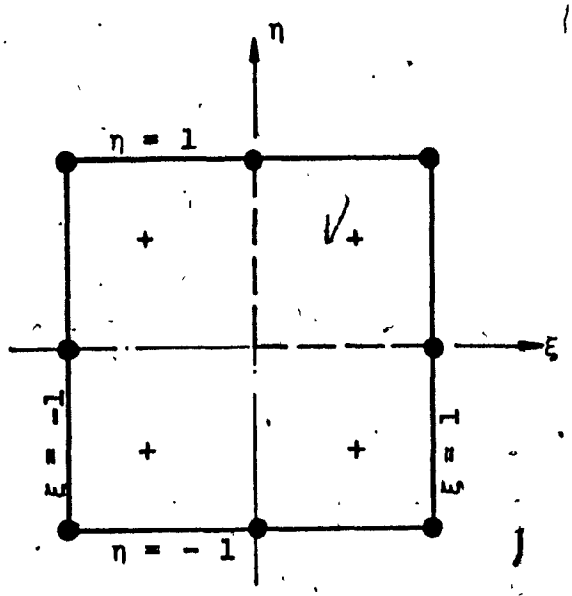

(b)

+ Integration Points

CHAPTER 4

COMPARISON OF THE FINITE ELEMENT MODEL WITH EXPERIMENTAL RESULTS

CHAPTER 4

COMPARISON OF THE FINITE ELEMENT MODEL WITH EXPERIMENTAL RESULTS

4.1. INTRODUCTION

The idealization of the material properties and stress-strain relationships, and the incremental finite element method of analysis used, impose some degree of approximation to the analytical model. The accuracy and versatility of the chosen finite element model is investigated using results of tests conducted at Concordia University and comparable results from other experimental studies. The following test results and analyses are presented in order of increasing complexity; ordinary beams, intermediate beams and beam panels.

4.2 BEAMS 2 AND 3 BY KRAHL ET AL

Three beams with the following properties (see Fig. 4.1(a)) were tested to study the effect of longitudinal reinforcement on the propagation of tensile cracks (23):

ℓ = 136"	f'_c = 3,740 psi
h = 12"	f_t = 458 psi
b = 6"	f_y = 44,000 psi

Beam 1 : No reinforcement

Beam 2 : 2 #5 (A_s = 0.62 in^2)

Beam 3 : 2 #9 (A_s = 2.00 in^2)

The reinforcement was located at an effective depth of 9.94". The beams were simply supported and loaded by two equal concentrated loads 50" from the supports. Beam 1 failed by the sudden propagation of the first flexural crack to the compression face. Beam 2 was under-reinforced ($A_s/bd = 0.0104$) and yielding of the reinforcement was observed. Failure of Beam 3, which was over-reinforced ($A_s/bd = 0.0335$), occurred by crushing of concrete at the compression face.

Beams 2 and 3 were analyzed using the proposed finite element model, with $\beta = 0.10$ and $\beta = 0.50$. The difference in β values had negligible effect on the numerical solution. With the lower β value, the model indicated yielding of steel at P = 4,000 lbs, while with the higher β value, yielding was indicated at P = 4,400 lbs. The computed failure load in both cases was 5,000 lbs. This value can be checked using the ordinary beam theory:

$$\text{Depth of equivalent compression block} = a = \frac{A_s f_y}{0.85\, f_c' b}$$

$$a = \frac{(0.62)44{,}000}{(0.85)3{,}740(6)} = 1.43"$$

$$\text{Ultimate flexural moment} = M_{ult} = A_s f_y (d - \frac{a}{2})$$

$$M_{ult} = (0.62)44{,}000(9.94 - \frac{1.43}{2}) = 251{,}655 \text{ in/lb}$$

$$P_{ult} = \frac{M_{ult}}{50} = 5{,}033 \text{ lbs}$$

The computed ultimate load for Beam 3 was 10,500 lbs for both β values, and failure was due to crushing of concrete at the vicinity of the load point. The computed load is 78% of the experimental value. This under-estimation is due to the difference between the actual and idealized loading patterns. In reality the load is applied over a finite area. In the finite element model, however, the load is applied at a point, which leads to a high stress concentration, and local crushing. The analytical result could be improved by distributing the load over an area (as in the actual loading) and/or using a finer grid in the vicinity of the load point.

The finite element mesh and the analytical crack patterns for Beam 2 and Beam 3 are shown in Fig. 4.1(b) and Fig.4.2. When obtaining the analytical crack patterns, the following approximations were introduced for the sake of simplicity and better physical description: stresses, material modes (yielding, cracking, etc.) and crack directions are determined at the integration points, and could be different for any other point within the element. Since the integration points are symmetrically located in the element, the values obtained at each integration point are assumed to be constant over that particular quarter of the element. Thus, if cracking occurs at an integration point, that particular quarter of the element is shown as cracked. Secondly, instead of indicating the crack direction with numerous parallel lines, the lines are "condensed" for easier comparison of experimental and analytical crack directions and only those lines near or along the

observed cracks are shown.

A plot of load versus crack depth, including the results of analyses by Colville and Abbasi (9), Suidan and Schnobrich (40), and Valliappan and Doolan (41), is shown in Fig. 4.3. The superiority of the isoparametric elements is evident from the plot. The number of nodes, the number and types of elements used in the analyses were as follows:

	No. of Nodes	No. of Elements	Type of Element
Ref. 41	131	213	Constant strain triangle
Ref. 9	133	108	Constant edge strain rectangle
Ref. 40	108	10	Quadratic edge displacement isoparametric brick
Present Study	62	15	Quadratic edge displacement isoparametric rectangle

In the other studies, the effect of biaxial tension-compression stresses on the cracking strength of concrete was not considered. Colville and Abbasi analyzed only Beam 3, whereas Suidan and Schnobrich analyzed Beam 2. In the latter investigation, a shear retention factor of 0.5 was used for cracked concrete, and in generating the stiffness matrix for the brick, the stiffness terms were evaluated at two different sets of points. A 3 x 3 x 2 point integration was adopted for elements that were expected to be critical. A 2 x 2 x 2 point integration (which follows the reduced integration concept) was adopted for all other elements.

Due to the insensitivity of the solution to the value of the shear retention factor used, a fixed value of $\beta = 0.1$ was used in all of the following analyses.

4.3 TEST SERIES BY ZIELINSKI

Beams "a", "b" and "c" shown in Fig. 4.4 were tested as part of a study on the ultimate strength in high shear and diagonal splitting failure of reinforced concrete beams (46). The test results indicated very high shear stresses not allowed by existing code requirements. All three beams contained the same amount of flexural reinforcement; 2 #10 bars ($A_s = 2.54$ in^2) as tension steel and 2 #3 bars ($A'_s = 0.22$ in^2) as compression steel. The tensile reinforcement was anchored by welding steel plates to the ends of the bars. The section and material properties were as follows:

$\ell = 80"$ $\quad f'_c = 4{,}100,\ 3{,}920,\ 3{,}870$ psi for "a","b" and "c", respectively

$h = 16"$ $\quad f_t = 313,\ 298,\ 298$ psi for "a","b" and "c", respectively

$b = 6"$ $\quad f_y = 44{,}700$ psi for #10 bars

$\quad\quad = 49{,}800$ psi for #2 and #3 bars

In Beam "a" bond was eliminated along portions of the length by encasing the tensile reinforcement in rubber tubes. Consequently, the beam worked as a tied arch throughout the loading. The web reinforcement was designed for the beam to fail by diagonal splitting and consisted of #3 bars spaced at 10" intervals. The beam was under a concentrated midspan load.

Failure occurred at 37.5 tons (82.5 kips). The crack pattern is shown in Fig. 4.5 (a).

The finite element mesh for Beam "a" consisted of 76 nodes and 18 elements, as shown in Fig. 4.6(a). The elimination of bond was simulated by disconnecting adjacent steel and reinforced concrete elements at their common nodes. The analysis indicated failure at 30 tons (66 kips) by local crushing when a single nodal force was used (the same value for the failure load was obtained for Beam "b" using a single nodal force.) However, when the load was distributed over a 6" length (as in the actual testing), the model indicated failure at 39 tons (85.8 kips). The crack pattern of the model is shown in Fig. 4.6(b).

Beam "b" was loaded the same way as Beam "a". However, the web reinforcement was computed according to ACI Code 318-63 and consisted of #3 bars at 4" intervals. The failure load was 39 tons (85.8 kips), and the crack pattern is shown in Fig. 4.5(b). The finite element mesh consisted of 51 nodes and 12 elements. The failure load indicated by the analysis was 42 tons (92.4 kips). The finite element mesh and the analytical crack pattern are illustrated in Figs. 4.7(a) and 4.7(b), respectively.

Beam "c" was under two equal concentrated loads at a distance of 18" from the supports. Like Beam "a", the web reinforcement was computed on the assumption of arch action at ultimate state, and consisted of 4 #3 bars between each

support and load point, plus 4 #2 bars at 10" intervals in the zero shear zone. Failure of Beam "c" occurred at 35.5 tons (78.1 kips). The crack pattern is shown in Fig. 4.5(c). The finite element mesh was similar to that of Beam "b". The model indicated failure at 33 tons (72.6 kips). The finite element mesh and the analytical crack pattern are illustrated in Fig. 4.8(a) and 4.8(b), respectively.

4.4 BEAM PANELS - CONCORDIA TESTS

4.4.1 Experimental Program

4.4.1.1 Description of testing

A series of tests on full-scale beam panels were conducted as part of continuing research at Concordia University on panelized building systems, for a better understanding of the load-carrying capacity and failure mechanisms of thin-wall ribbed panels and for the verification of the applicability of the finite element model.

The panels were 44" x 89" and had a wall thickness of 1.5". 6" thick ribs along the perimeter provided lateral rigidity to the panels and also accommodated the reinforcing bars. All the panels contained a 6 x 6 - 6/6 welded wire mesh as the web reinforcement, and 2 #3 bars in the vertical and upper (compression) ribs. The panels were simply supported and top loaded. The testing arrangement is illustrated in Fig. 4.9 and a typical panel is shown in Fig. 4.10. The

main variables were the amount of tensile flexural steel and shear span ratio. The notation "P ijk" used for the panels indicated these variables:

"i" denoted the amount of tensile flexural steel

1 - 2 #3 bars

2 - 2 #4 bars

3 - 2 #10 bars

"j" denoted the type of loading

1 - midspan loading

2 - third point loading

"k" denoted the sample number for a particular i,j combination.

The tensile flexural steel was welded to steel angles at the ends prior to casting to avoid possible bond and anchorage failures. The load was applied at 2.5 kip increments, and cracks were marked on both sides as they appeared. Deflection readings were taken at 5 kip intervals by dial gauges accurate to 0.001".

4.4.1.2 Material properties

Compression strength of concrete was determined from tests on standard 6" x 12" cylinders. The beam panels and cylinders were tested approximately three months after casting and the following relationships suggested in European Concrete Committee's "Recommendations for an International

Code of Practice" (pp.32-34) were used to determine the tensile strength of the concrete:

$$f'_c \text{ (90 days)} = 1.2\ f'_c \text{ (28 days)}$$

$$f_t \text{ (90 days)} = 1.05\ f_t \text{ (28 days)}$$

and at 28 days $f_t = 1.38\ (f'_c)^{2/3}$ where f_t and f'_c are expressed in lbs/in^2.

The following values were used in the computations:

Panel Designation	f'_c (psi) (average of 3 cylinders)	f_t (psi)
P 111, P 121	5482	399
P 211, P 221	5648	407
P 311, P 321	5277	389

Strength of reinforcing steel was determined by tensile tests. The stress-strain diagrams obtained from the tests are given in Fig. 4.11. The following values for yield strength were used in the computations:

Reinforcement Designation	Yield Strength f_y (psi) (average of 3 samples)
Gauge 6 wire	78,506
# 3 bar	60,088
# 4 bar	57,500

#10 bars were not tested and a yield strength of 50,000 psi was assumed as specified in the design. Knowledge of the exact value was not significant since in this case, yielding of steel did

not occur.

4.4.1.3 General observations

The first cracks to appear were the vertical flexural cracks in the lower (tension) rib or in the web, just above the lower rib, along the load point (see Appendix A). These cracks were generally observed at a load of 12.5 - 25 kips. In panels with existing cracks, instead of new crack formation existing cracks widened and extended. As the load was increased the first flexural cracks extended and new cracks formed beside them. Shear-flexure cracks were observed at a load of 20 - 30 kips. These cracks were extending from the lower rib towards the load point and propagated upwards as the load was increased. The third type of cracks were the diagonal splitting cracks which formed approximately along lines connecting the support and load points. These cracks were differentiated from shear-flexure cracks by their sudden, audible formation and extension over the whole web (in some cases the cracks even penetrated into the ribs.) Unlike shear-flexure cracks, diagonal splitting cracks were not the continuation of flexural cracks and did not necessarily originate at or near the lower rib. Generally, the splitting cracks appeared after the formation of the shear-flexure cracks. In some cases, as the load was increased new splitting cracks appeared besides the existing ones. Failure of the panels invariably occurred by crushing of concrete along the diagonal connecting the support and load point.

For the panels under third point loading, crushing was in the shorter segment.

4.4.1.4 Description of individual panels - specific observations

(i) P 111: The first flexural crack was observed at 12.5^k, and propagated to 3/4 of the depth at 20^k. Shear-flexure cracks appeared at 25 kips. At 45 kips, the vertical flexural crack penetrated into the upper rib. The first diagonal splitting crack (DSC) appeared at 47.5^k on the right-hand side (RHS), and was followed by another one at 55^k on the left-hand side (LHS). A third DSC appeared, on the RHS at 57.5^k. At 60^k, this last DSC penetrated into the compression rib and failure occurred by crushing of concrete in the web under the load point. P 111 was under-reinforced and was designed to fail in flexure. Strain hardening of the #3 bars, however, lead to a higher load carrying capacity than designed for and to the development of diagonal splitting cracks.

(ii) P 211: The first flexural crack was observed at 12.5^k and propagated to the top of the web at 20^k. Shear-flexure cracks appeared at 17.5^k. The first DSC appeared at 40^k on the LHS, and a second one appeared at 52.5^k on the RHS. A third DSC appeared at the RHS when the load reached 60^k. Meantime, another splitting crack was propagating from the load point to the support, along the first DSC. These two cracks joined and penetrated to the support area, and led to the failure of the panel at 68.5^k. P 211 was also under-rein-

forced, however, the higher amount of reinforcement as compared to P 111, permitted considerable "arch action" to develop, and the panel worked as a tied arch until the flexural tensile steel yielded.

(iii) P 311: This panel contained shrinkage cracks near midspan, and as a result new flexural cracks did not appear until 30^k. However, shear cracks appeared at 25^k and were accompanied by diagonal splitting cracks on both load-support segments. A third DSC appeared on the LHS at 55^k and propagated to 3/4 of the upper rib at 62.5^k. Failure occurred at 90^k when a fourth DSC appeared along the third DSC and extended to the support, leading to crushing of the web above the support area.

(iv) P 121: This panel was identical to P 111, except for being loaded at the third point. Flexural cracks appeared at 17.5^k and shear-flexure cracks were observed at 25^k. The first DSC appeared in the shorter segment (LHS) at 30^k, and was followed by the second DSC on the RHS at 45^k. At 47.5^k, a third DSC appeared along the shorter load-support segment. The cracks propagated to the middle of the upper rib by 52.5^k. At 60^k another diagonal crack appeared in the shorter segment, above the existing cracks. Failure occurred at 64^k by crushing of the compression "strut" along the shorter diagonal.

(v) P 221: The general behavior was similar to P 121. The first DSC appeared at 42.5^k in the shorter segment (LHS). At 45^k a second DSC appeared in the longer segment. Failure

occurred at 67.5^k when a new diagonal crack appeared below the first DSC which meantime propagated in both directions, to the support and load point. As in P 121, crushing occurred along the shorter diagonal strut.

(vi) P 321: The first flexural crack was observed at 17.5^k, and propagated to the top of the web at 30^k. The first shear-flexure crack appeared at 22.5^k and was followed by the first DSC at 35^k which appeared in the longer segment (RHS). The second DSC appeared in the shorter segment at 50^k. Failure occurred at 87.5^k by crushing along the shorter diagonal as in P 121 and P 221. However, relatively fewer cracks were observed.

4.4.2 Finite Element Study

The results of the finite element study are described below. The different mesh used and the analytical crack patterns are illustrated in Appendix B.

4.4.2.1 Beam panels loaded at midspan

Making use of symmetry, only half of the panels were analyzed. The finite element mesh consisted of 96 nodes and 25 elements.

(i) P 111: The computed load for the first flexural crack was 23.6^k. At 25^k, the first crack reached the top of the web. Thereafter, the load was applied in 5^k increments. At 40^k, the model indicated cracks similar to the experiment-

ally observed diagonal cracks. Ignoring the plastic modulus of the #3 bars led to the underestimation of the load carrying capacity of the panel and to the failure of the model at 50^k due to the yielding of the tensile flexural steel. The program was then modified for a non-zero plastic modulus for the #3 bars only. The value used for the plastic modulus was 1,100,000 psi as recommended by the European Concrete Committee. At 55^k, the horizontal component of the wire mesh located up to 1/3 of the depth was in yield. The load increment was then reduced to 2.5^k. At 57.5^k, the first flexural crack penetrated into the upper rib, and the horizontal steel up to mid-depth was in yield. It should be noted that flexural failure of reinforced concrete members may be initiated by excessive straining of the tensile steel and excessive sectional rotation. This critical strain value is usually taken as 0.5%. The steel strain in the lower rib at 57.5^k was .0057 in/in, thus the failure load was assumed to be 57.5^k.

(ii) P 211: The computed load for the first flexural crack was 23.5^k. This crack propagated to 3/4 of the depth at 25^k. At 35^k, the model indicated cracks similar to the experimentally observed shear cracks. Yielding of the tensile flexural steel was first indicated at 65^k, and spread upward and to the sides as the load was increased. At 77.5^k, the horizontal steel located up to 1/3 of the depth was in yield, and the steel strain in the lower rib was in the order of .0055 in/in, indicating excessive rotation. Consequently, 77.5^k was assumed to be the failure load.

P 211 was used to study the effect of the number and size of (a) elements, and (b) load increments on the accuracy of the solution. In addition to the standard mesh, a coarse mesh consisting of 65 nodes and 16 elements, and a fine mesh consisting of 133 nodes and 36 elements were used in the analyses. In order to decrease the execution time, the original amount of steel was reduced by applying a factor taken as

$$1 - \frac{E_c}{E_s} \approx .84$$

The computed load for the first flexural crack using the coarse mesh was 25.1^k. This crack extended to 3/4 of the depth at 27.5^k. At 35^k shear-flexure cracks were indicated and the first flexural crack reached the top of the web. Cracking along the diagonal occurred between 40 and 45 kips. Yielding of the tensile flexural steel was indicated at 57.5^k. At 70^k, the horizontal web steel began to yield, and at 77.5^k yielding of the horizontal web steel located up to mid-depth was indicated, and this load was assumed to be the failure load.

The computed first crack load for the medium (standard) mesh was 23.6^k, and this crack propagated to 3/4 of the depth at 25^k. Three different load increments were used thereafter. In the first case, the load was increased at 10^k increments from 25^k to 65^k, and then the increment was reduced to 2.5^k. In the second case the load increment was taken as 5^k, from 25^k to 55^k, and 2.5^k thereafter. In the

third case, a constant value of 2.5^k was used. In all the cases, the model indicated yielding of tensile flexural steel in the lower rib at 55^k and yielding of the horizontal web steel at 65^k. Yielding of horizontal steel located up to mid-depth was indicated at 67.5^k for all three cases. The size of the load increments was observed to have very little effect on the solution. With the larger load increments, the displacements were slightly larger.

Using the fine mesh, the first crack load was computed as 23.5^k. Since this value was almost identical to the one obtained using the medium mesh (23,469 lbs. vs. 23,647 lbs), an incremental analysis was found to be unnecessary.

(iii) P 311: The first crack load was computed as 18.1^k. At 30^k shear-flexure type cracks and at 40^k cracks similar to diagonal splitting cracks were indicated. Cracking in the upper rib was indicated at 60^k. This, however, was not a continuation of a flexural crack, but was due to diagonal splitting. The model indicated plastification of cracked concrete at 97.5^k, in the web, below the load point. At 100^k, crushing of concrete was indicated at the same location and the execution was terminated. However, due to reasons which will be discussed in the next section, 97.5^k at which concrete plasticity occurred was assumed to be the failure load.

4.4.2.2 Beam panels under third point loading

The panels were analyzed using a mesh which consisted of 147 nodes and 40 elements.

(i) P 121: As in P 111, the plastic modulus for the #3 bars was set as 1,100,000 psi. The computed load for the first flexural crack was 24.9^k. This crack reached the top of the web, and penetrated into the upper rib at 30^k. Cracks along the shorter diagonal were indicated at 35^k and 40^k. Similar cracks along the longer diagonal were indicated at 45^k. Yielding of the tensile flexural steel also occurred at this load. At 55^k, the model indicated yielding of the horizontal web steel. At 60^k, horizontal steel located up to 2/3 of the depth was in yield, and the strain in the main flexural steel in the lower rib was .0056 in/in indicating excessive rotation. Therefore, the failure load was assumed to be 60^k.

(ii) P 221: The first crack load was computed as 24.8^k. The flexural crack reached the top of the web at 30^k. The model indicated cracking along diagonals at 45^k. Yielding of the tensile flexural steel was indicated at 55^k. At 60^k, the horizontal component of the web reinforcement was in yield. The model indicated plastification of concrete in the shorter segment, above the support area at 65^k, which was assumed to be the failure load.

(iii) P 321: The computed first crack load was 19.6^k.

The cracks extended to 1/2 of the depth at 35^k. Shear cracks were indicated at 40^k. At 55^k, the model indicated cracking along the diagonals. Failure load was assumed to be 95^k, at which stage plastification of cracked concrete in the web, below the load point was indicated.

4.5 DISCUSSION OF THE RESULTS AND CONCLUDING REMARKS

The comparisons with test results indicate that the finite element model can quite accurately predict the behavior of reinforced concrete beams and beam panels subject to monotonically increasing loads. The analytical and observed crack directions and locations, as well as the failure loads, are in good agreement. Obviously, discrete cracks as in actual members cannot be represented with the model. Instead, zones of cracked concrete are indicated.

Two factors which may influence the solution are the number and size of (a) elements and (b) load increments.

For a given type of element, a smoother crack pattern will be obtained using a larger number of elements. Reducing the size (thus increasing the number) of elements leads to the "softening" of the model. The comparison of two different mesh for P 211 indicated that the load-displacement diagram (see Appendix C for the load-displacement diagrams) for the coarse mesh is above the diagram obtained by using a finer mesh. Also, the first crack load is higher in the case of a coarse mesh. These observations are in agreement with those reported in (6).

A technique in specifying load increments, especially for cases where sufficient information on the failure load is not available, would be to apply a certain load, determine the stresses, and multiply the values with the smallest factor such that the cracking limit (or any other change in material modes) is reached. This technique was used in determining the first crack load. The technique, however, leads to an uncontrolled number and size of load increments, especially when a fine mesh is used in the analysis. Therefore, this technique was abandoned for the incremental analysis and the program was written for the application of load increments of arbitrary size. This has the advantage of treating any number of elements simultaneously. Cervenka (6) reported that the size of the load increment had little effect on the results, and generally, deflections were slightly higher for large increments.

In the case of P 211, which was analyzed by 2.5^k, 5^k and 10^k increments, the above observations were verified, indicating that the load-displacement diagram in the case of large load increments will be below the one obtained using smaller load increments. It is not advisable to use a very large load increment just after the first crack load (i.e., after scaling the stresses to the elastic limit), as this may lead to an irregular crack pattern and even to instability and failure. Smaller load increments, near collapse state will also be preferable in order to obtain an accurate value for the failure load. A conclusion on the computer time requirements

as a function of the load increment size cannot be drawn, because larger load increments may require more iterations than smaller increments before equilibrium can be reached. However, for P 211, the computer time required in the cases of 5^k and 2.5^k increments were 11% and 23% higher, respectively, than that required in the case of 10^k increments.

Based on the comparisons with test results, it can be concluded that the assumed material stress-strain relationships and the criteria for cracking and plasticity correctly represent the behaviour of the concrete-steel composite. The value for the first crack load obtained by the analysis was in all cases higher than the experimental value. This results from the geometrical and physical imperfections in the reinforced concrete members and to a lesser extent, from the overstiffness of the finite element. The load-displacement diagrams also indicate the overstiffness of the model. However, the difference between the analytical and experimental load-displacement diagrams was basically due to the manner in which the experimental measurements were taken. The vertical displacements were measured along the supports and under the lower rib, along the load point. The net displacement along the load point was computed as

$$\Delta_{net} = \Delta_2 - \tfrac{1}{2}\Delta_1 - \tfrac{1}{2}\Delta_3$$

in the case of midspan loading and as

$$\Delta_{net} = \Delta_2 - \tfrac{2}{3}\Delta_1 - \tfrac{1}{3}\Delta_3$$

in the case of third point loading, where

Δ_2 = displacement along the load point

Δ_1, Δ_3 = displacements along the supports (closer to and further away from the load point, respectively, in the case of third point loading.)

Following the formation of the diagonal cracks, however, relative displacement of the central block with respect to the end blocks (the term block is used for portions of the panel separated by the diagonal cracks) occurred. Thus, the measurements taken actually did not represent displacements within a continuous body. This is evident in the load-displacement diagrams, as the difference between observed and analytical displacements increases rapidly at higher loads at which diagonal splitting cracks were observed. However, the similarity between the general trend of the analytical and experimental diagrams is worth noting.

A very important difference in the modelling of beams, and beam panels was observed following the analyses of P 311, P 221 and P 321. In the program, a factor of 0.9 is applied to the concrete compression strength obtained from cylindrical samples, due to the differences in casting, compacting, curing and due to the discontinuities introduced to the structural member by the presence of reinforcing steel. For cracked concrete, a reduced factor of 0.7 is applied to represent the weakening of concrete due to the presence of cracks. Cracked concrete is assumed to go plastic when the normal stress along the crack direction reaches the uniaxial compressive strength.

Crushing is assumed to occur when the limit compressive strain is reached, which is set as -0.003 in/in unless specified otherwise. In the case of P 311, plastification of cracked concrete was indicated at 97.5^k (compared to the observed failure load of 90^k). Theoretically, the load had to be increased further for crushing and(consequently for failure) to occur. Similarly, in P 321, plastification occurred at 95^k, in the shorter segment (the lower value as compared to P 311 is due to the fact that the larger portion of the applied load is carried by the shorter segment.) However, observation of the beam panels indicated that failure actually occurred not due to compression crushing but as a result of reaching a limit tensile strain perpendicular to the plane of the panel. This can be checked as follows:

$$\text{Strain along the compression stress} = \frac{-0.7f'_c}{E_c}$$

$$= \frac{-(0.7)5,277}{4,400,000} = -.00084 \text{ in/in}$$

$$\text{Lateral strain} = (\nu)(.00084) \approx (.17).00084 = .00014 \text{ in/in}$$

Note that although the compression strain is much less than the limiting value of - .003 in/in, the lateral strain is within the range of .0001 - .0002 in/in, accepted as the limiting tensile strain in concrete. The presence of the wire mesh in the mid-plane introduces a discontinuity which also influences the spalling of the concrete.

In the light of the above discussion, it seems to be appropriate to neglect uniaxial plasticity of concrete and assume crushing when the uniaxial stress reaches the predefined compressive strength. The reduction factor of 0.70 seems reasonable if one compares the computed and observed failure loads (97.5^k vs. 90^k for P 311, 65^k vs. 67.5^k for P 221, and 95^k vs. 87.5^k in the case of P 321.) This can also be compared with the capacity reduction factor for columns according to ACI practice.

Plasticity of uncracked concrete (biaxial compression) did not occur in any of the beam panels analyzed. This was due to the fact that the cracks penetrated to the top of the web at relatively small loads, and only a portion of the upper rib at and around the load point was subject to biaxial compression. However, due to the relatively large thickness of the rib, the compression stresses were not critical. However, in cases where the thickness is constant, the model may indicate biaxial plasticity. But, as in the case of uniaxial plasticity, actual failure will probably occur due to limiting tensile strain, rather than a limiting compressive strain. Thus, in addition to economy in computational effort, neglecting biaxial plasticity of concrete may lead to a better representation of the actual behavior.

Although the program was prepared for the analysis of reinforced concrete members, the analysis capability can be extended to rock mechanics with minor modifications. The

finite element model can be used in the elastic analysis of isotropic materials. In order to extend the capability of the model to study reinforced concrete members under cyclic loads, additional modes (closing and re-opening of cracks, etc.) have to be included and stress-strain curves have to be specified with unloading paths and nonlinearities due to bond-slip and crack surface deterioration have to be introduced.

The conclusions that are drawn from this study can be summarized as follows:

1) Both for beams and beam panels, the crack directions and locations as well as the ultimate loads observed experimentally and obtained analytically are in good agreement.

2) Comparisons of the load-displacement diagrams in the case of beam panels indicated that the analytical displacements are smaller than those measured experimentally. The discrepancy was mainly due to the assumption of continuity in the finite element model.

3) Plasticity of cracked as well as uncracked concrete was included in the finite element model. Results indicate that, neglecting concrete plasticity will not only reduce the computational effort but may also lead to a better analytical representation.

4) Effect of the size of load increments on the solution is found to be negligible. Generally, with larger load increments, the displacements are larger.

5) With a finer mesh, a smoother crack pattern will be obtained and the analytical model will be more flexible.

6) The finite element model will be a valuable tool to the designer as it offers a complete picture of the stress distribution both in concrete and steel throughout the structure, at all load stages. Analysis of members for various reinforcement configurations, material properties and dimensions can be carried out rapidly with little effort. Although smaller load increments and a finer mesh are generally preferable, the analyst has to decide upon the trade-off between the accuracy and the economy of the solution.

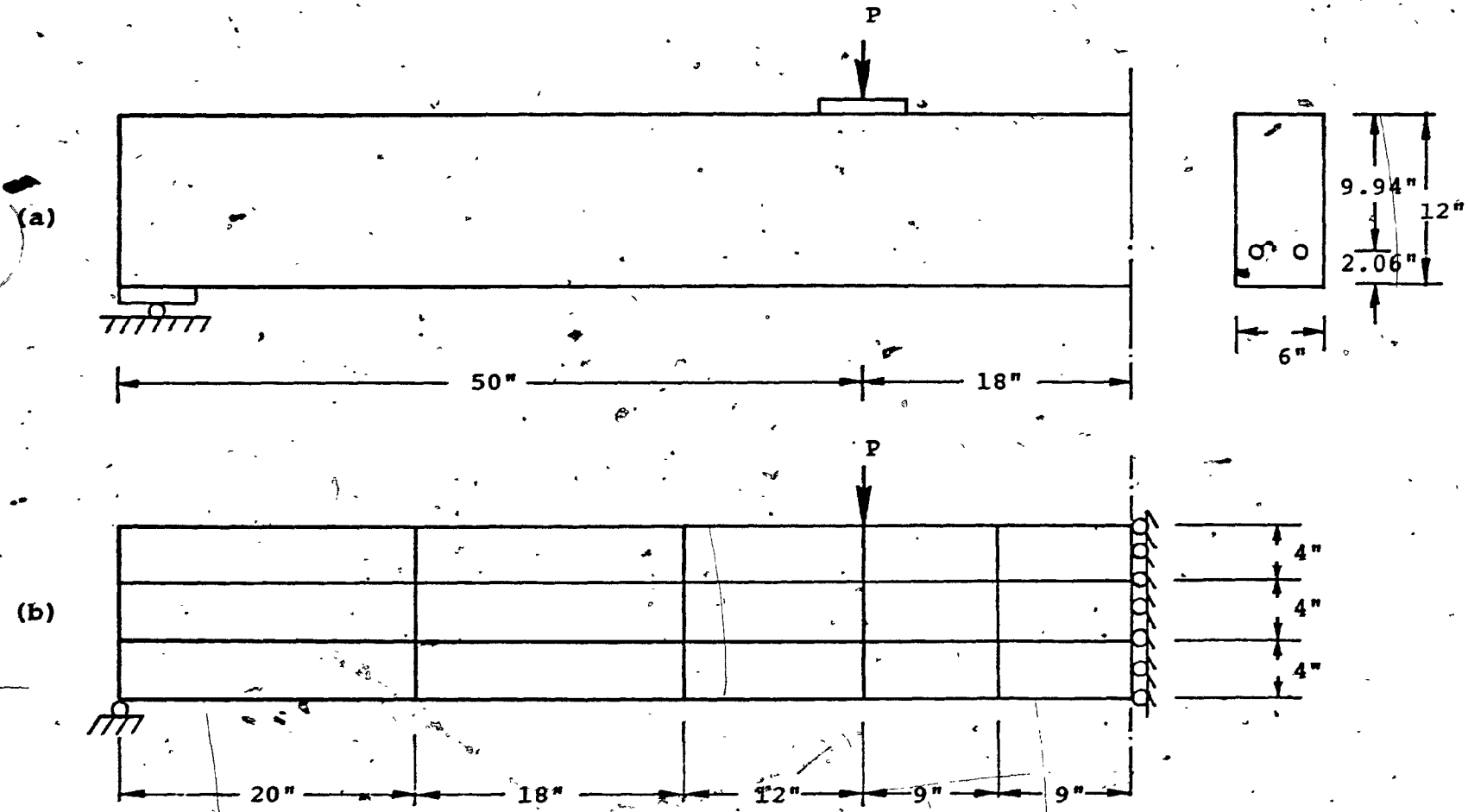

FIG. 4.1 BEAMS 2 AND 3 BY KRAHL ET AL [23]

(a) Beam Layout

(b) Finite Element Mesh

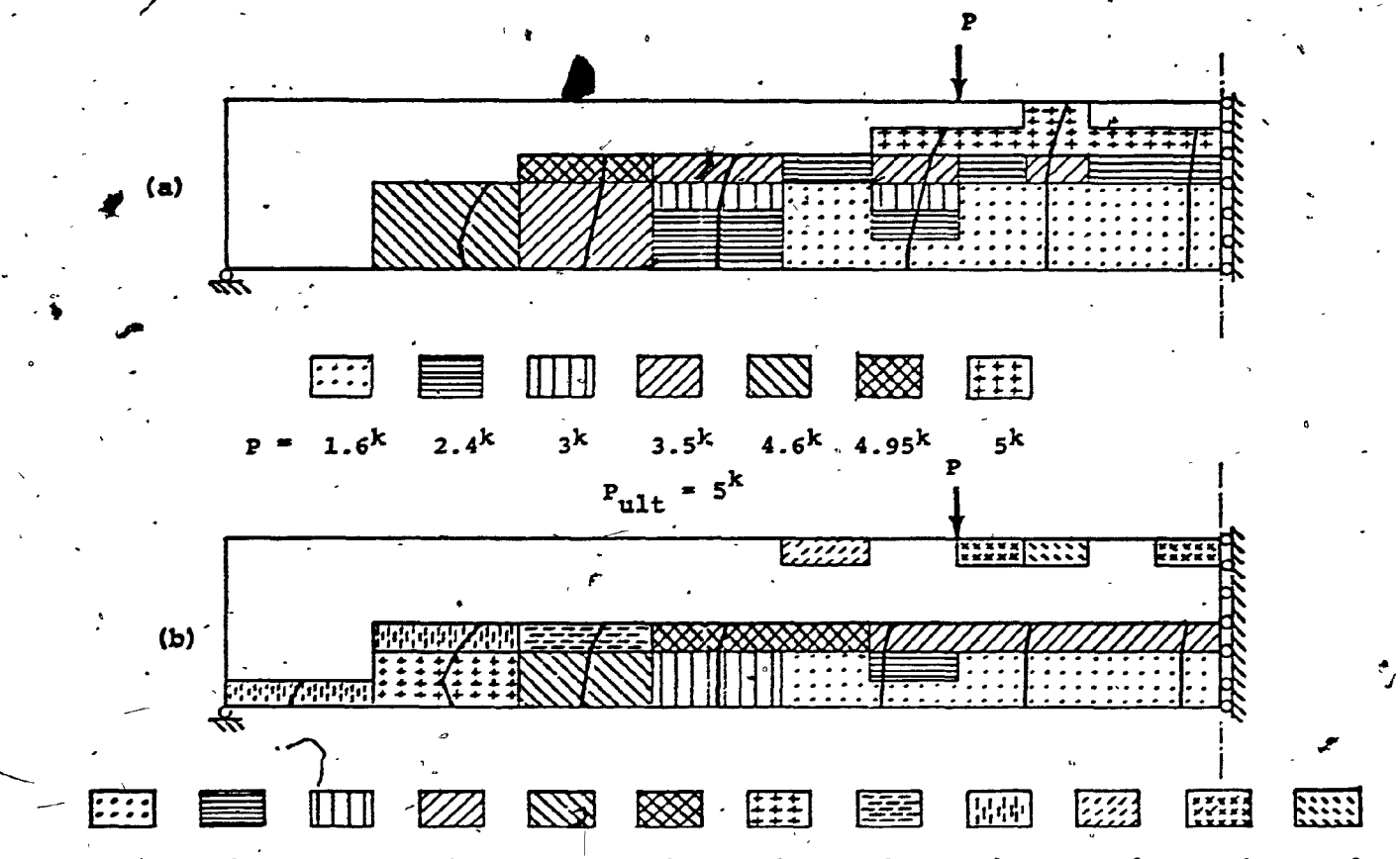

FIG.4.2 ANALYTICAL CRACK PATTERNS - (a) Beam 2
(b) Beam 3

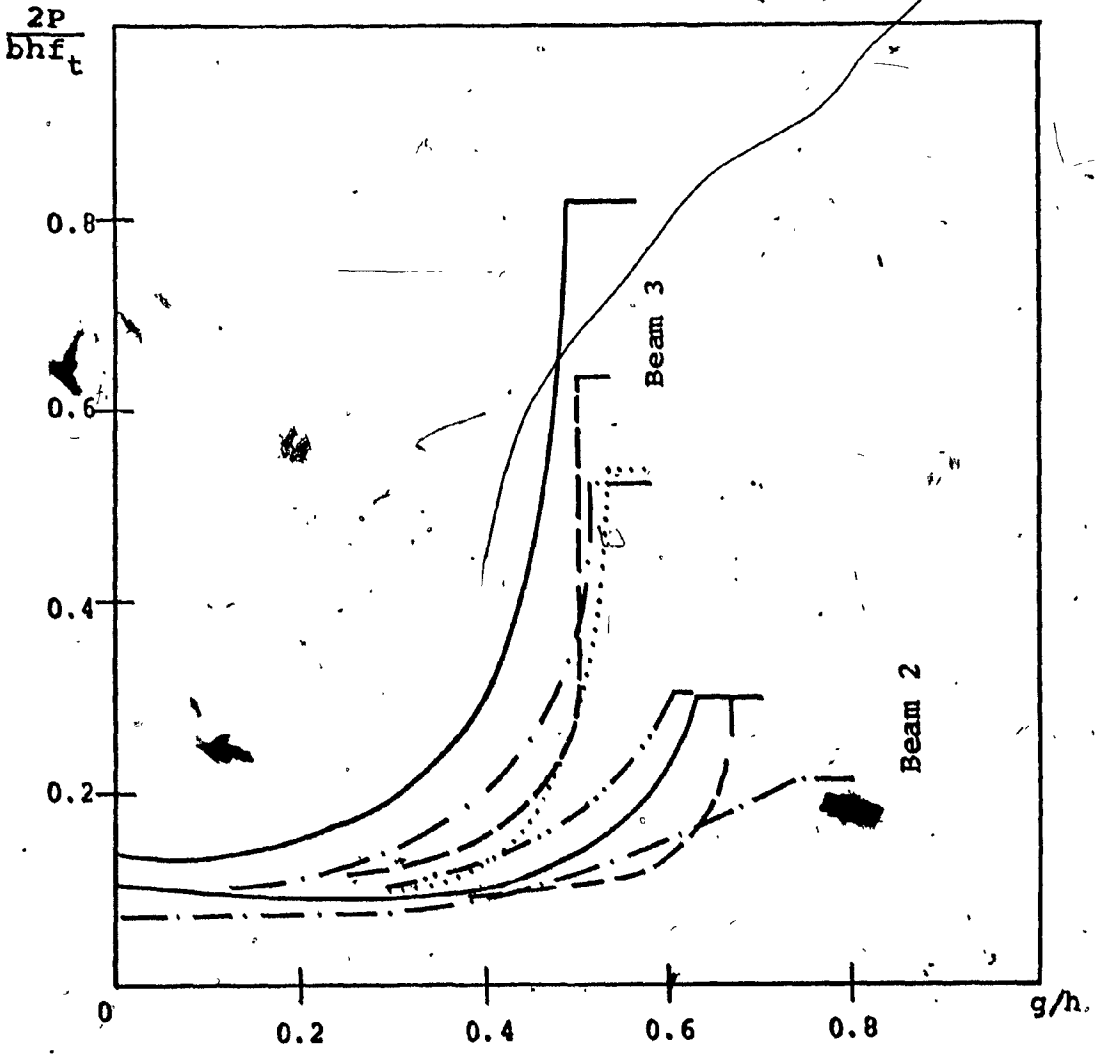

——— Krahl et al [23]

—.—.— Valliappan and Doolan [41]

..... Colville and Abbasi [9]

—..— Suidan and Schnobrich [40]

— — — Present study

FIG. 4.3 LOAD-CRACK DEPTH DIAGRAM - BEAMS 2 AND 3

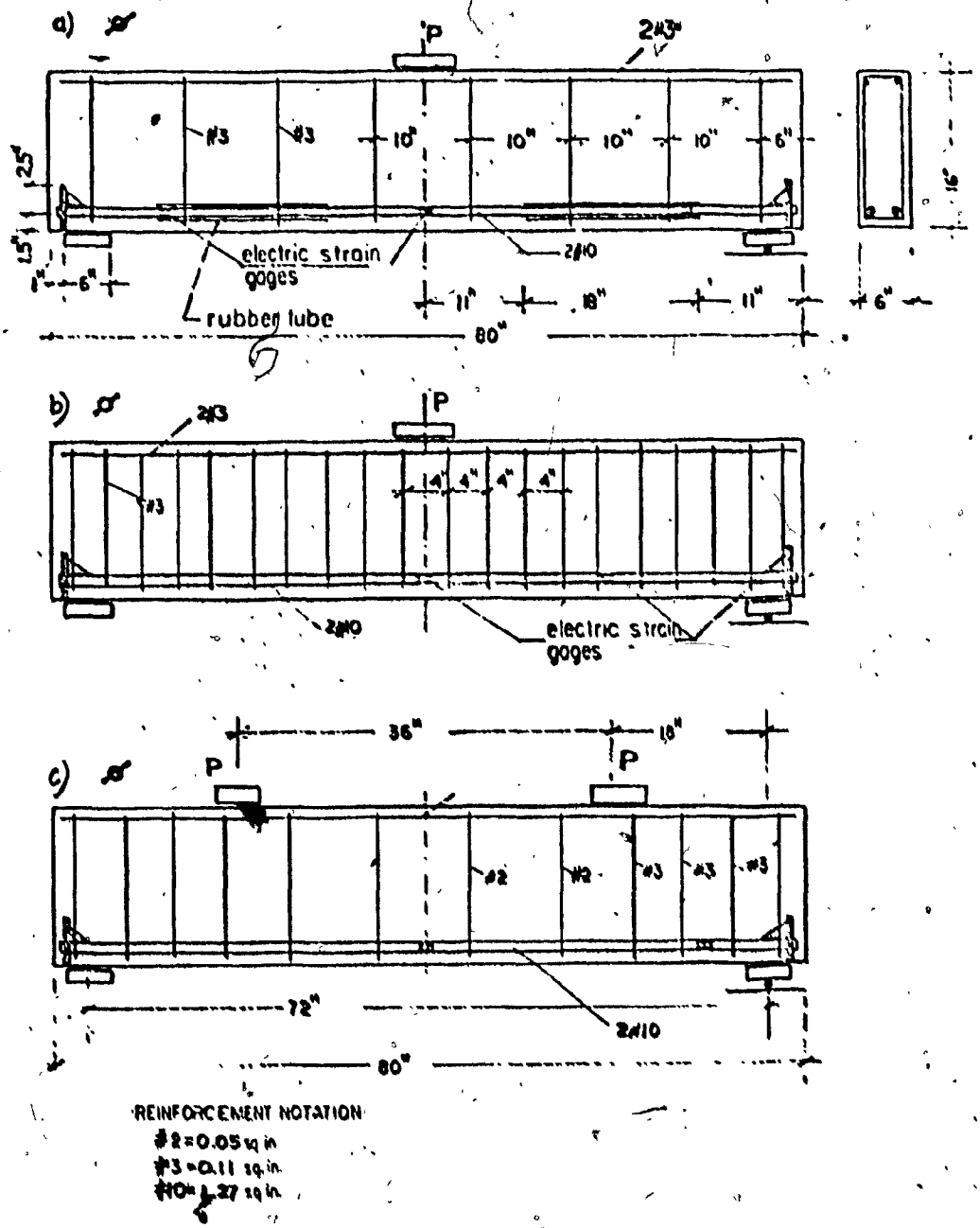

FIG. 4.4 BEAMS "a", "b" AND "c" BY ZIELINSKI

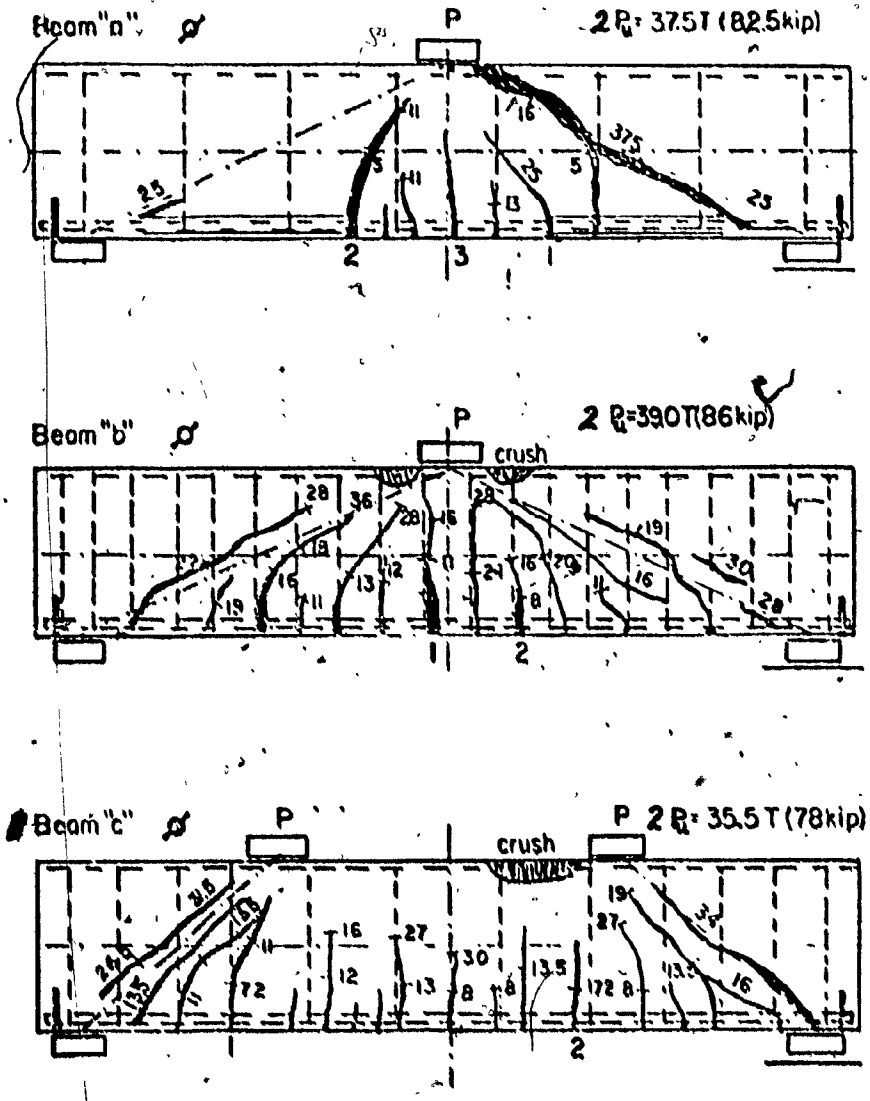

FIG. 4.5 EXPERIMENTAL CRACK PATTERNS - BEAMS "a", "b" AND "c"

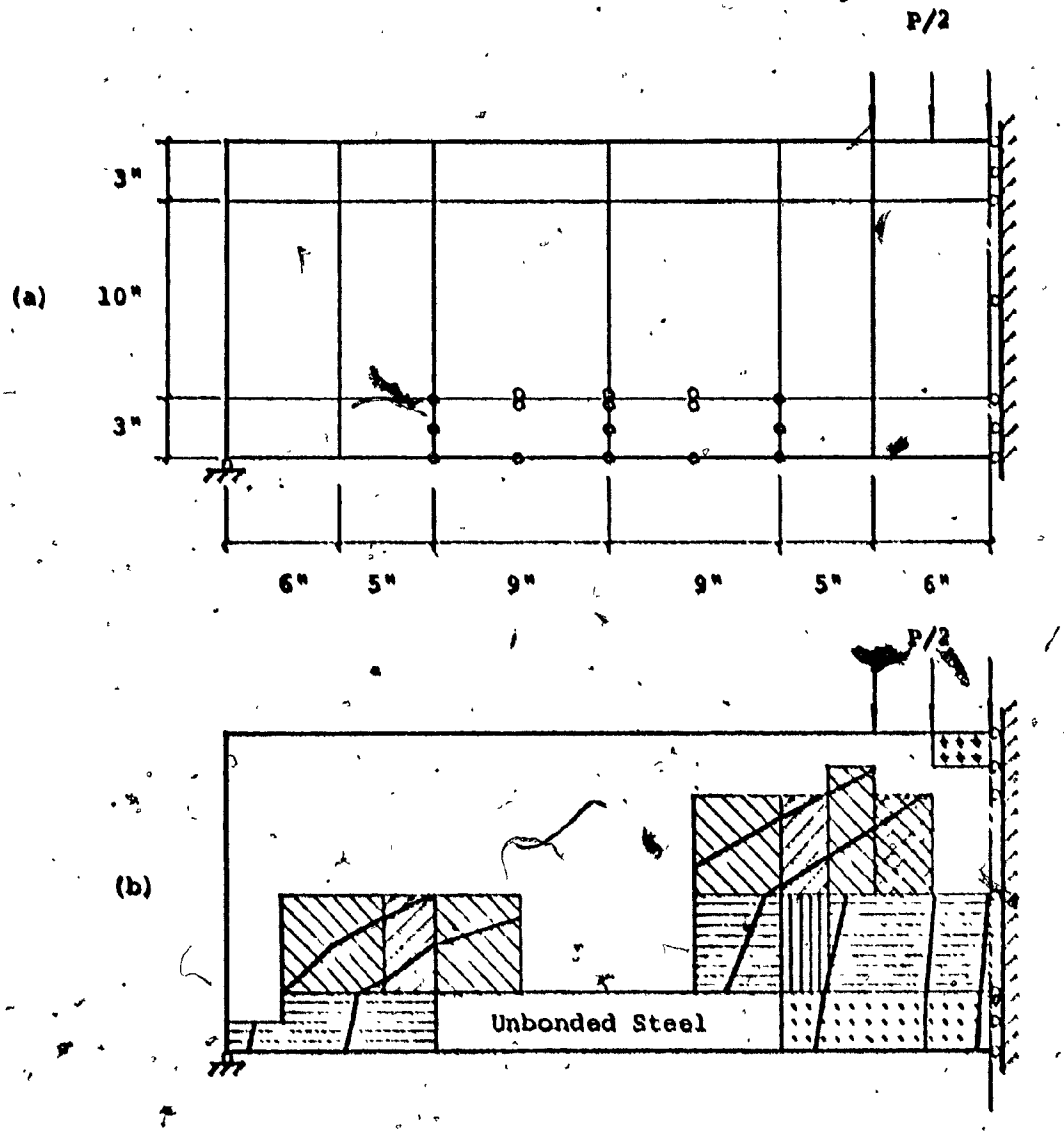

FIG. 4.6 BEAM "a" - (a) Finite Element Mesh

(b) Analytical Crack Pattern

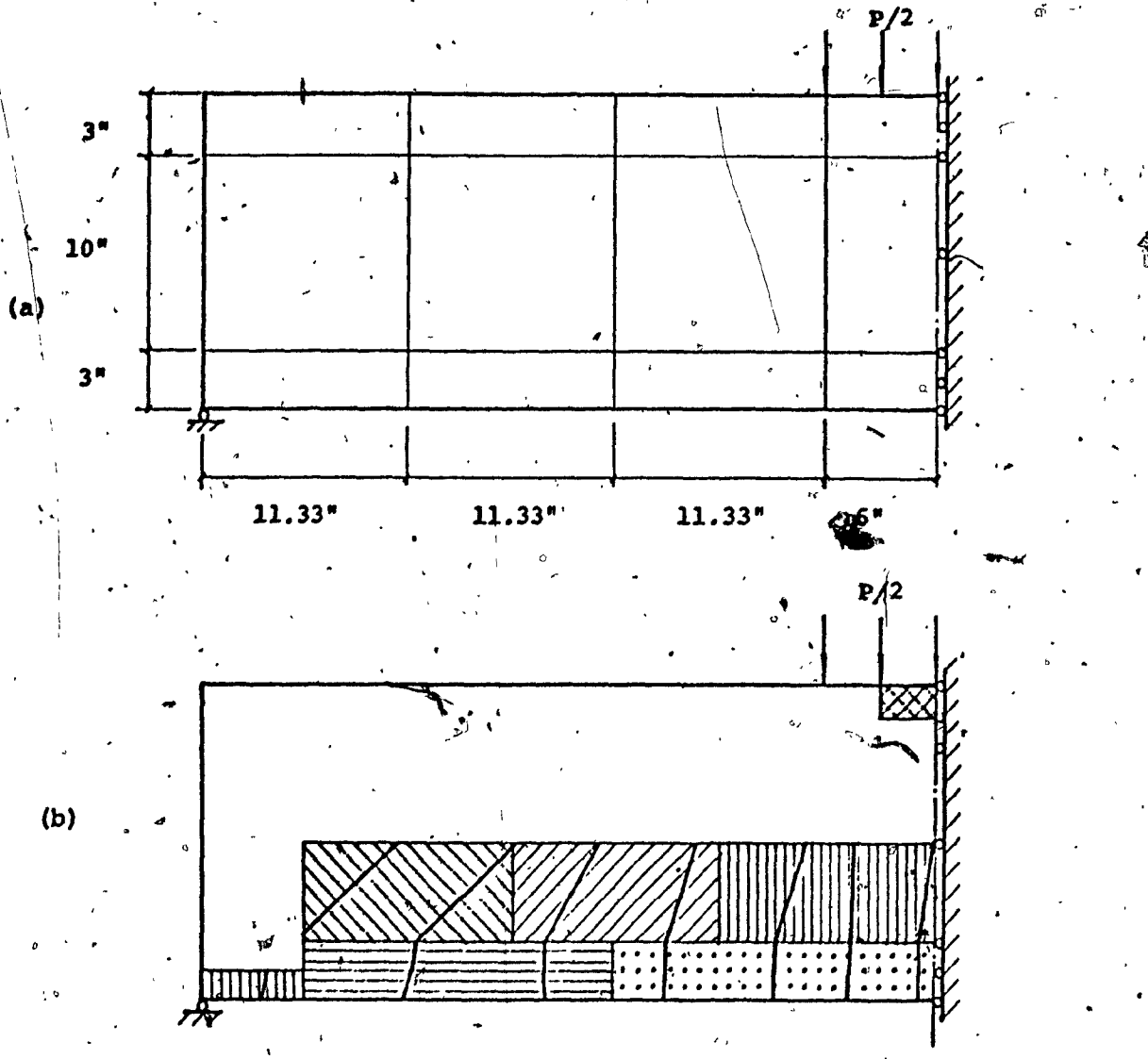

FIG. 4.7 BEAM "b" - (a) Finite Element Mesh
(b) Analytical Crack Pattern

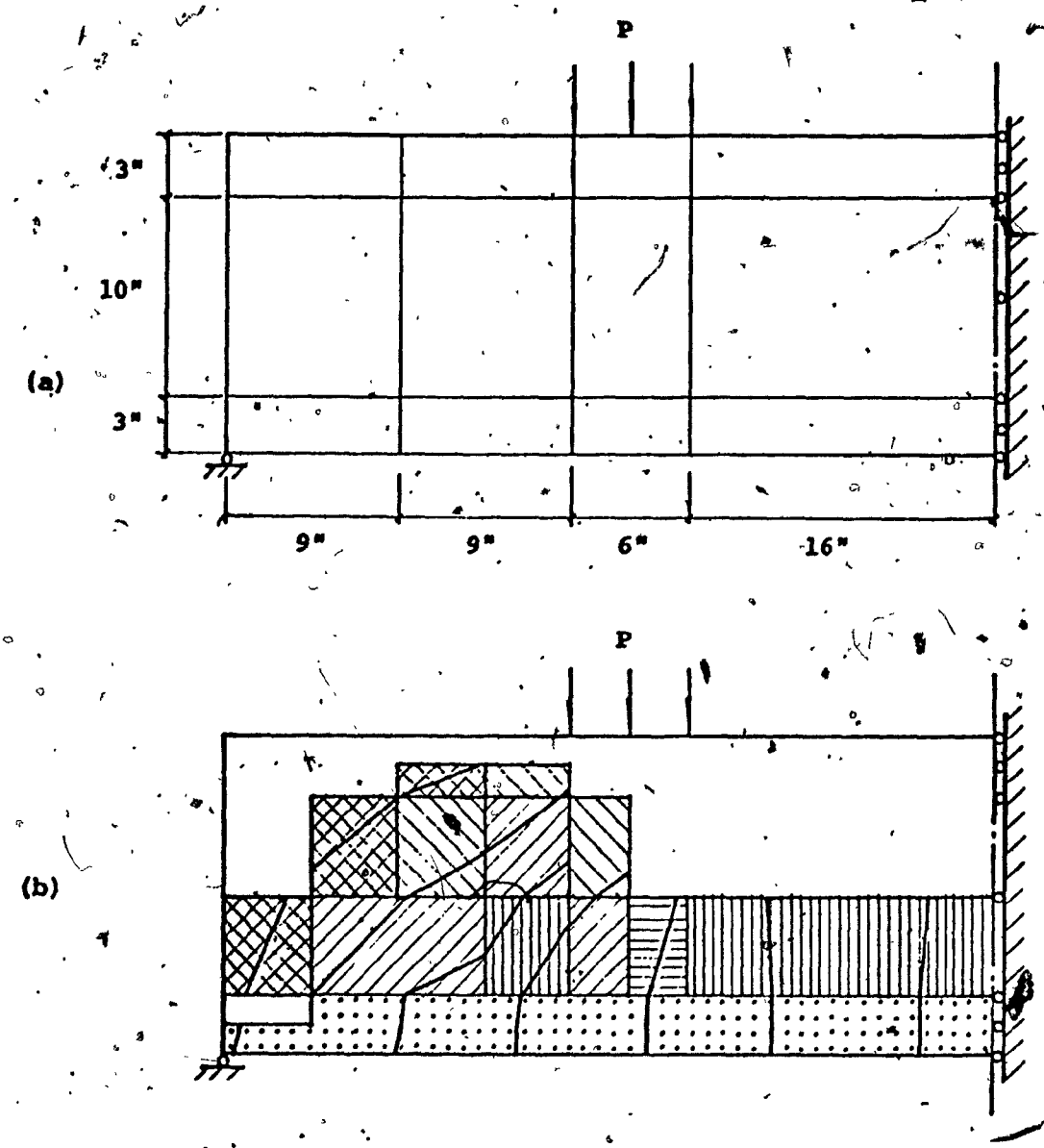

FIG.4.8 BEAM "c" - (a) Finite Element Mesh
(b) Analytical Crack Pattern

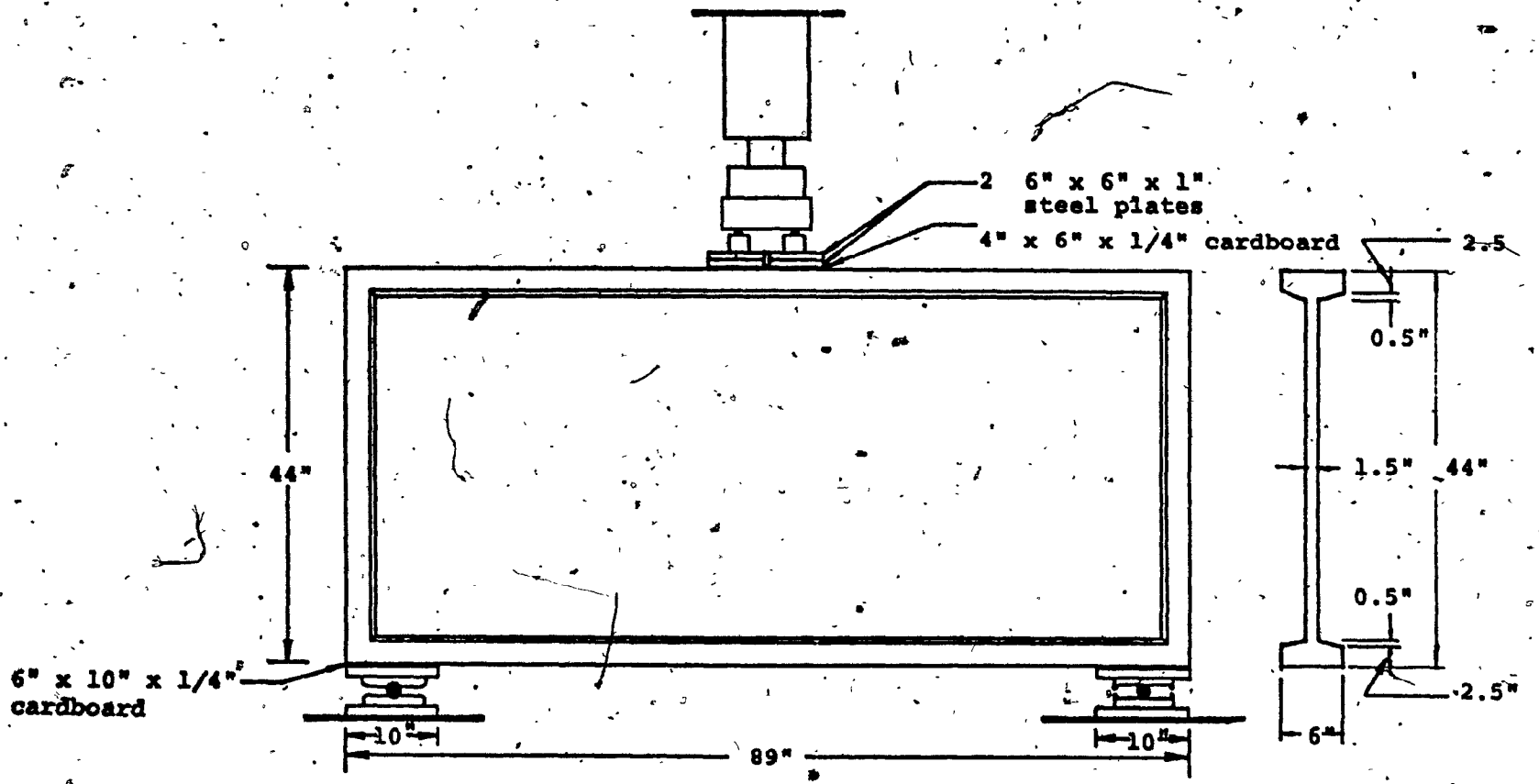

FIG. 4.9 TESTING ARRANGEMENT

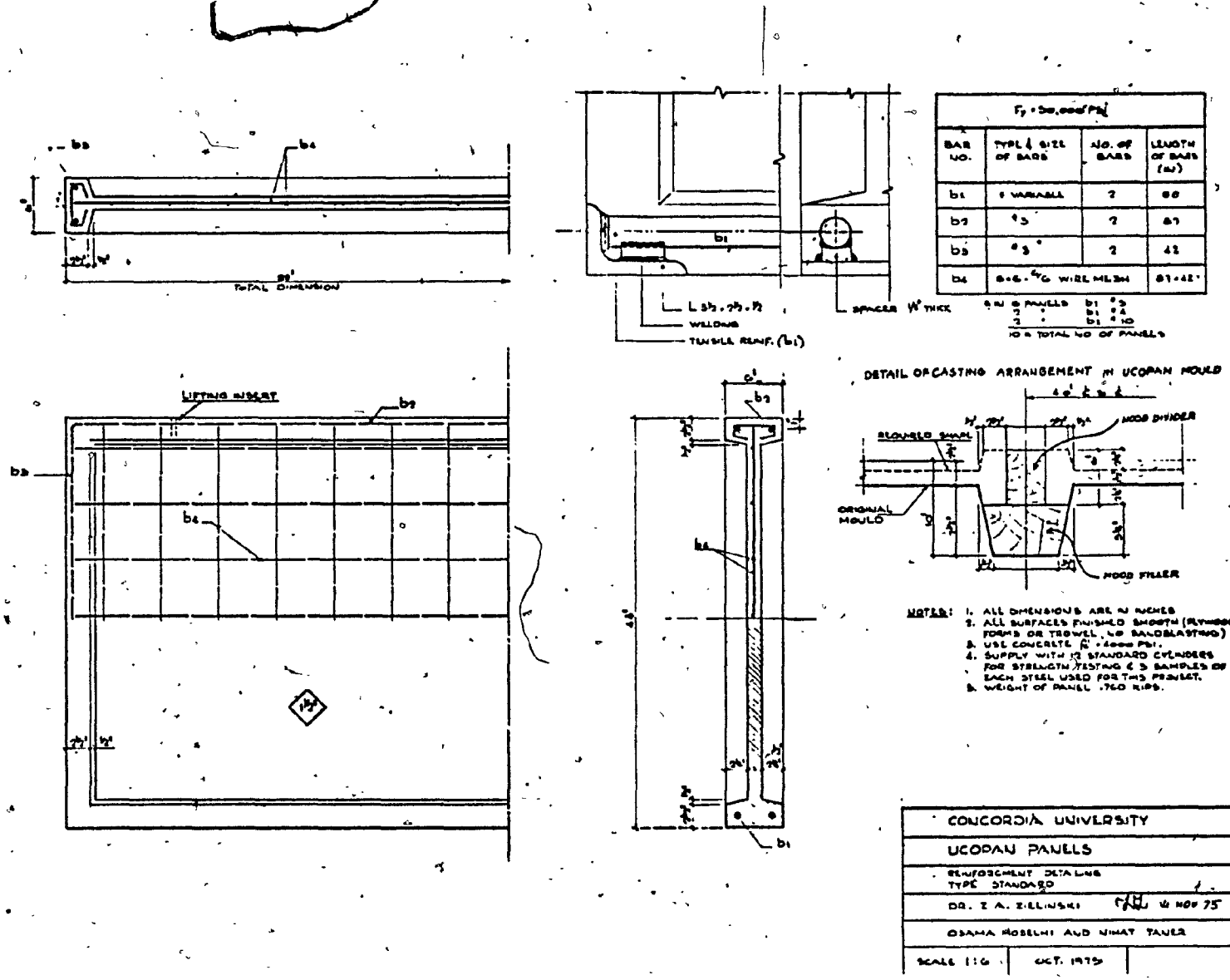

F_y = 300,000 PSI			
BAR NO.	TYPE & SIZE OF BARS	NO. OF BARS	LENGTH OF BARS (in)
b1	# VARIABLE	2	88
b2	#5	2	83
b3	#3	2	41
b4	6×6 - 4/6 WIRE MESH		81×42

# IN 8 PANELS	
2	b1 #5
2	b1 #4
2	b1 #10

10 = TOTAL NO OF PANELS

NOTES:
1. ALL DIMENSIONS ARE IN INCHES
2. ALL SURFACES FINISHED SMOOTH (PLYWOOD FORMS OR TROWEL, NO SANDBLASTING)
3. USE CONCRETE f'_c = 4000 PSI.
4. SUPPLY WITH 10 STANDARD CYLINDERS FOR STRENGTH TESTING & 3 SAMPLES OF EACH STEEL USED FOR THIS PROJECT.
5. WEIGHT OF PANEL = 760 KIPS.

CONCORDIA UNIVERSITY	
UCOPAN PANELS	
REINFORCEMENT DETAILING TYPE STANDARD	
DR. Z. A. ZIELINSKI	W NOV 75
OSAMA MOSELHI AND NIMAT TANUS	
SCALE 1:6	OCT. 1975

FIG. 4.10 TYPICAL PANEL

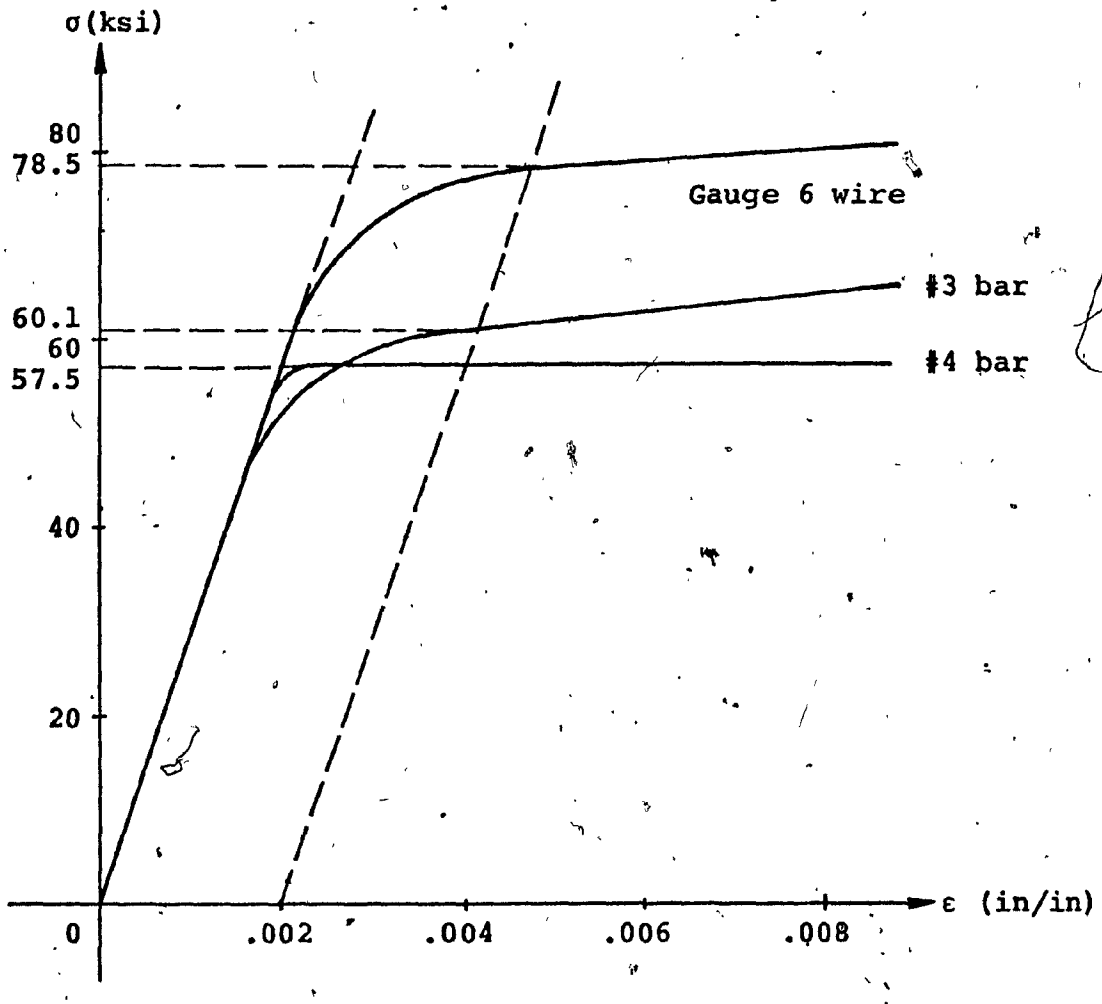

FIG. 4.11 REINFORCEMENT STRESS-STRAIN RELATIONSHIP

CHAPTER 5

ANALYSIS OF BEAM PANELS USING SIMPLIFIED FORMULAE DEVELOPED FOR DEEP BEAMS

CHAPTER 5

ANALYSIS OF BEAM PANELS USING SIMPLIFIED FORMULAE DEVELOPED FOR DEEP BEAMS

5.1 INTRODUCTION

Behaviour of a reinforced concrete beam through different stages of loading can be described by the changes in the stress distribution and the consequent variation in the crack patterns. During the initial stage of loading concrete is uncracked and the beam can be analyzed on the basis of elastic theory. The first flexural crack occurs when the tensile stress at the extreme fibre reaches the uniaxial tensile strength f_t. This crack propagates to the compression zone until the flexural reinforcement develops the tension force necessary to balance the external moment. In the case of very little flexural reinforcement, flexural cracking may lead to the failure of the beam.

Normal and shear stresses develop as a result of the combined action of bending moment and shear force. In terms of principal stresses, this corresponds to a state of biaxial tension-compression as a result of which inclined shear-flexure cracks appear. In the case of insufficient web reinforcement, inclined cracking can be a limit on the usable capacity of the structure. It should be noted that inclined shear cracks develop as a result of bond. Thus, in unbonded beams such cracks are not expected, and these beams work as a tied arch following the first flexural crack.

If there is sufficient reinforcement to take over

flexural and inclined cracking, the reinforced concrete member may work until it reaches the ultimate flexural strength either by yielding of the tensile steel or by crushing of the concrete (generally where the deepest flexural crack is located, i.e., where the depth of the compression zone is minimum.) Formulae to determine the depth of the compression zone and the ultimate moment using an equivalent rectangular stress block for concrete are well known and used in practice.

The work stages described above, namely

(i) elastic behavior in uncracked state
(ii) appearance of the first flexural crack
(iii) inclined cracking due to bond
(iv) ultimate flexural strength

are adequate to describe the behavior of ordinary beams. In deep beams and beam panels, however, after the appearance of inclined cracks, the applied load is transmitted to the supports by direct compression (as in the case of a tied arch), provided that the tensile reinforcement is carried to and anchored beyond the support. Biaxial tension-compression stresses exist along the diagonals connecting the support and load points, and failure may occur by splitting or crushing of concrete along these diagonals. Failure due to diagonal crushing did not receive much attention since it occurred in relatively few cases as compared to diagonal splitting. In the following sections relevant formulae used to define strength of deep beams are summarized, and their applicability

to beam panels is investigated using the results of Concordia tests.

5.2 SUMMARY OF SIMPLIFIED FORMULAE

Based on the analogy between the diagonal splitting of deep beams and the indirect tensile (Brazilian) test of concrete cylinders, Brock (4) used the following relationship to express ultimate shear force V_s at diagonal splitting (see Fig. 5.1).

$$f_{ti} = \frac{2P}{\pi DL} = \frac{2(V_s/\sin\alpha)}{\pi(h/\sin\alpha)b} = \frac{2V_s}{\pi hb} \qquad (5.1a)$$

$$V_s = V_{ult} = \frac{\pi}{2} f_{ti} hb = K f_{ti} hb \qquad (5.1b)$$

It should be noted that the splitting strength varies with shape and size of samples. For example, in the case of cubes loaded diagonally, instead of $K \simeq 1.57$, 1.36 must be used to express the splitting force. It is also known that, the value of splitting stress obtained from larger samples is lower than that obtained from smaller samples. Taking into consideration experimental results, Ramakrishnan and Ananthanarayana [36] suggested that $K = 1.12$ will be a reasonable lower bound value for beams which fail by the diagonal tension mode..

Kong et al (22) developed the following empirical formula to define the ultimate strength in shear of deep beams (see Fig. 5.2).

$$V_{ult} = C_1\left(1 - 0.35\,\frac{x}{h}\right) f_{ti}\, hb + C_2\, \Sigma A_s\, \frac{y}{h} \sin^2\alpha \quad (5.2)$$

where

C_1 = an empirical coefficient equal to 1.4 for normal concrete, and 1.0 for lightweight concrete

x = horizontal distance from the inside edge of support to the outside edge of the load plate (clear shear span)

C_2 = an empirical coefficient equal to 18,900 psi for plain round bars, and 43,500 psi for deformed bars

A_s = area of individual web bar (main longitudinal tensile bars are considered as web bars)

y = depth measured from the top of the beam at which an individual bar intersects the line joining the inside edge of the support to the outside edge of the load plate

α = acute angle between the bar being considered and the line described in the definition of y, above

The applicability of the formula is limited to cases where the x/h ratio does not depart from the experimental range of 0.23 to 0.70, and where the main longitudinal reinforcement is anchored at the ends.

According to Zielinski (46,47), occurrence of diagonal splitting cracks does not terminate the work of a flexural member, provided that there is sufficient web reinforcement to take over the splitting force. For practical purposes, the actual curvilinear variation of the biaxial stresses between the support and load point is replaced by a simplified rectangular stress block. This assumption is comparable to the simplification of the flexural compression zone in reinforced concrete beams according to the ultimate strength method. As shown in Fig. 5.3, the biaxial stress condition depends on the geometry of the support segment and can be defined as

$$f_{ct} = \frac{S}{hb}\cos\alpha = \frac{H}{hb} \qquad (5.3a)$$

$$f_{tc} = \frac{S}{ab}\sin\alpha = \frac{V}{ab} \qquad (5.3b)$$

$$\frac{f_{ct}}{f_{tc}} = \frac{Ha}{Vh} = \frac{a^2}{h^2} \qquad (5.3c)$$

where

a = shear span (measured from center of support to center of load area)

α = arctan $(\frac{h}{a})$

and f_{ct}, and f_{tc} represent compression and tension stresses, respectively, in concrete subject to biaxial tension-compression. Using Suwalski-Zalewski criterion, the limiting value of f_{tc} at

which diagonal splitting will occur, is given as

$$f_{tc} = \frac{f'_c}{\frac{f'_c}{f_t} + \frac{a^2}{h^2}} \qquad (5.4)$$

Note that a and h should be interchanged if $a/h < 1$. The corresponding load can be expressed as

$$V_s = f_{tc}\, ab = \frac{f'_c}{\frac{f'_c}{f_t} + \frac{a^2}{h^2}}\, ab \qquad (5.5a)$$

The presence of web reinforcement will increase the splitting force slightly

$$V_s = f_{tc}\, ab + f_s\, \Sigma A_s \cos\theta \qquad (5.5b)$$

where

f_s = stress in steel at cracking

$= E_s \varepsilon_t \approx 29 \times 10^6 \times (.0001 \text{ to } .0002) \approx 3000 - 6000$ psi

A_s = area of individual web bar located along the diagonal (main flexural tensile steel is included)

θ = angle between the web bar and the principal tension direction

The shear load can be expressed in terms of f_{ct} as

$$V = \frac{h^2 b}{a} f_{ct} = \left(\frac{h^2 b}{a}\right) \frac{f_t}{\frac{f_t}{f_c} + \frac{h^2}{a^2}} \qquad (5.6a)$$

if there is no web reinforcement, and as

$$V = f_{ct} \left(\frac{h^2 b}{a} + \frac{E_s}{E_c} \Sigma A_s \sin\theta\right) \qquad (5.6b)$$

if there is web reinforcement.

Note that, contrary to Brock; and Ramakrishnan and Ananthanarayana, the effects of both the shear span and the web reinforcement are included. Diagonal splitting is accompanied by a sudden increase in the steel stress because from the moment of splitting, the total tension force must be carried by the web reinforcement. In the case of insufficient amount of web reinforcement, this will be the limit strength for the deep beam. However, if the reinforcement can take over the splitting force, the member will be able to work further, until the reinforcement yields or concrete fails in diagonal compression. The ultimate load defined by yielding of the steel is expressed as

$$V_{ult} = \Sigma A_s f_y \cos\theta \qquad (5.7a)$$

The recommended upper bound value for f_y is 44,000 psi.

Diagonal compression failure has to be checked on the basis of bearing area

$$\sigma_{comp} = \frac{V/\sin\alpha}{B/\sin\alpha} = \frac{V}{B}$$

thus

$$V_{ult} = B f_c' \qquad (5.7b)$$

where B = bearing area

5.3 APPLICATION OF SIMPLIFIED FORMULAE TO THE ANALYSIS OF BEAM PANELS

5.3.1 Splitting Analogy

Cylindrical samples tested in splitting are subject to biaxial tension-compression stresses. Along the longitudinal axis, these stresses are

$$f_{tc} = \frac{2P}{\pi DL} \tag{5.8a}$$

and

$$f_{ct} = \frac{-6P}{\pi DL} = -3f_{tc} \tag{5.8b}$$

According to Suwalski-Zalewski criterion, splitting will occur when

$$f_{tc} = \frac{f_t}{1 + \frac{3f_t}{f_c'}} = f_{ti} \tag{5.9}$$

For example, if $f_t \approx 0.1\, f_c'$, the splitting strength would be

$$f_{ti} \approx .77\, f_t$$

The computed splitting stresses and corresponding loads for the beam panels are given in Table 5.1.

5.3.2 Empirical Approach by Kong et al

According to Kong et al, the ultimate load will be expressed as

$$V_{ult} = 1.4(1 - .35 \frac{x}{h}) f_{ti}\, hb + 43.5 \Sigma A_s \frac{y}{h} \sin^2\alpha$$

For beam panels loaded at midspan

$$\frac{x}{h} = .65$$

and

$1.4(1 - .35 \frac{x}{h}) f_{ti}\, hb = 1.08\, f_{ti}\, hb$ (compare with Eq.(5.1b))

For beam panels under third point loading

$$\frac{x}{h} = .35$$

and

$1.4(1 - .35 \frac{x}{h}) f_{ti}\, hb = 1.23\, f_{ti}\, hb$

The computed ultimate loads are presented in Table 5.2.

5.3.3 Zielinski's Approach

For beam panels loaded at midspan

$a = 36.5"$

$h = 44"$

$a/h = .83 < 1$

Therefore, a and h must be interchanged.

a = 44" h = 36.5" a/h = 1.21

For beam panels under third point loading

(i) in the shorter segment

a = 44" h = 23.3" a/h = 1.89

(ii) in the longer segment

a = 49.7" h = 44" a/h = 1.13

Assuming that strain at cracking = .0001 in/in

$f_s \approx$ 3ksi.

The loads at which diagonal splitting cracks will occur are presented in Table 5.3. Note that the main tensile bars are included as web bars.

The ultimate loads defined by yielding of reinforcement and crushing of concrete, are given in Tables 5.4 and 5.5, respectively. Comparison of the observed and computed ultimate loads are presented in Table 5.6.

Formulae based on cylinder splitting analogy underestimated the ultimate capacity seriously for over-reinforced and/or asymmetrically loaded beam panels. Formulae by Kong et al, and Zielinski, based on the assumption of reinforcement yielding at ultimate state led to erroneous results (overestimation by approximately 100%) for over-reinforced panels.

For under-reinforced beam panels, Zielinski's formula on diagonal splitting gave very good results (P_4/P_0 = 1.00, .91, .95 and .93, for P 111, P 211, P 121 and P 221, respectively). This formula is practical and simple to use and will be helpful to the designer for routine and approximate checks.

For over-reinforced beam panels, diagonal compression failure may govern and bearing strength must be checked. Results indicate that, instead of uniaxial compression strength f_c', a reduced value (.6 to .7 f_c') should be used for bearing strength.

TABLE 5.1 - ULTIMATE LOAD (P_{ult}) ACCORDING TO SPLITTING ANALOGY

Panel	f'_c (ksi)	f_t (ksi)	f_{ti} (ksi)	P_{ult} [4] (kips)	P_{ult} [36] (kips)
P 111	5.482	.399	.327	67.8	48.4
P 211	5.648	.407	.335	69.4	49.6
P 311	5.277	.389	.319	66.2	47.2
P 121	5.482	.399	.327	50.9	36.3
P 221	5.648	.407	.335	52.1	37.2
P 321	5.277	.389	.319	49.7	35.4

TABLE 5.2 - ULTIMATE LOAD (P_{ult}) ACCORDING TO KONG ET AL

		$43.5 \Sigma A_s \frac{y}{h} \sin^2 \alpha$			
Panel	Kf_{ti} hb	Longitudinal bars	Horizontal wires	Vertical wires	P_{ult} (kips)
P 111	23.3	6.5	3.1	.8	67.4
P 211	23.9	11.8	3.1	.8	79.2
P 311	22.7	74.7	3.1	.8	202.6
P 121	26.5	8.3	3.9	.1	58.2
P 221	27.2	15.0	3.9	.1	69.3
P 321	25.9	95.0	3.9	.1	187.4

TABLE 5.3 - SPLITTING LOAD (P_s) ACCORDING TO ZIELINSKI

			$3 \Sigma A_s \cos\theta$			
Panel	f_{tc}	$f_{tc}ab$	Longitudinal bars	Horizontal wires	Vertical wires	P_s (kips)
P 111	.361	28.7	.5	.5	.3	60
P 211	.368	29.3	.9	.5	.3	62
P 311	.351	27.9	5.9	.5	.3	69.2
P 121_s	.317	39.5	.6	.5	.1	61.1
P 121_ℓ	.365	27.2	.4	.4	.5	85.5
P 221_s	.324	40.3	1.1	.5	.1	63
P 221_ℓ	.373	27.8	.8	.4	.5	88.5
P 321_s	.308	38.3	6.7	.5	.1	68.4
P 321_ℓ	.356	26.5	5.1	.4	.5	97.5

TABLE 5.4 - ULTIMATE LOAD (P_{ult}) DEFINED BY YIELDING OF REINFORCEMENT (f_y = 44 ksi for all steel)

	$44 \Sigma A_s \cos\theta$			
Panel	Longitudinal bars	Horizontal wires	Vertical wires	P_{ult} (kips)
P 111	7.5	6.9	4.9	38.6
P 211	13.5	6.9	4.9	50.6
P 311	86.0	6.9	4.9	195.6
P 121_s	8.6	7.9	1.8	27.5
P 121_ℓ	6.4	5.9	7.6	59.7
P 221_s	15.5	7.9	1.8	37.8
P 221_ℓ	11.7	5.9	7.6	75.6
P 321_s	98.7	7.9	1.8	162.6
P 321_ℓ	74.1	5.9	7.6	262.8

TABLE 5.5 - ULTIMATE LOAD (P_{ult}) DEFINED BY CRUSHING OF CONCRETE

Bearing area = 1.5 x (12 + 3 + 3) = 27 in^2		
Panel	f'_c (ksi)	P_{ult} (kips)
P 111	5.482	148.0
P 211	5.648	152.5
P 311	5.277	142.5
P 121	5.482	148.0
P 221	5.648	152.5
P 321	5.277	142.5

TABLE 5.6 - COMPARISON OF OBSERVED vs. COMPUTED ULTIMATE LOADS

Panel	P_0	P_1	P_1/P_0	P_2	P_2/P_0	P_3	P_3/P_0	P_4	P_4/P_0	P_5	P_5/P_0	P_6	P_6/P_0	P_7	P_7/P_0
P 111	60	67.8	1.13	48.4	.81	67.4	1.12	60	1.00	38.6	.64	148.0	2.47	57.5	.96
P 211	68.5	69.4	1.01	49.6	.72	79.2	1.16	62	.91	50.6	.74	152.5	2.23	77.5	1.13
P 311	90	66.2	.74	47.2	.52	202.6	2.25	69.2	.77	195.6	2.17	142.5	1.58	97.5	1.08
P 121	64	50.9	.80	36.3	.57	58.2	.91	61.1	.95	27.5	.43	148.0	2.31	60	.94
P 221	67.5	52.1	.77	37.2	.55	69.3	1.03	63	.93	37.8	.56	152.5	2.26	65	.96
P 321	87.5	49.7	.57	35.4	.40	187.4	2.14	68.4	.78	162.6	1.86	142.5	1.63	95	1.09

P_0 = Observed
P_1 = Table 5.1 K = 1.57
P_2 = Table 5.1 K = 1.12
P_3 = Table 5.2
P_4 = Table 5.3
P_5 = Table 5.4
P_6 = Table 5.5
P_7 = Finite Element Analysis

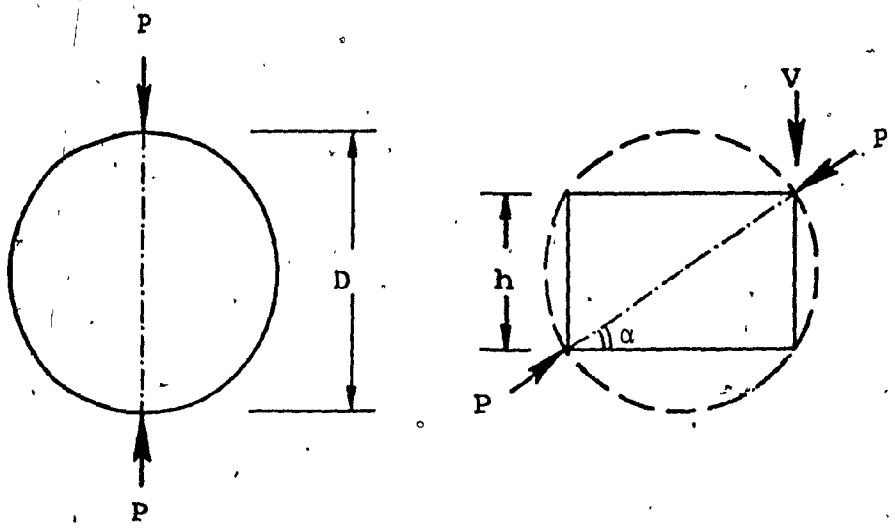

FIG. 5.1 SPLITTING ANALOGY FOR DEEP BEAMS

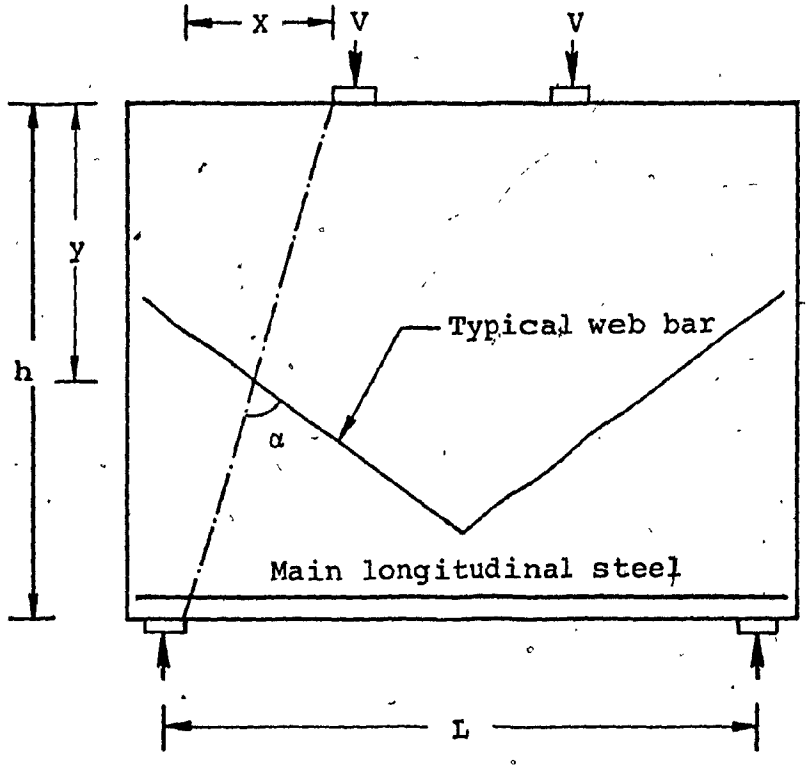

FIG. 5.2 DESCRIPTION OF VARIABLES USED IN THE EMPIRICAL FORMULA BY KONG ET AL

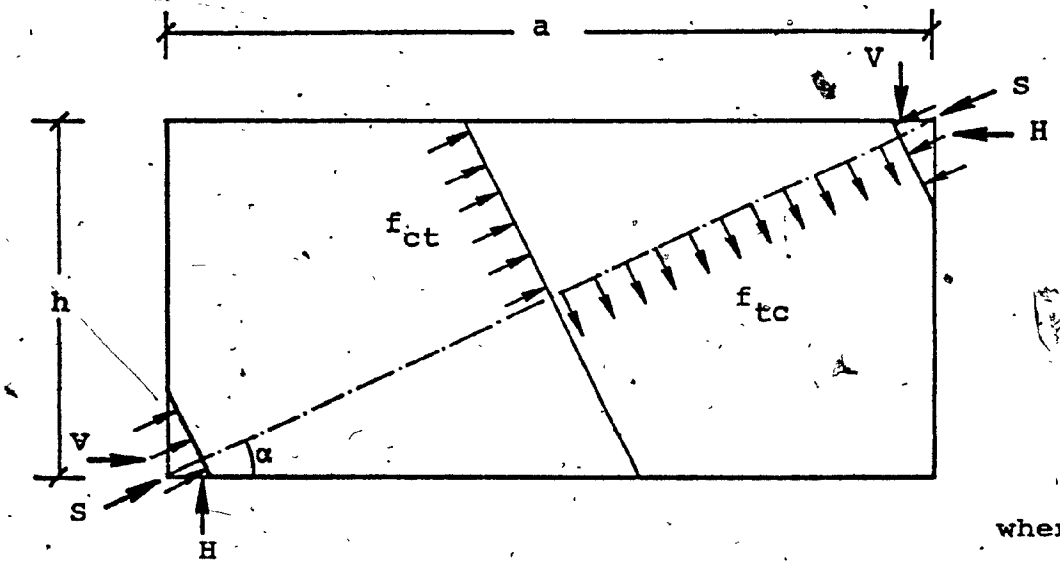

$$\alpha = \arctan\left(\frac{h}{a}\right)$$

$$V = S \sin\alpha$$

$$H = S \cos\alpha$$

$$f_{ct} = \frac{H}{hb}$$

$$f_{tc} = \frac{V}{ab}$$

where b = width of member

FIG. 5.3 ASSUMED STRESS DISTRIBUTION UNDER DIAGONAL COMPRESSION ACCORDING TO ZIELINSKI

REFERENCES

REFERENCES

[1] Abdulezer, A., "Ultimate Strength in Diagonal Splitting of Reinforced Concrete Thin Wall Ribbed Panels", M.Eng. Thesis, Department of Civil Engineering, Sir George Williams University, Montreal, Canada, (1974).

[2] ACI Committee 318, Building Code Requirements for Reinforced Concrete (ACI-318-71), American Concrete Institute, Detroit, (1972).

[3] Beskos, D.E., "Fracture of Plain Concrete Under Biaxial Stresses", Cement and Concrete Research, Vol. 4, No. 6, (1974), pp.979-985.

[4] Brock, G., Discussion of "The Riddle of Shear Failure and Its Solution", by N.J.Kani, ACI Journal Proceedings, Vol. 61, No. 12, (December 1964), pp.1587-1590.

[5] Browning, J.S., "A Study of the Strength of Mortar Cubes in Biaxial Tension and Compression", M.S.Thesis, Department of Civil Engineering, North Carolina State University, Raleigh, (1966).

[6] Cervenka, V., "Inelastic Finite Element Analysis of Reinforced Concrete Panels Under In-Plane Loads", Ph.D. Thesis, Department of Civil Engineering, University of Colorado, Boulder, (1970).

[7] Chen, A.C. and Chen, W., "Constitutive Relations for Concrete", Journal of the Engineering Mechanics Division, ASCE, Vol.101, No. EM4, (August 1975), pp.465-481.

[8] Cohn, M.Z., ed., Inelasticity and Non-Linearity in Structural Concrete, Solid Mechanics Division, University of Waterloo, Study No. 8, (1973).

[9] Colville, J., and Abbasi, J., "Plane Stress Reinforced Concrete Finite Elements", Journal of the Structural Division, ASCE, Vol. 100, No. ST5, (May 1974), pp.1067-1083.

[10] Cook, R.D., "Improved Two-Dimensional Finite Element", Journal of the Structural Division, ASCE, Vol. 100, No.ST9, (September 1974), pp.1851-1863.

[11] Cook, R.D., "Avoidance of Parasitic Shear in Plane Element", Journal of the Structural Division, ASCE, Vol. 101, No.ST6, (June 1975), pp.1239-1253.

[12] Desai, C.S., and Abel, J.F., Introduction to the Finite Element Method, Van Nostrand Reinhold Co. New York, (1972).

[13] Egeland, O., "Application of Finite Element Techniques to Plasticity Problems", Finite Element Methods in Stress Analysis, ed. Holand, I. and Bell K., Technical University of Norway, (1969), pp.435-450.

[14] Fenwick, R.C. and Paulay, T., "Mechanisms of Shear Resistance of Concrete Beams", Journal of the Structural Division, ASCE, Vol.94, No. ST10, (October 1968), pp. 2325-2350.

[15] Franklin, H.A., "Nonlinear Analysis of Reinforced Concrete Frames and Panels", Ph.D.Thesis, Department of Civil Engineering, University of California, Berkeley, (1970).

[16] Hand, F.R., "Nonlinear Layered Finite Element Analysis of Reinforced Concrete Plates and Shells", Ph.D.Thesis, Department of Civil Engineering, University of Illinois, Urbana, (1972).

[17] Isenberg, J., and Adham, S., "Analysis of Orthotropic Reinforced Concrete Structures", Journal of the Structural Division, ASCE, Vol. 96, No.ST12, (December 1970) pp.2607-2624.

[18] Joint ASCE-ACI Task Committee 426, "The Shear Strength of Reinforced Concrete Members", Journal of the Structural Division, ASCE, Vo.99, No.ST6, (June 1973), pp. 1091-1187.

[19] Kani, G.N., "The Riddle of Shear Failure and Its Solution", ACI Journal, Proceedings, Vol. 61,No.4, (April 1964), pp.441-462.

[20] Kong,F.K., Robins, P.J. and Cole, D.F., "Web Reinforcement Effects on Deep Beams", ACI Journal, Proceedings, Vol.67, No.12, (December 1970), pp.1010-1017.

[21] Kong, F.K. and Robins, P.J., "Web Reinforcement Effects on Lightweight Concrete Deep Beams",ACI Journal, Proceedings, Vol. 68, No.7, (July 1971), pp.514-520.

[22] Kong, F.K., Robins, P.J., Singh, A. and Sharp,G.R., "Shear Analysis and Design of Reinforced Concrete Deep Beams", The Structural Engineer, Vol.50, No.10, (October 1972), pp.405-409.

[23] Krahl,N.W., Khachaturian,N., and Siess, C.P., "Stability of Tensile Cracks in Concrete Beams", Journal of the Structural Division, ASCE, Vol.93,No.ST1, (February 1967), pp.235-254.

[24] Kupfer, H.B. and Gerstle, K.H., "Behaviour of Concrete Under Biaxial Stresses", Journal of the Engineering Mechanics Division, ASCE, Vol.99, No.EM4, (August 1973), pp.853-866.

[25] Kupfer, H., Hilsdorf, H.K. and Rusch,H., "Behaviour of Concrete Under Biaxial Stresses",ACI Journal, Proceedings, Vol. 66, No.8, (August 1969), pp.656-666.

[26] Leonhardt, F., Discussion of "Strength and Behaviour of Deep Beams in Shear", by H.A.R. de Paiva and C.P.Siess, Journal of the Structural Division, ASCE, Vol. 92, No.ST2, (April 1966), pp.427-432.

[27] Liu, T.C.Y., Nilson, A.H., and Slate, F.O., "Stress-Strain Response and Fracture of Concrete in Uniaxial and Biaxial Compression", ACI Journal, Proceedings, Vol.69, No.5, (May 1972), pp.291-295.

[28] Liu,T.C.Y., Nilson,A.H. and Slate, F.O., "Biaxial Stress-Strain Relations for Concrete", Journal of the Structural Division,ASCE,Vol.98, No.ST5, (May 1972), pp.1025-1034.

[29] Mirza, M.S. and Mufti, A.A., "Nonlinear Finite Element Analysis of Reinforced Concrete Structures", Finite Element Methods in Engineering, The University of New South Wales, (1974), pp.403-417.

[30] Mufti,A.A., Mirza, M.S., McCutcheon,J.O., and Spokowski, R., "A Study of Non-Linear Behaviour of Structural Concrete Elements", Proceedings of the Specialty Conference on Finite Element Method in Civil Engineering, ed. McCutcheon,J.O., Mirza, M.S., Mufti,A.A., McGill University, Montreal, (1972), pp.767-802.

[31] Nam,C. and Salmon,C.G.,"Finite Element Analysis of Concrete Beams", Journal of the Structural Division,ASCE, Vol.100,No.ST12, (December 1974),pp.2419-2432.

[32] Ngo,D. and Scordelis, A.C.,"Finite Element Analysis of Reinforced Concrete Beams", ACI Journal, Proceedings, Vol.64,No.3, (March 1967),pp.152-163.

[33] Nilson,A.H., "Nonlinear Analysis of Reinforced Concrete by the Finite Element Method",ACI Journal, Proceedings, Vol.65,No.9, (September 1968),pp.759-766.

[34] de Paiva, H.A.R. and Siess,C.P., "Strength and Behaviour of Deep Beams in Shear", Journal of the Structural Division,ASCE,Vol.91,No.ST5,(October 1965),pp.19-41.

[35] Popovics,S., "A Review of Stress-Strain Relationships for Concrete",ACI Journal, Proceedings,Vol.67,No.3 (March 1970),pp.243-248.

[36] Ramakrishnan,V., and Ananthanarayana, Y.,"Ultimate Strength of Deep Beams in Shear", ACI Journal, Proceedings, Vol.65,No.2,(February 1968),pp.87-98.

[37] Robins, P.J., and Kong, F.K., "Modified Finite Element Method Applied to R.C.Deep Beams", Civil Engineering and Public Works Review, (November 1973), pp.963-966.

[38] Scordelis, A.C., "Finite Element Analysis of Reinforced Concrete Structures", Proceedings of the Specialty Conference on Finite Element Method in Civil Engineering, ed. McCutcheon,J.O., Mirza,M.S., Mufti,A.A., McGill University, Montreal (1972), pp.71-113.

[39] Subedi,N.K., "Design of Reinforced Concrete Sections Subjected to Membrane Forces", The Structural Engineer, Vol.53,No.7,(July 1975),pp.289-292.

[40] Suidan,M. and Schnobrich,W.C., "Finite Element Analysis of Reinforced Concrete",Journal of the Structural Division, ASCE,Vol.99,No.ST10,(October 1973),pp.2109-2121.

[41] Valliappan,S. and Doolan,T.F.,"Nonlinear Stress Analysis of Reinforced Concrete",Journal of the Structural Division, ASCE,Vol.98,No.ST4,(April 1972),pp.885-897.

[42] Valliappan, S. and Nath,P., "Tensile Crack Propagation in Reinforced Concrete - Finite Element Technique", International Conference on Shear, Torsion and Bond in Reinforced and Prestressed Concrete, Coimbatore, India, (January 1969).

[43] Wilson,E.L.,"Solid Sap - A Static Analysis Program for Three-Dimensional Solid Structures", Report UC SESM 71-19, Structural Engineering Laboratory, University of California, Berkeley, (revised), (December 1972).

[44] Wu,H., "Dual Failure Criterion for Plain Concrete", Journal of the Engineering Mechanics Division,ASCE, Vol.100,No.EM6, (December 1974),pp.1167-1181.

[45] Yuzugullu,O., "Finite Element Approach for the Prediction of Inelastic Behaviour of Shear Wall-Frame Systems", Ph.D.Thesis,Department of Civil Engineering, University of Illinois, Urbana, (1972).

[46] Zielinski,Z.A., "Behaviour and Ultimate Strength of Rectangular Reinforced Concrete Beams in Bending and High Shear", Engineering School Bulletin No.81, North Carolina State University, Raleigh, (1967).

[47] Zielinski, Z.A., "A New Approach to Ultimate Strength of Reinforced Concrete Beams in Inclined Cracking and Reduction of Web Reinforcement in Bridge Girders", Discussion by Suter, G.T., and Author's Closure, ACI, Second International Symposium on Concrete Bridge Design, Paper SP 26-17, Vol.1, (April 2nd, 1969), pp.411-456.

[48] Zielinski, Z.A., and Browning, J.S., "Strength Investigation of Cement Mortar in Bi-Directional Compression and Tension", (in Polish), Inzynieria i Budownictwo, (Engineering and Construction), No. 3, (March 1967).

[49] Zienkiewicz, O.C., The Finite Element Method in Engineering Science, McGraw-Hill, London, (1971).

[50] Zienkiewicz, O.C., Valliappan, S., and King, I.P., "Stress Analysis of Rock as a 'No Tension' Material", Geotechnique, Vol.18, (March 1968),pp.56-66.

[51] Zienkiewicz, O.C., Valliappan,S., and King,I.P., "Elasto-Plastic Solutions of Engineering Problems, 'Initial Stress' Finite Element Approach", International Journal for Numerical Methods in Engineering, Vol.1, (January 1969),pp.75-100.

APPENDIX "A"

TEST PHOTOGRAPHS

(1) BEAM PANEL IN TESTING FRAME

(2) LOADING ARRANGEMENT

(3) TYPICAL SHEAR-FLEXURE CRACKS

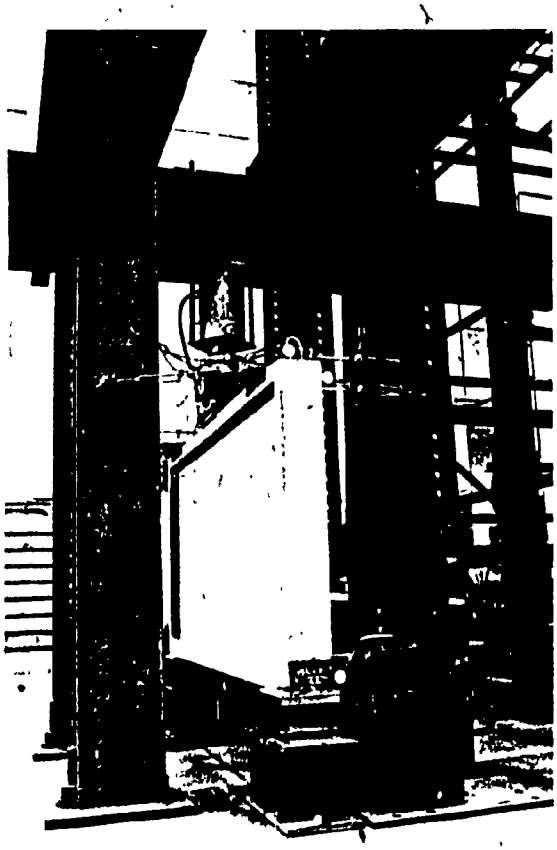

(1)

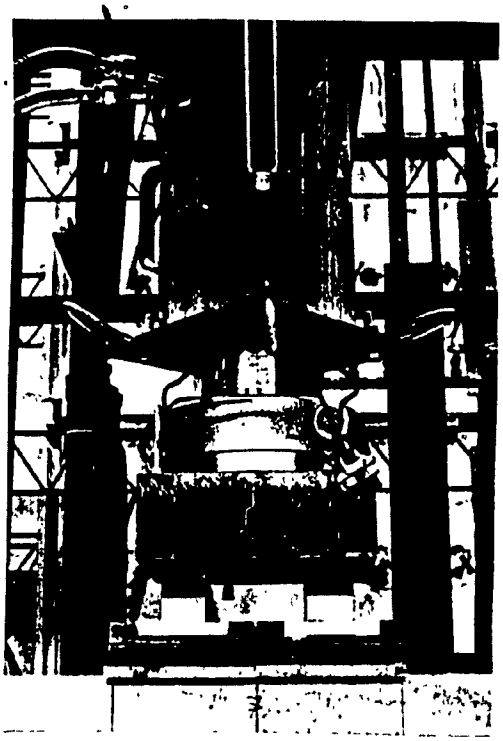

(2)

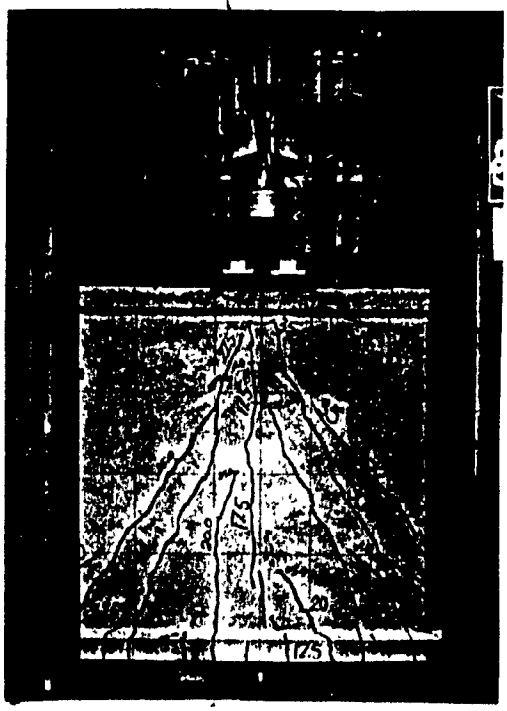

(3)

BEAM PANELS LOADED AT MIDSPAN

(4) - P 111

(5) - P 211

(6) - P 311

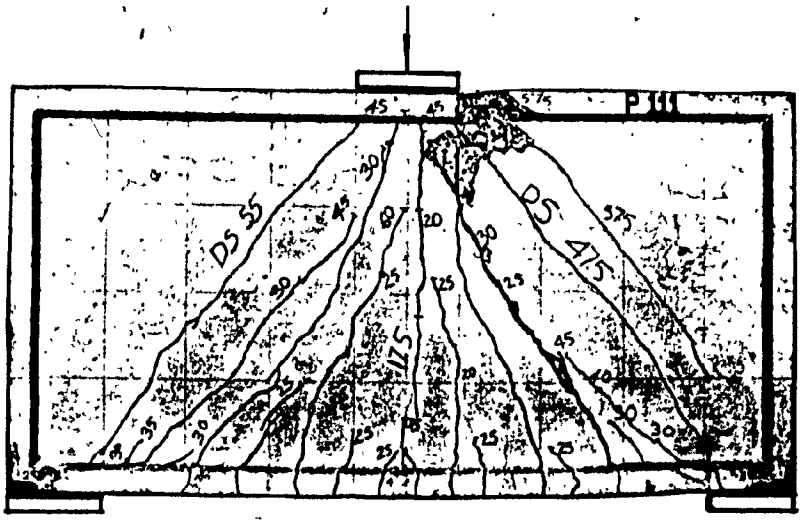
P311
DS 55
DS 475

(4)

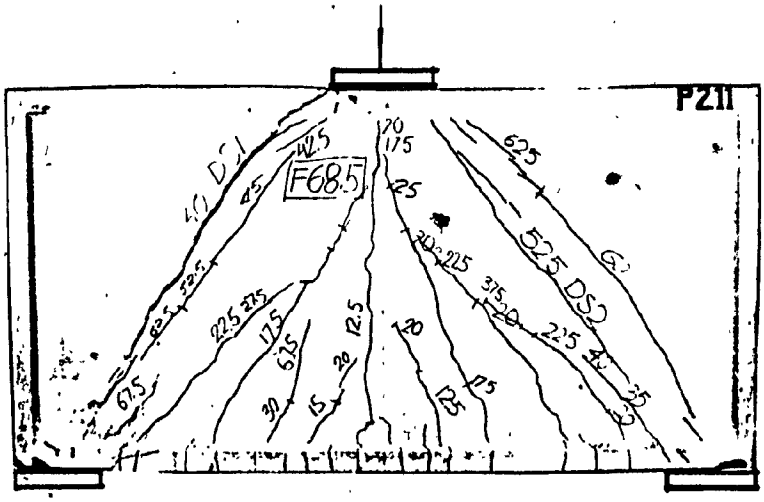
P211
F68.5
DS1
DS2
525

(5)

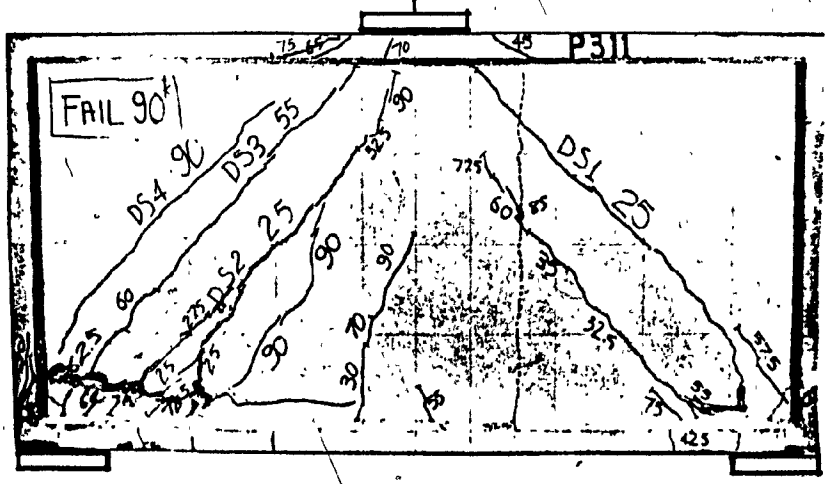
P311
FAIL 90#
DS4 90
DS3 55
DS2 25
DS1 25

(6)

BEAM PANELS UNDER THIRD POINT LOADING

(7) - P 121

(8) - P 221

(9) - P 321

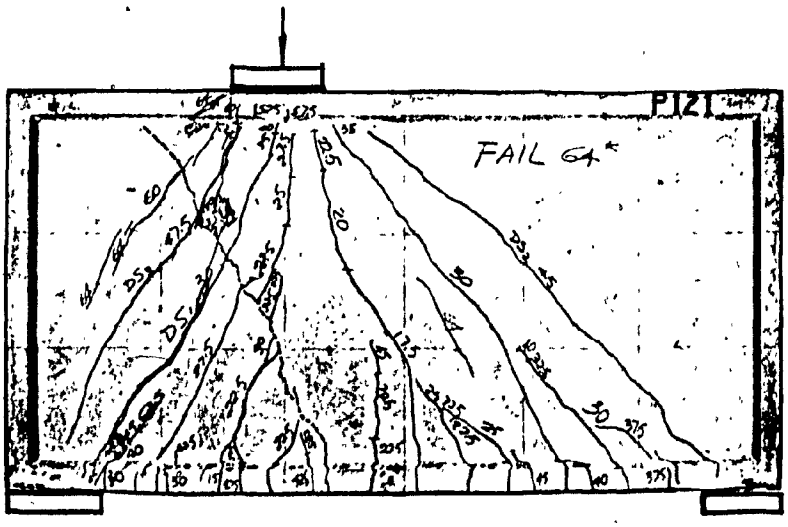

(7)

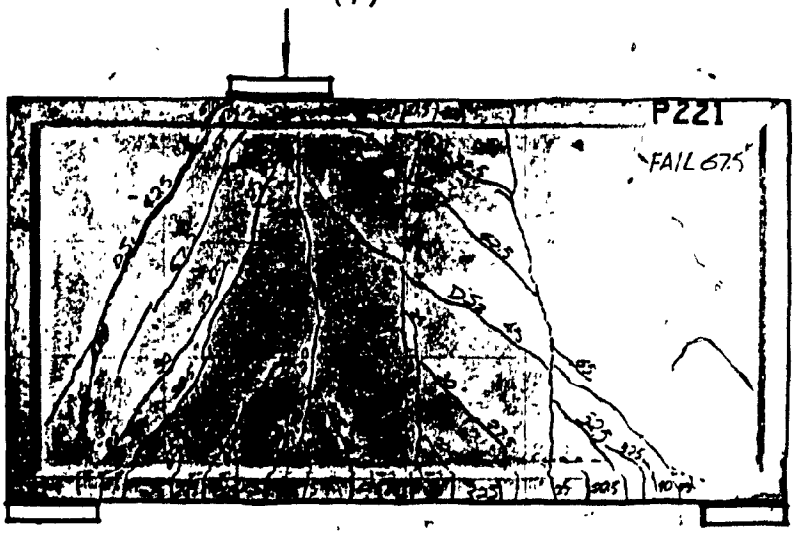

(8)

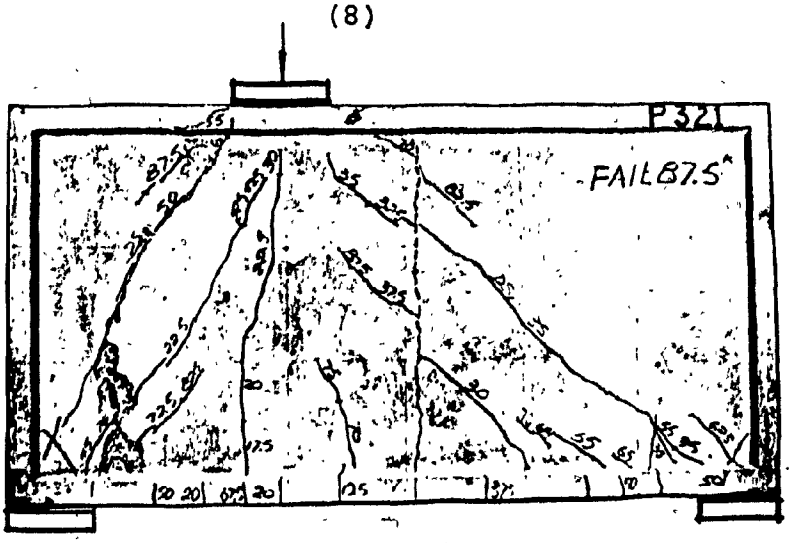

(9)

APPENDIX "B"

FINITE ELEMENT MESH AND ANALYTICAL CRACK PATTERNS - BEAM PANELS

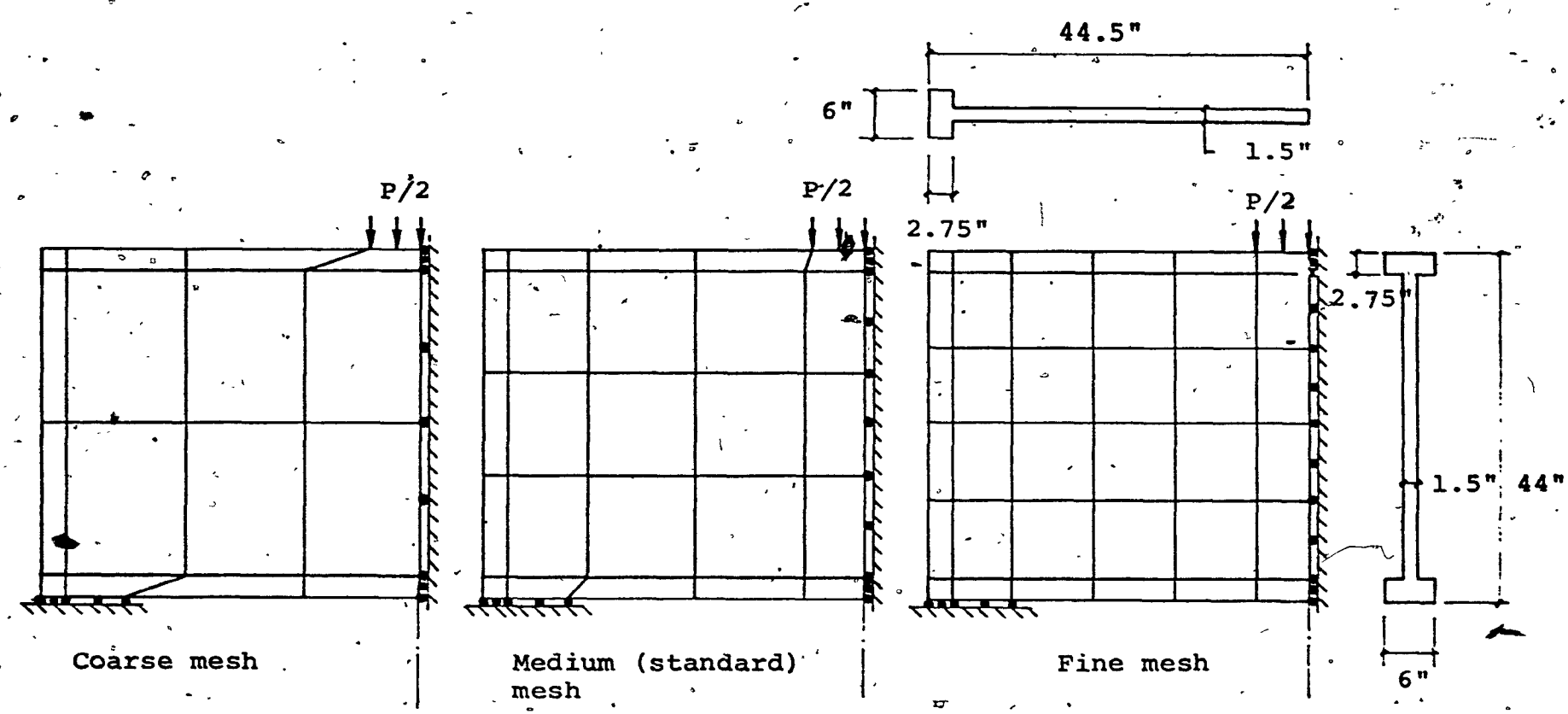

FIG. B.1 FINITE ELEMENT MESH USED FOR BEAM PANELS LOADED AT MIDSPAN

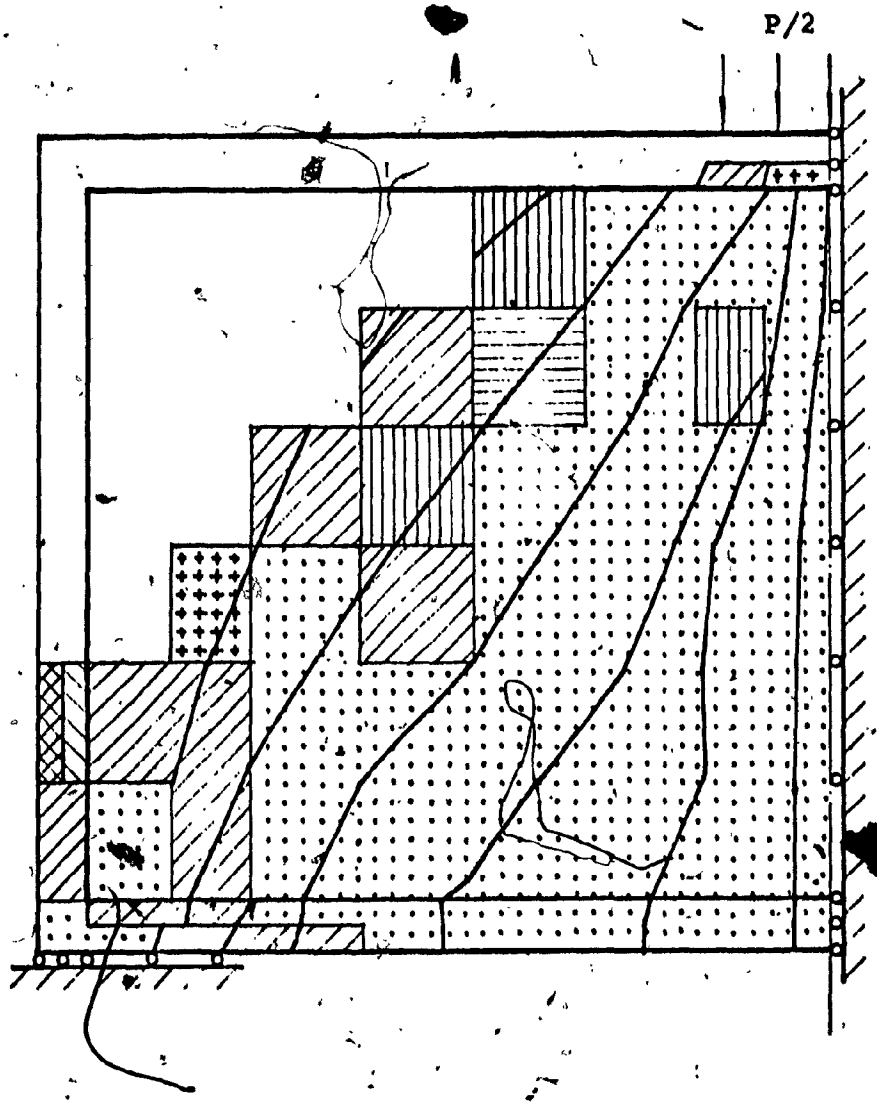

P = 25^{k} 30^{k} 35^{k} 40^{k} 50^{k}

55^{k} 57.5^{k}

P_{ult} = 57.5^{k}

FIG. B.2 ANALYTICAL CRACK PATTERN - P 111

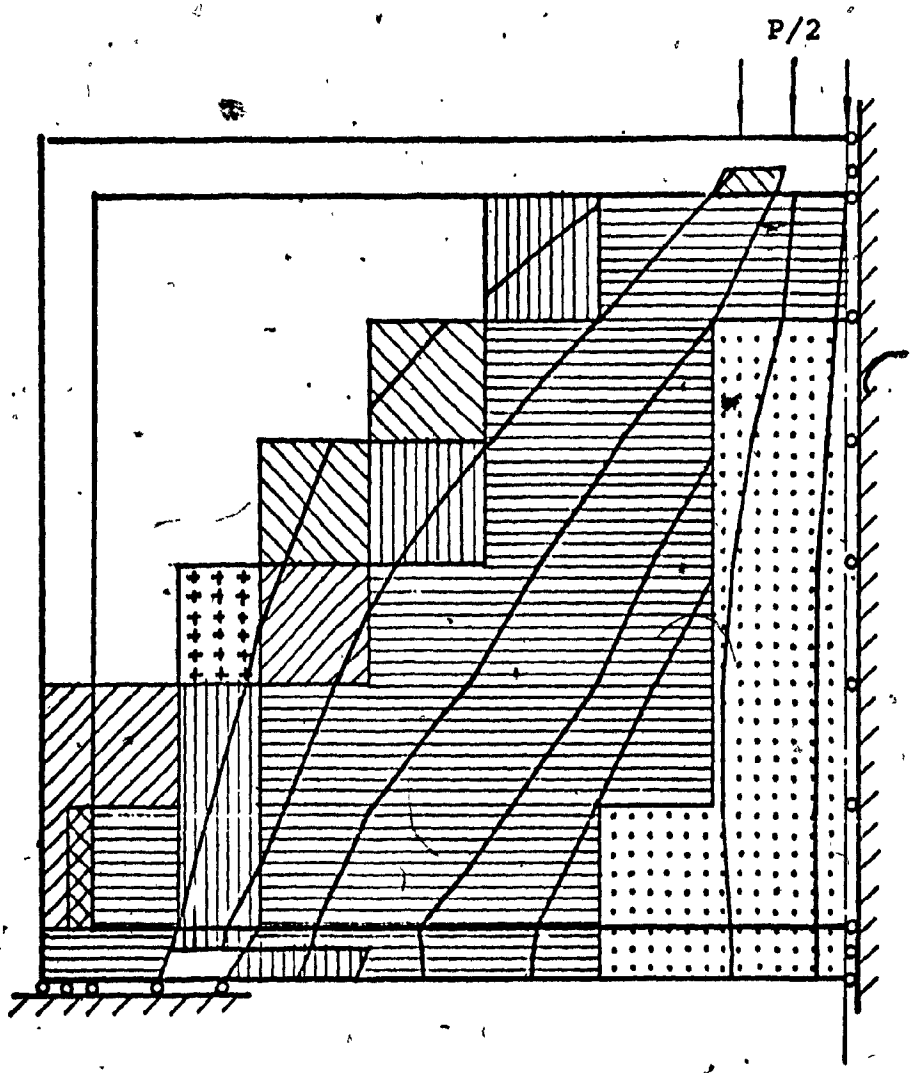

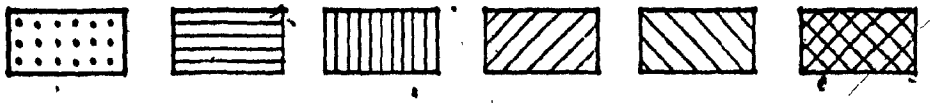

P = 25^k 35^k 40^k 45^k 50^k 65^k

75^k

P_{ult} = 77.5^k

FIG. B.3 ANALYTICAL CRACK PATTERN - P 211

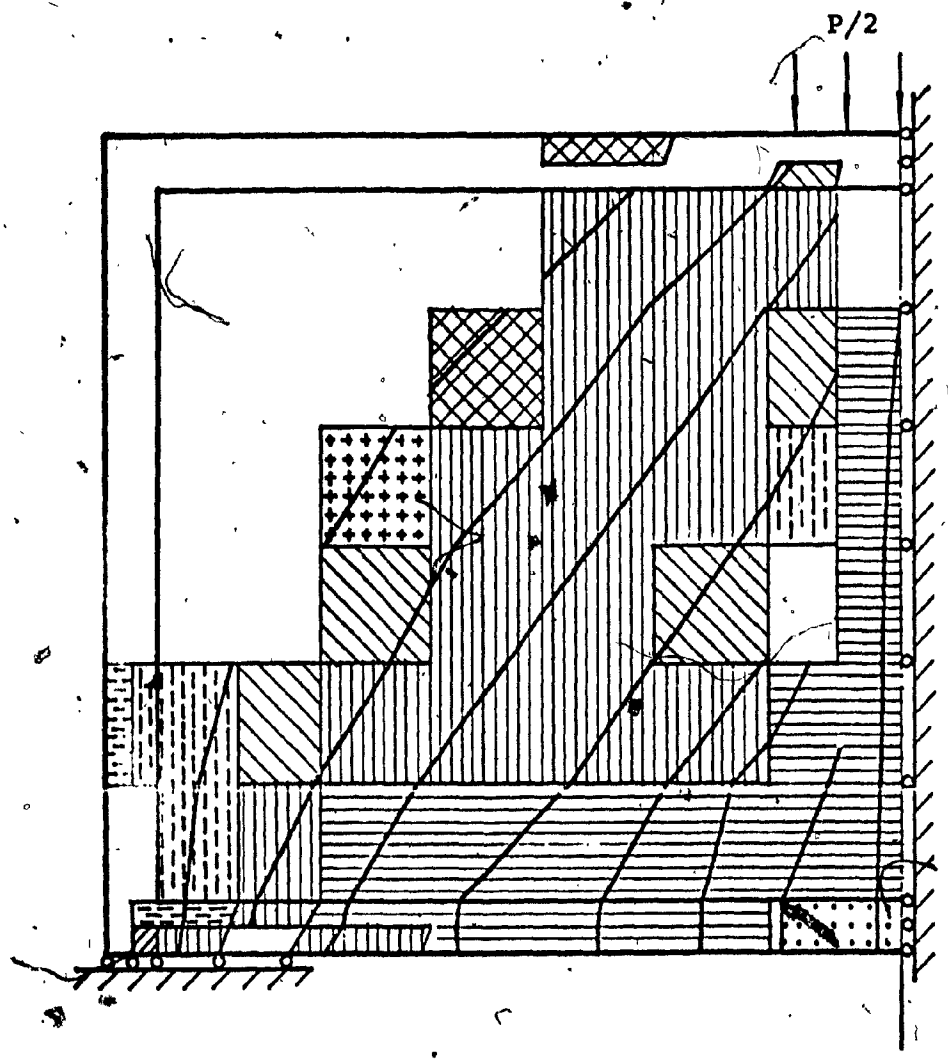

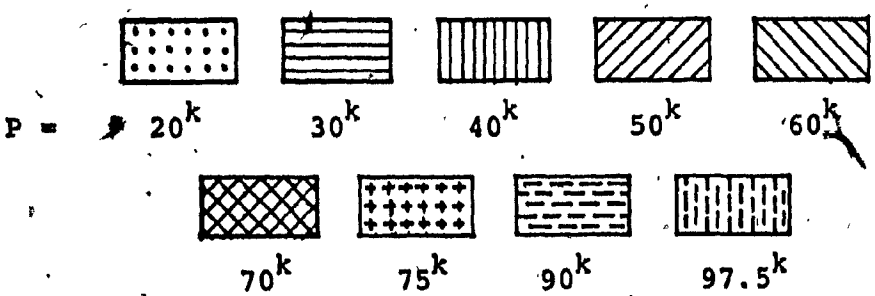

$P_{ult} = 97.5^{k}$

FIG. B.4 ANALYTICAL CRACK PATTERN - P 311

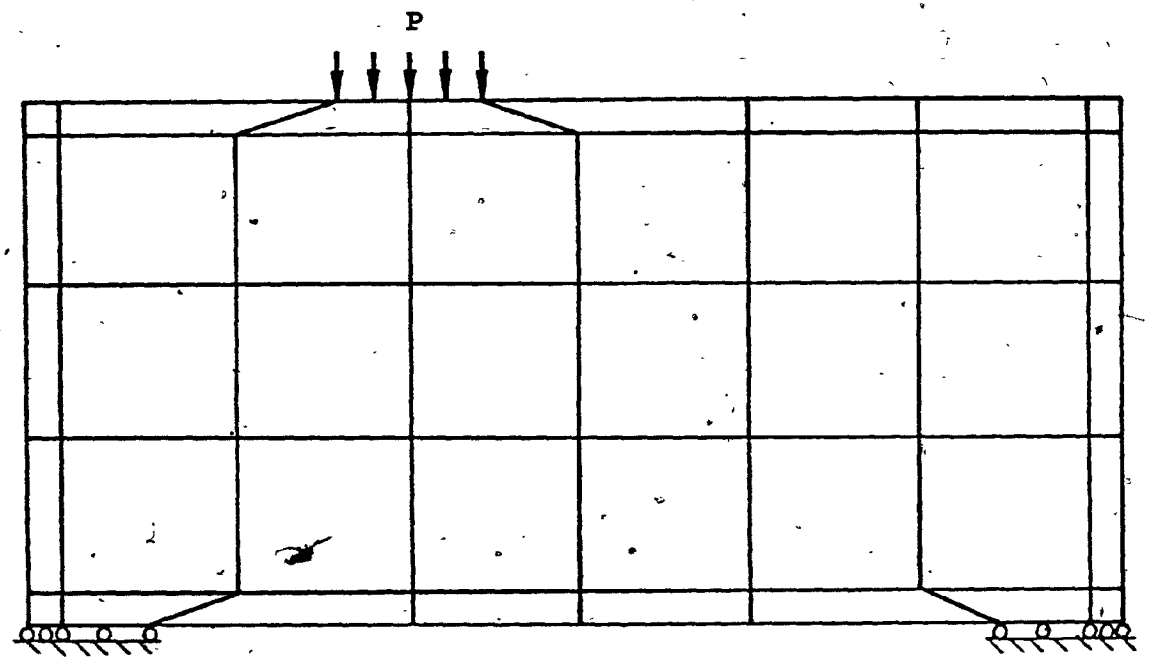

FIG. B.5 FINITE ELEMENT MESH USED FOR BEAM PANELS UNDER THIRD POINT LOADING

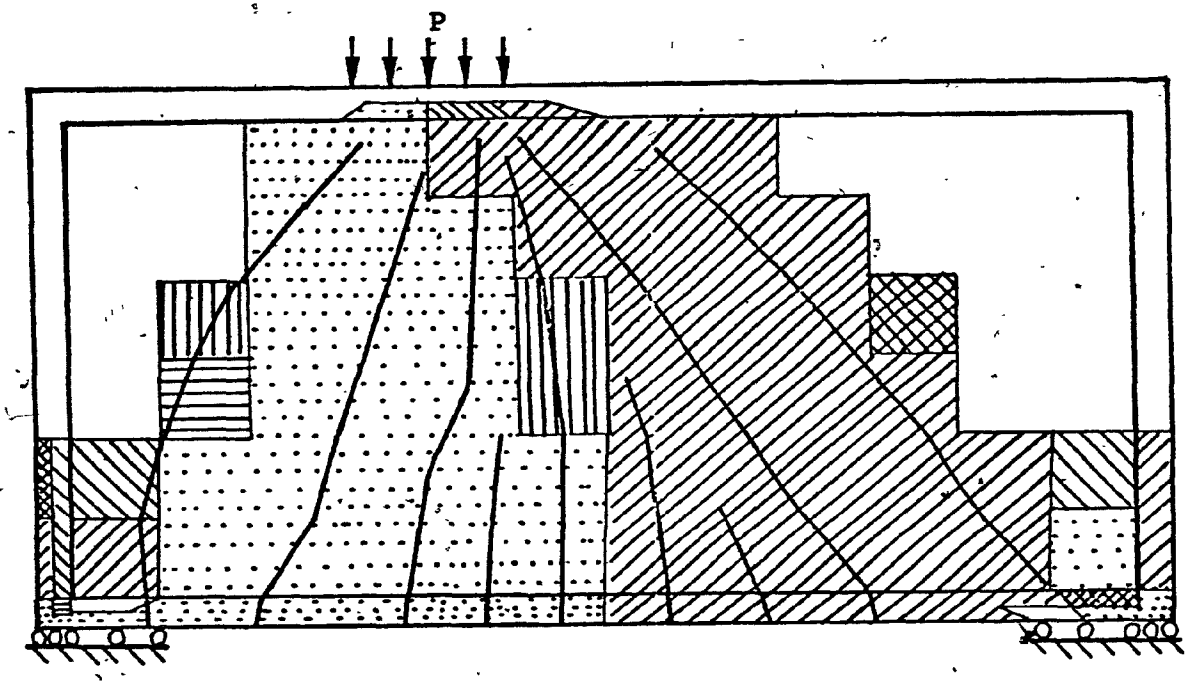

P = 30^k 35^k 40^k 45^k 50^k 60^k

$P_{ult} = 60^k$

FIG. B.6 ANALYTICAL CRACK PATTERN - P 121

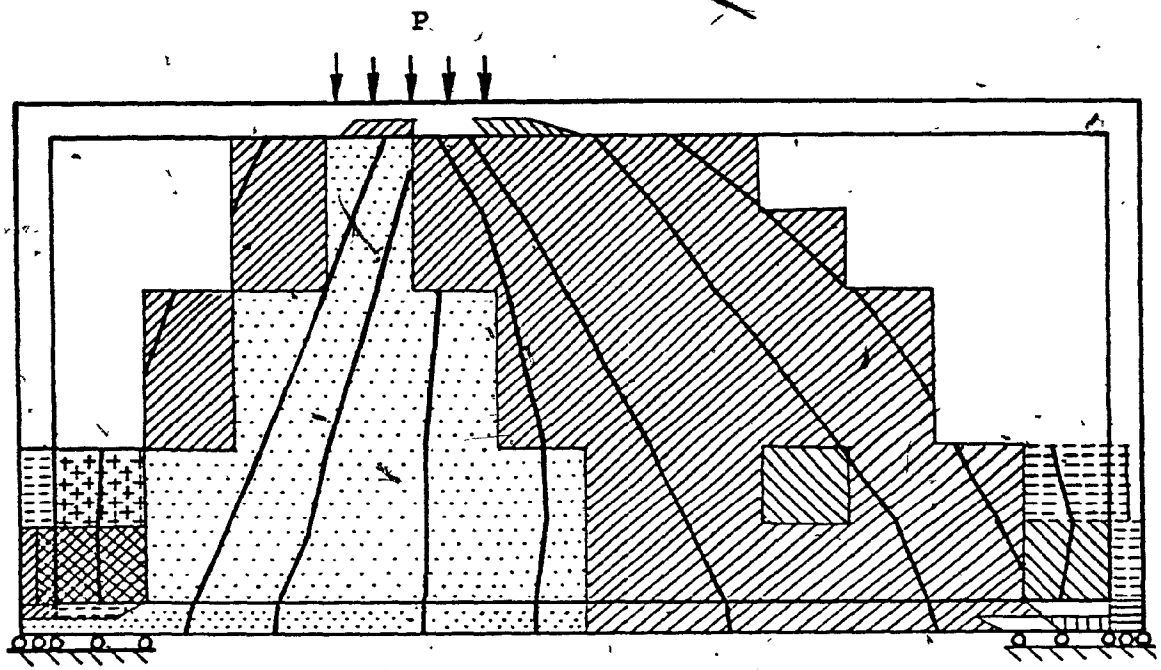

P = 30k 35k 40k 45k 50k 55k 60k

65k

P_{ult} = 65k

FIG. B.7 - ANALYTICAL CRACK PATTERN - P 221

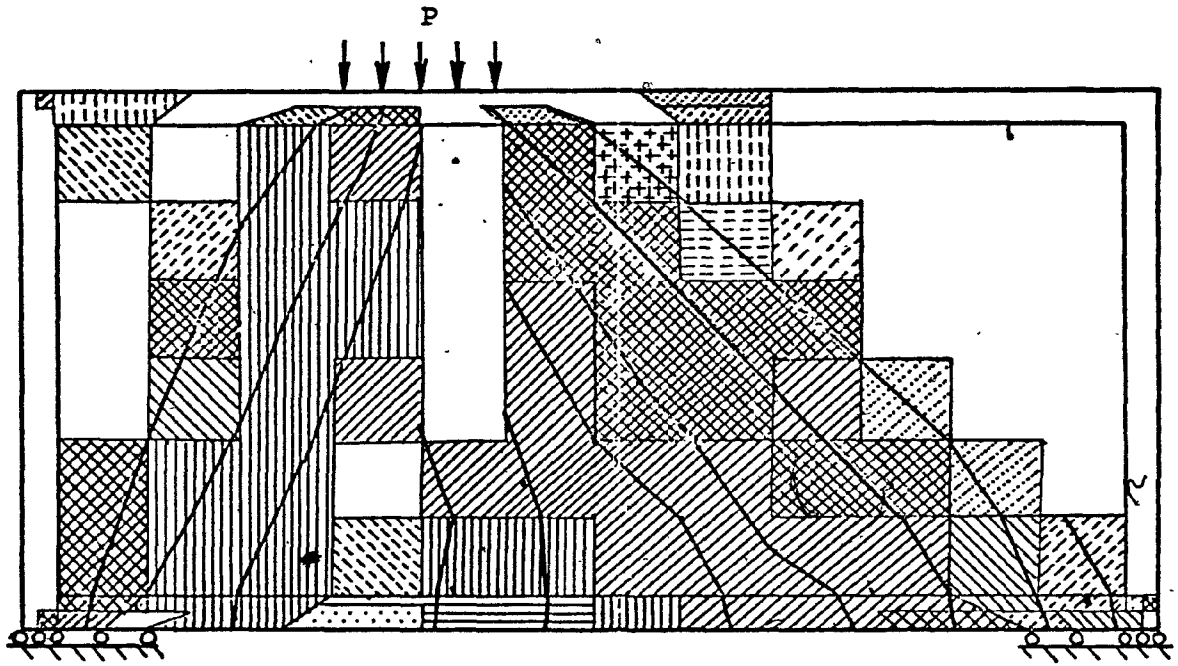

P = 20^k 25^k 35^k 40^k 45^k 55^k 60^k

65^k 70^k 75^k 90^k 92.5^k

P_{ult} = 95^k

FIG. B.8 ANALYTICAL CRACK PATTERN - P 321

APPENDIX "C"

LOAD-DISPLACEMENT DIAGRAMS OF THE BEAM PANELS

BEAM PANELS LOADED AT MIDSPAN

(1) - P 111

(2) - P 211

(3) - P 311

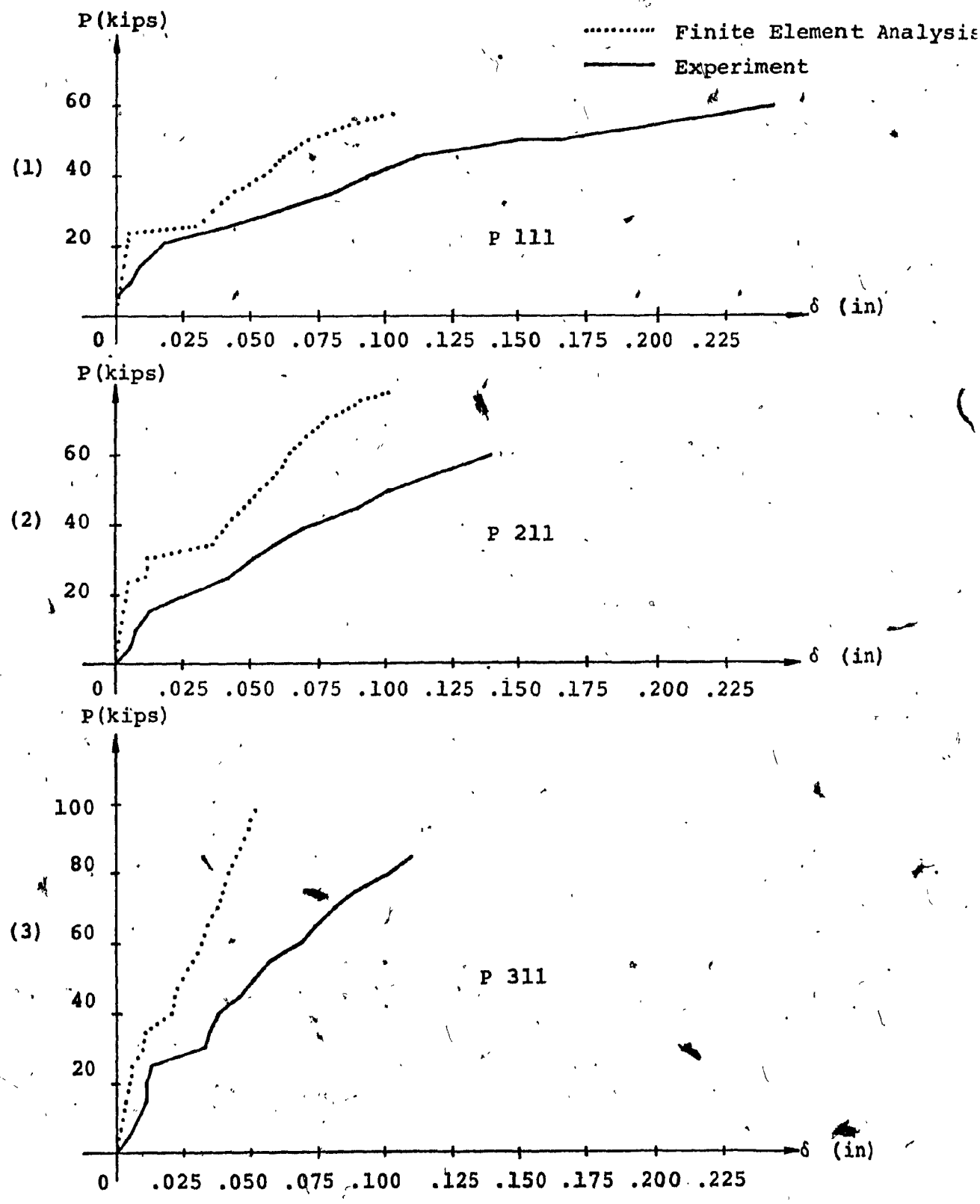
P(kips)
Finite Element Analysis
Experiment
(1)
60
40
20
0
P 111
δ (in)
.025 .050 .075 .100 .125 .150 .175 .200 .225
P(kips)
(2)
60
40
20
0
P 211
δ (in)
.025 .050 .075 .100 .125 .150 .175 .200 .225
P(kips)
100
80
(3)
60
40
20
0
P 311
δ (in)
.025 .050 .075 .100 .125 .150 .175 .200 .225

BEAM PANELS UNDER THIRD POINT LOADING

(4) - P 121

(5) - P 221

(6) - P 321

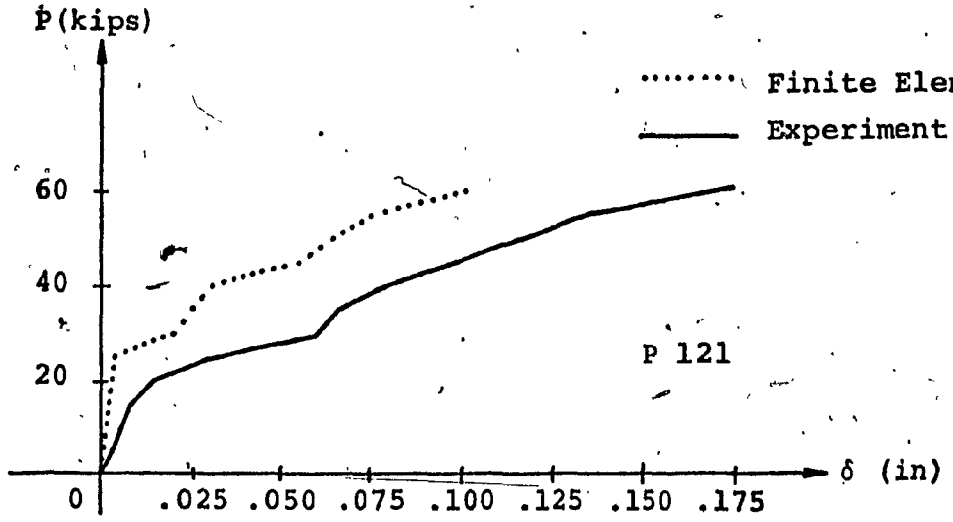
P(kips)
Finite Element Analysis
Experiment
60
40
20
0
.025 .050 .075 .100 .125 .150 .175
δ (in)
P 121

(4)

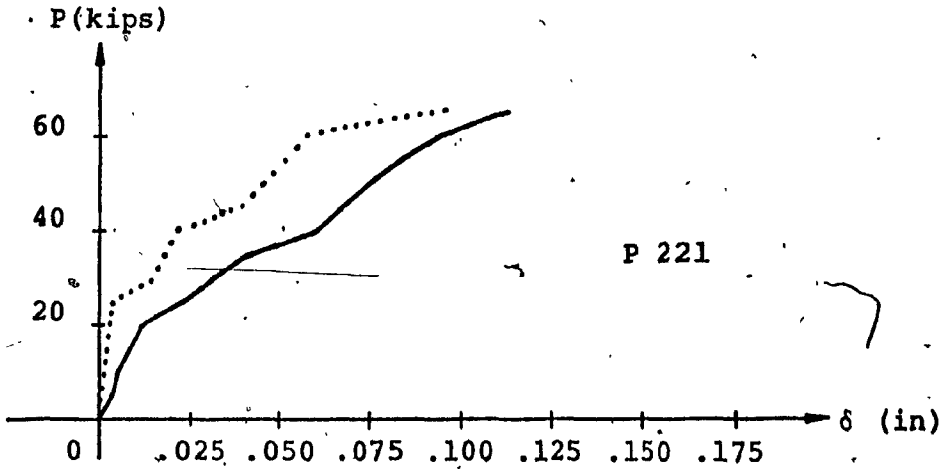
P(kips)
60
40
20
0
.025 .050 .075 .100 .125 .150 .175
δ (in)
P 221

(5)

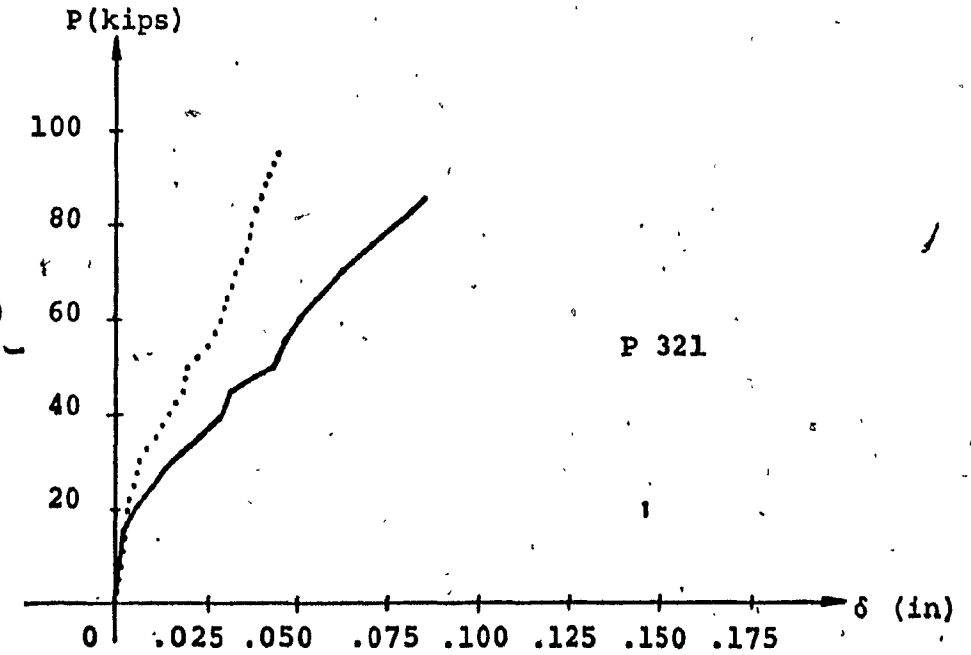
P(kips)
100
80
60
40
20
0
.025 .050 .075 .100 .125 .150 .175
δ (in)
P 321

(6)

COMPARISON OF DIFFERENT MESH AND LOAD INCREMENTS

(7) - P 211 (MESH)

(8)+ - P 211 (LOAD INCREMENTS)

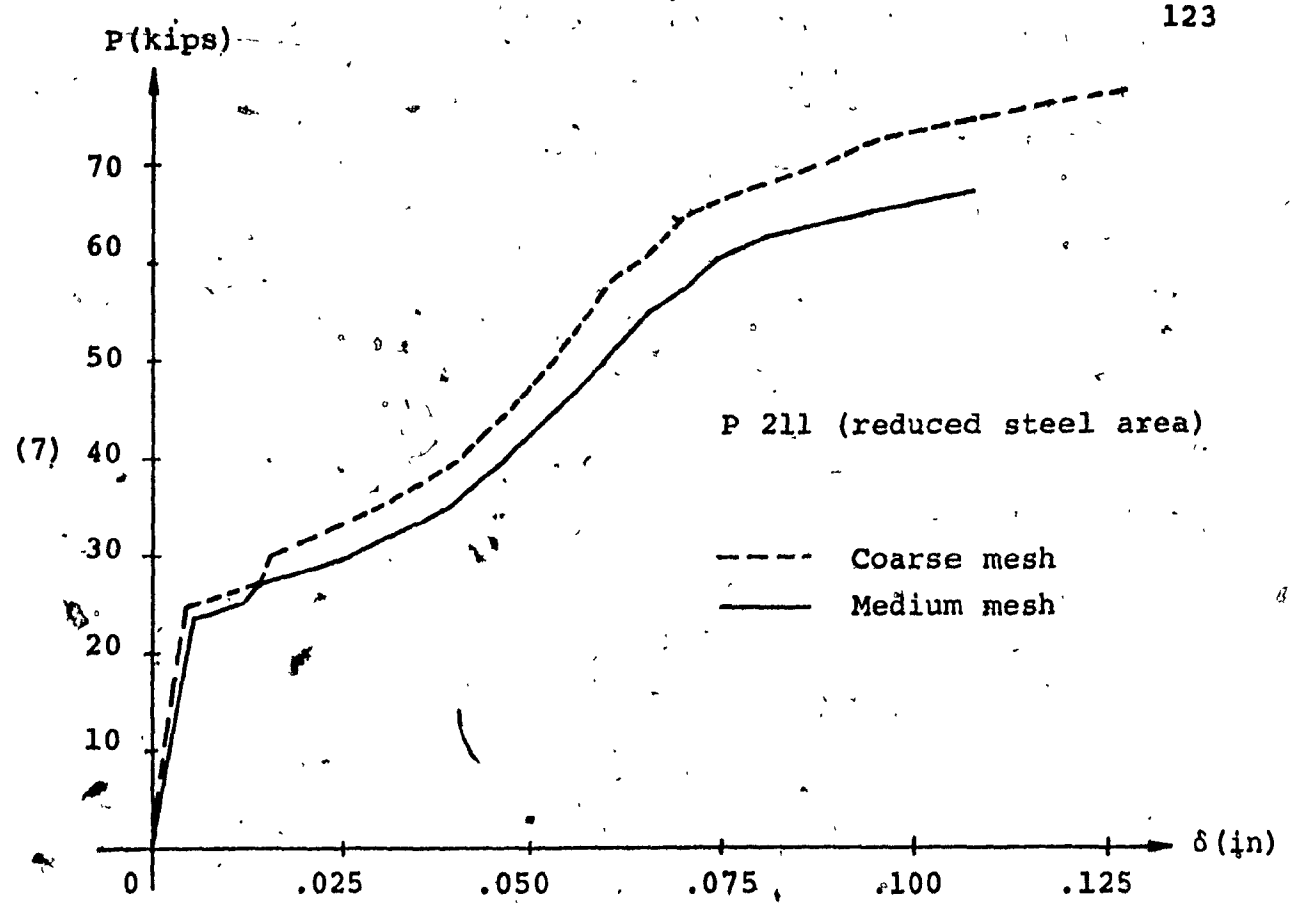
P(kips)
70
60
50
40
30
20
10
0
.025
.050
.075
.100
.125
δ(in)
P 211 (reduced steel area)
Coarse mesh
Medium mesh

(7)

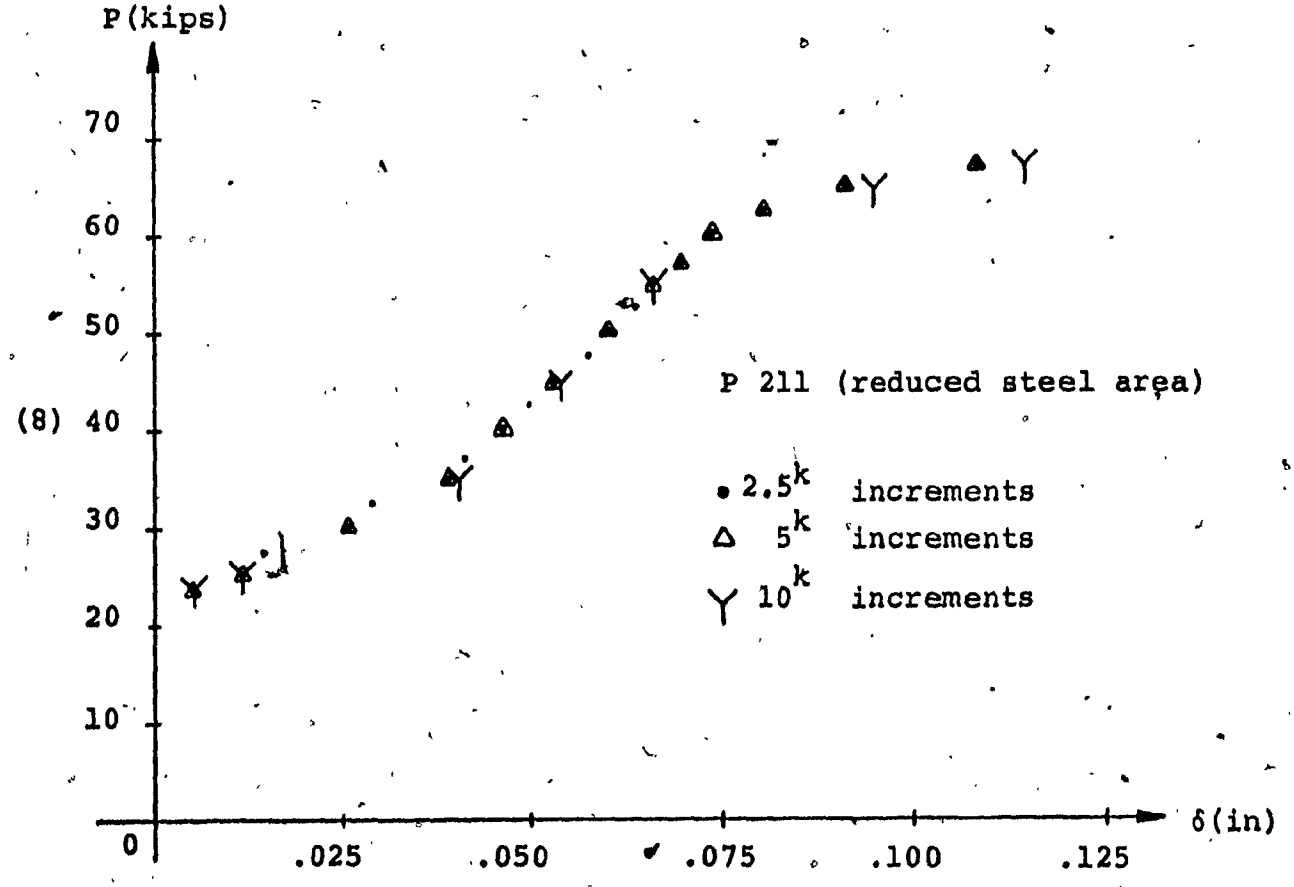
P(kips)
70
60
50
40
30
20
10
0
.025
.050
.075
.100
.125
δ(in)
P 211 (reduced steel area)
2.5k increments
5k increments
10k increments

(8)

APPENDIX "D"

COMPUTER PROGRAM - DATA DESCRIPTION AND LISTING

APPENDIX "D"

COMPUTER PROGRAM - DATA DESCRIPTION AND LISTING

In this version of the program, up to 149 nodes, 40 elements and 9 different types of material properties can be specified. All computations are done in core and require approximately 100 K. These limitations can be easily relaxed according to user needs. TAPE 10 and TAPE 11 are used as direct access files. The data on TAPE 10 are updated following each incremental solution and permits the user to run a job in parts (see NOCH below). The data for plotting the finite element mesh, stresses, cracks and displacements are written on TAPE 11. The necessary input data cards are explained below.

(1) NOPROB (I5):

Number of problems to be solved. One set of the following cards is required for each problem.

(2) NOCH (I5):

Execution control card. Specify one of the following:

0 - complete run

1 - up to elastic limit

2 - continue after previous execution, do not print previous stresses

3 - continue after previous execution, print previous stresses

(3) TITLE (8A10):

Heading or problem description. If NOCH > 1, data cards described in 4 through 7 are not required.

(4) NUMNP, MUMEL, NELTYP (3I5):

Number of node points, elements and different types of material properties.

(5) N, KOD(N), Y(N), DI(N), FI(N), INCR (2I5, 4F10.0, I5):

Node number, boundary condition indicator, coordinates, known forces and/or displacements along x and y axes, respectively, and increment for nodal data generation. The following code for boundary conditions is adopted:

0 - Free joint

1 - Restraint in x-direction (horizontal roller)

2 - Restraint in y-direction (vertical roller)

3 - Fixed joint (hinge)

For three or more nodes along a straight line, it is sufficient to give the data for only the end points. Data for the intermediate nodes is generated by specifying INCR as the difference between consecutive nodes. For the generated nodes the boundary condition indicator is set identical to that of the previous node.

(6) (PELMAT(I,J),J = 1,13)(8F10.0):

Two cards are required for each type of material properties. The first card should contain t, E_s, E_c, ν, p_1, θ_1, p_2, θ_2 and the second card should contain f'_c, f_t, f_{y_1}, f_{y_2} and ε_ℓ, where p_1, p_2, θ_1, θ_2, f_{y_1}, f_{y_2} represent the reinforcement ratio, angle between the direction of the reinforcement and the x-axis, and yield strength, respectively, in directions 1 and 2. If punched as zero (or left blank) on data cards, the following values will be used in the calculations:

$E_s = 29{,}000{,}000$ psi

$E_c = 33\, w^{1.5}\sqrt{f'_c}$ where w = 150 pcf

$\nu = 0.17$

$f_t = 1.38\, (f'_c)^{2/3}$

$\varepsilon_\ell = -.003$ in/in

(7) N,(INODE(N,J),J = 1,9),INCR (10I5):

Element, nodes (counterclockwise, starting from the lower left corner), material type and increment for element data generation (INCR = difference between corresponding nodes of consecutive elements). For generated elements, the material type is set identical to that of the previous element.

(8) IDIFOR,IPOINT,DISPMX,TLR,BETA,MCIK,MLIMIT (2I5, 3F10.0, 2I5):

Control parameters, as explained below.

IDIFOR:

Displacement output control. Specify one of the following:

0 - Do not print nodal displacements.

1 - Print displacements of the node specified by IPOINT only.

2 - Print nodal displacements.

IPOINT:

Location where the limit deformation is checked. Thus if DISP(IPOINT) exceeds the limit deformation, execution is terminated. For node I, if the limit deformation is checked along the x-direction (y-direction), IPOINT = 2xI-1 (2xI).

DISPMX:

Limit deformation.

TLR:

Tolerance level to check convergence. If, at the N^{th} iteration

$$(P_{max})_N \leq TLR \times (P_{max})_1$$

where P_{max} represents the component of the nodal force

vector, largest in absolute value, convergence is assumed, and the iteration process is terminated.

BETA:

Shear retention factor.

MCIK:

Stresses are printed either after each load increment or after each iteration. MCIK indicates the load increment following which the stresses will be printed after each iteration.

MLIMIT:

Number of load increments (maximum 25).

(9) (DIV(I),I = 1,MLIMIT)(8F10.0):

Load increment ratios

$$\{P\}_N = (1 + DIV(N)) \times \{P\}_{N-1}$$

DESCRIPTION OF VARIABLES

VA (3,4), VB (3,4), VC (3,4), VD (3,4)

Auxiliary stress, strain vectors - element level

(stress or strain component, integration point)

EXS (3,4)

Excess stress vector - element level

FI (298), DI (298)

Incremental force and displacement vectors, respectively

PR (16)

Equivalent nodal forces vector - element level

DA (3,3)

Auxiliary elasticity matrix

DEP (3,3)

Elasto-plastic matrix

TITLE (8)

Problem description or heading

COMMON/ISOPAR/

XX (8), YY (8)

Cartesian coordinates - element level

D (3,3,4)

Elasticity matrix - element level

EST (16,16)

Element stiffness matrix

OS (2,2)

Element stiffness submatrix

XI (14)

Stiffness terms - element level

FI (14)

Functions to be integrated to form XI

XN (8), YN (8)

Partial deviatives of shape functions in local coordinates $\partial Ni/\partial \xi$ and $\partial Ni/\partial \eta$ respectively

V (8,4), Z (8,4)

Partial derivatives of shape functions in general coordinates, $\partial Ni/\partial x$ and $\partial Ni/\partial y$ respectively

(shape function, integration point)

A (2)

Coordinates of Gauss integration points

DET

Determinant of Jacobian matrix

KOUNT

Counter for integration points

COMMON/DATA/

KOD (149), X (149), Y (149)

Boundary condition indicator, and Cartesian coordinates for nodal points, respectively (see data description)

INODE (40,9)

Element data (see data description)

PELMAT (9,13)

Material data (see data description)

DC (3,3,9)

Composite material elasticity matrix (maximum 9 different types)

COMMON/VALU/

DISP (298), FORCE (298)

Force and displacement vectors, respectively

S (298,46)

System stiffness matrix

(total degress of freedom, half band width)

COMMON/IO/

NR,NW

Input, output tape numbers

COMMON/STRS/

CS (40,3,4)

Concrete stresses

(element, stress component, integration point)

SS (40,2,4)

Steel stresses

CSI (3,4)

Incremental concrete stesses - element level

(stress component, integration point)

SSI (2,4)

Incremental steel stresses - element level

S1, S2

Principal stressess - at integration point

SNI (3,4)

Strain increment vector - element level

ALPHA, THETA

Principal angle for composite material and concrete respectively

FE

Auxiliary angle

CRF (40,4) CRS (40,4)

Directions of first and second cracks, respectively - element level (element, integration point)

MCRACK (40,4) Crack modes

0 - uncracked concrete

1 - cracked concrete

2 - concrete with two cracks

MCRUSH (40,4) Modes in compression

0 - elastic concrete

1 - crushed concrete

2 - plastic concrete

COMMON/LET/

NUMNP, NUMEL, NELTYP

see data description

THICK

Element thickness

NTOT

Total degrees of freedom = 2* NUMNP

NB

Half band width

LEF

Material type - element level

COMMON/NONLIN/

see data description

LIST OF SUBROUTINES

BANDWD	:	Determine half band width
CHOLE 1	:	Decompose the system stiffness matrix
CHOLE 2	:	Solve for displacements
ELASMX	:	Evaluate the elasticity matrices
FORDIS	:	Print forces and displacements
FUNC	:	Evaluate derivatives of the shape functions
INTEG	:	Evaluate element stiffness matrix terms using Gaussian quadrature
LIMIT	:	Scale forces, displacements, strains and stresses to the elastic limit
MASTER	:	Generate the system stiffness matrix
MODIFY	:	Modify the stystem stiffness matrix for known displacements
MOHR	:	Determine principal angle and pricipal stresses
NEWSTF	:	Modify stress-strain matrices and regenerate the system stiffness matrix
SHAPE	:	Evaluate strain-displacement matrices (to determine strains), and/or multiply by the Jacobian (to compute equivalent nodal forces)
STIFF	:	Generate element stiffness matrices
STRESS	:	Determine strains and stresses (element level)
XDATA	:	Read and generate input
XPRINT	:	Print concrete and steel stresses and crack directions at the integration points

```
      PROGRAM SAPRCS(INPUT,OUTPUT,TAPE1=INPUT,TAPE2=OUTPUT,TAPE10,TAPE11
     *)
      DIMENSION VA(3,4),VB(3,4),VC(3,4),VD(3,4),EXS(3,4),FI(298),DI(298)
     *,PR(16),DA(3,3),DEP(3,3),TITLE(8)
      COMMON/ISOPAR/XX(8),YY(8),D(3,3,4),EST(16,16),OS(2,2),XI(14),F(14)
     *,XN(8),YN(8),V(8,4),Z(8,4),A(2),DET,KOUNT
      COMMON/DATA/KOD(149),X(149),Y(149),INODE(40,9),PELMAT(9,13),DC(3,3
     *,9)
      COMMON/VALU/DISP(298),FORCE(298),S(298,46)
      COMMON/IO/NR,NW
      COMMON/STRS/CS(40,3,4),SS(40,2,4),CSI(3,4),SSI(2,4),SIG2,SNI(3,4)
     *,ALPHA,THETA,FE,CRF(40,4),CRS(40,4),MCRACK(40,4),MCRUSH(40,4)
      COMMON/LET/NUMNP,NUMEL,NELTYP,THICK,NTOT,NB,LEF
      COMMON/NONLIN/MLIMIT,DIV(25),MCIK,TLR,IDIFOR,IPOINT,DISPMX,BETA
C
C     ***************************************
C     *                                     *
C     *              SAPRCS                 *
C     *  A FINITE ELEMENT COMPUTER PROGRAM FOR *
C     *   NONLINEAR STRESS ANALYSIS OF PLANAR  *
C     *      REINFORCED CONCRETE STRUCTURES    *
C     *                                     *
C     ***************************************
C
C     COORDINATES OF GAUSS INTEGRATION POINTS
      A(1)=-0.577350269189&3
      A(2)=-A(1)
C     DATA SET REFERENCE NUMBERS
      NR=1
      NW=2
C     NOPROB=NUMBER OF PROBLEMS TO BE SOLVED
      READ(NR,10) NOPROB
      DO 11 IP=1,NOPROB
      READ(NR,16) NOCH,(TITLE(J),J=1,8)
      WRITE(NW,17) IP,NOCH,(TITLE(J),J=1,8)
C     NOCH=0  GO AHEAD
C     NOCH=1  LIMIT ONLY
C     NOCH=2  CONTINUE WHERE PREVIOUS EXECUTION STOPPED, DO NOT PRINT STRESSES
C     NOCH=3  CONTINUE WHERE PREVIOUS EXECUTION STOPPED, PRINT STRESSES
      IF(NOCH.GT.1) GO TO 830
      CALL XDATA
C     DETERMINE HALF BAND WIDTH = NB
      CALL BANDWD
      IF(NB.GT.46) GO TO 9999
      WRITE(11) NUMNP,NUMEL,NELTYP,NTOT,NB
      WRITE(11) (X(I),Y(I),KOD(I),I=1,NUMNP)
      WRITE(11) ((INODE(I,J),J=1,9),I=1,NUMEL)
      DO 9 IJK=1,NUMEL
      DO 9 KJI=1,4
      MCRACK(IJK,KJI)=0
      MCRUSH(IJK,KJI)=0
      CRF(IJK,KJI)=0.0
    9 CRS(IJK,KJI)=0.0
C     EVALUATE THE ELASTICITY MATRICES
      CALL ELASMX
      DO 7 IKI=1,NTOT
      DO 7 JLJ=1,NB
    7 S(IKI,JLJ)=0.0
C     GENERATE THE ELEMENT STIFFNESS MATRICES
```

```
      DO 20 N=1,NUMEL
      LEF=INODE(N,9)
      DO 21 K=1,4
      DO 22 IK=1,3
      DO 22 JL=1,3
   22 D(IK,JL,K)=DC(IK,JL,LEF)
   21 CONTINUE
      THICK=PELMAT(LEF,1)
      DO 24 IK=1,8
      JL=INODE(N,IK)
      XX(IK)=X(JL)
   24 YY(IK)=Y(JL)
      CALL STIFF
C     ADD THE ELEMENT STIFFNESS MATRIX TO THE SYSTEM STIFFNESS MATRIX
      CALL MASTER(N)
   20 CONTINUE
C     MODIFY THE STIFFNESS MATRIX FOR KNOWN DISPLACEMENTS
      CALL MODIFY
C     CALCULATION OF NODAL DISPLACEMENTS BY THE CHOLESKY ALGORITHM
C     DECOMPOSITION
      CALL CHOLE1(KOT)
      IF(KOT.EQ.1) GO TO 9995
C     SOLUTION
      CALL CHOLE2(FORCE,DISP)
C     SCALE THE FORCES, DISPLACEMENTS, STRAINS AND STRESSES TO THE FIRST LIMIT
      CALL LIMIT
      MODSUM=0
      MI=0
 1010 MI=MI+1
      REWIND 10
      WRITE(10) NUMNP,NUMEL,NELTYP,NTOT,NB
      WRITE(10) (X(I),Y(I),KOD(I),I=1,NUMNP)
      WRITE(10) ((INODE(I,J),J=1,9),I=1,NUMEL)
      WRITE(10) ((PELMAT(I,J),J=1,13),I=1,NELTYP)
      WRITE(10) (((DC(I,J,K),I=1,3),J=1,3),K=1,NELTYP)
      WRITE(10) (DISP(I),FORCE(I),(S(I,J),J=1,NB),I=1,NTOT)
      DO 827 KZ=10,11
      WRITE(KZ) ((CS(I,1,K),CS(I,2,K),CS(I,3,K),SS(I,1,K),SS(I,2,K),I=1,
     *NUMEL),K=1,4)
      WRITE(KZ) ((CRF(I,J),CRS(I,J),MCRACK(I,J),MCRUSH(I,J),I=1,NUMEL),J
     *=1,4)
      WRITE(KZ) MI
  827 CONTINUE
      IF(MI.GT.MLIMIT) GO TO 11
      IF(NOCH.EQ.1) GO TO 11
      IF(NOCH.EQ.0) GO TO 835
  830 READ (10) NUMNP,NUMEL,NELTYP,NTOT,NB
      READ (10) (X(I),Y(I),KOD(I),I=1,NUMNP)
      READ (10) ((INODE(I,J),J=1,9),I=1,NUMEL)
      READ (10) ((PELMAT(I,J),J=1,13),I=1,NELTYP)
      READ (10) (((DC(I,J,K),I=1,3),J=1,3),K=1,NELTYP)
      READ (10) (DISP(I),FORCE(I),(S(I,J),J=1,NB),I=1,NTOT)
      READ (10) ((CS(I,1,K),CS(I,2,K),CS(I,3,K),SS(I,1,K),SS(I,2,K),I=1,
     *NUMEL),K=1,4)
      READ (10) ((CRF(I,J),CRS(I,J),MCRACK(I,J),MCRUSH(I,J),I=1,NUMEL),J
     *=1,4)
      READ (10) MI
```

```
      READ(NR,5000) IDIFOR,IPOINT,DISPMX,TLR,BETA,MCIK,MLIMIT,(DIV(I),I=
     *1,MLIMIT)
      WRITE(NW,5001) IDIFOR,IPOINT,DISPMX,TLR,BETA,MCIK,MLIMIT,(DIV(I),I
     *=1,MLIMIT)
      CALL FORDIS(FORCE,DISP,IDIFOR,IPOINT)
      IF(NOCH.EQ.3) CALL XPRINT
      NOCH=0
  835 KARA=0
      WRITE(NW,1065) MI
      TOLERA=0.0
      DO 1000 I=1,NTOT
      FI(I)=0.0
      DI(I)=0.0
      IF(FORCE(I).EQ.0.0) GO TO 1000
      FI(I)=DIV(I)*FORCE(I)
      FORCEI=ABS(FI(I))
      IF(FORCEI.GT.TOLERA) TOLERA=FORCEI
      FORCE(I)=FORCE(I)-FI(I)
 1000 CONTINUE
C     ITERATION TERMINATED IF INCREMENTAL FORCES ARE WITHIN A TOLERANCE
C     (TAKEN AS A CERTAIN PERCENTAGE OF THE LARGEST FORCE AT THE BEGINNING
C     OF THE ITERATION, TLR=PERCENTAGE)
      TOLERA=TLR*TOLERA
C     BEGIN THE ITERATION PROCESS
      ICO=0
 1020 CONTINUE
      NCC=0
      NCP=0
      NSY=0
      ICO=ICO+1
      IF(ICO.GT.15) GO TO 9994
      DO 1001 I=1,NUMNP
      IF(KOD(I).EQ.0) GO TO 1001
      IF(KOD(I).EQ.1) GO TO 1002
      KI=2*I
      ICHECK=2
      GO TO 1003
 1002 IF(KOD(I).EQ.2) GO TO 1001
      KI=2*I-1
      ICHECK=1
 1003 IF(KARA.EQ.1) GO TO 1004
      FORCE(KI)=FORCE(KI)-FI(KI)
 1004 FI(KI)=0.0
      IF(ICHECK.EQ.2) GO TO 1002
 1001 CONTINUE
      CALL CHOLER(FI,DI)
C     CUMULATION OF DISPLACEMENTS
      DO 1005 I=1,NTOT
      FI(I)=0.0
 1005 DISP(I)=DISP(I)+DI(I)
      IF(DISPMX.EQ.0) GO TO 1019
      YOL=ABS(DISP(IPOINT))
      IF(YOL.GT.DISPMX) GO TO 9997
 1019 CONTINUE
      DO 1060 I=1,NUMEL
      LEF=INODE(I,9)
      CCONP=PELMA(LEF,9)
```

```
                CTENSN=PELMAT(LEF,10)
                CALL STRESS(7,0)
                DO 1061 K=1,4
          175   DO 1023 J=1,3
           1023 EXS(J,K)=0.0
                IF(NCRUSH(I,K).EQ.1) GO TO 1061
                IF(NCRACK(I,K).EQ.0) GO TO 1180
                C1=-0.9*CCOMP
          180   IF(NCRACK(I,K).GT.0) C1=-0.7*CCOMP
                C2=C1*C1
C               INCREMENTAL STRESSES
C               VO(I,J)=STRESSES FROM PREVIOUS LOADING
C               VD(I,J)=STRESSES FROM PRESENT LOADING
          185   DO 1024 J=1,3
                VO(J,K)=CSI(I,J,K)
                CSI(I,J,K)=CSI(I,J,K)+CSI(J,K)
           1024 VO(J,K)=CSI(I,J,K)
                IF(NCRACK(I,K).EQ.1) GO TO 1150
          190   NEW CRACK FORMATION
                CALL MOHR(I,K)
                IF(S1.LT.0.0) GO TO 1290
                IF(NCRUSH(I,K).EQ.0) GO TO 1131
                NCRUSH(I,K)=0
          195   NCP=NCP+1
           1131 IF(S2.LT.0.0) GO TO 1270
C               CHECK BIAXIAL TENSION
                IF(S1.GT.S2) GO TO 1190
                IF(S2.GT.CTENSN) GO TO 1186
          200   GO TO 1180
           1190 IF(S1.GT.CTENSN) GO TO 1184
                GO TO 1180
C               CHECK TENSION-COMPRESSION
           1270 TENSON=S1-S2*CTENSN/CCOMP
          205   IF(TENSON.GT.CTENSN) GO TO 1184
                GO TO 1186
           1290 IF(S2.LT.0.0) GO TO 1160
                IF(NCRUSH(I,K).EQ.0) GO TO 1132
                NCRUSH(I,K)=0
          210   NCP=NCP+1
           1132 TENSON=S2-S1*CTENSN/CCOMP
                IF(TENSON.GT.CTENSN) GO TO 1185
                GO TO 1180
           1184 FE=THETA+1.5707963268
          215   VA(1,K)=S1
                VA(2,K)=PELMAT(LEF,4)*S1
                CSI(I,1,K)=S2-VA(2,K)
                GO TO 1186
           1185 FE=THETA
          220   VA(1,K)=S2
                VA(2,K)=PELMAT(LEF,4)*S2
                CSI(I,1,K)=S1-VA(2,K)
           1186 ANGLE=FE-1.5707963268
                T1=COS(ANGLE)
          225   T2=SIN(ANGLE)
                EXS(J,K)=(VA(1,K)-VA(2,K))*T1*T2+EXS(J,K)
                T1=T1*T1
                T2=T2*T2
```

```
                EXS(1,K)=VA(1,K)*T1+VA(2,K)*T2+EXS(1,K)
230             EXS(2,K)=VA(1,K)*T2+VA(2,K)*T1+EXS(2,K)
                NCC=NCC+1
                NCRACK(I,K)=1
                CRF(I,K)=FE
                GO TO 1180
235          1170 IF(CS(I,1,K).LT.0.0) GO TO 1170
C       FORMATION OF SECOND SET OF CRACKS IN CRACKED CONCRETE
                IF(CS(I,1,K).LT.CTENSN) GO TO 1180
                NCRACK(I,K)=5
                CRS(I,K)=CRF(I,K)
240             CRF(I,K)=CRF(I,K)+1.5707963267
                GO TO 1172
C       PLASTICITY OF UNCRACKED CONCRETE
C       T3=YIELD CRITERION (VON MISES)
          1180 T3=S1*S1+S2*S2-S1*S2
245             IF(T3.GT.C2) GO TO 1182
                NCRUSH(I,K)=0
                GO TO 1180
          1182 CALL STRESS(I,DISP,1)
C       T1=EQUIVALENT STRAIN (VON MISES CRITERION)
250             T1=SNI(1,K)*SNI(1,K)+SNI(2,K)*SNI(2,K)-SNI(1,K)*SNI(2,K)+1.5*SNI(3
                *,K)*SNI(3,K)
                T1=-SQRT(T1)
C       PELMAT(LEF,13) = MAX. ALLOWABLE COMPRESSION STRAIN IN CONCRETE
                IF(T1.GT.PELMAT(LEF,13)) GO TO 1159
255     C       CRUSHED CONCRETE
                NCRUSH(I,K)=1
                NCC=NCC+1
                EXS(1,K)=CS(I,1,K)+EXS(1,K)
                EXS(2,K)=CS(I,2,K)+EXS(2,K)
260             EXS(3,K)=CS(I,3,K)+EXS(3,K)
                GO TO 1061
          1159 CALL STRESS(I,DI,1)
                IF(NCRUSH(I,K).EQ.2) GO TO 1032
C       SCALING
265             T2=VC(1,K)*VC(1,K)+VC(2,K)*VC(2,K)-VC(1,K)*VC(2,K)+3.0*VC(3,K)*VC(
                *3,K)
                T2=SQRT(T2)
                T3=SQRT(T3)
                T3=(T3-CCOMP)/(T3-T2)
270     C       T3 IS THE SCALING FACTOR
                DO 1163 J=1,3
                SNI(J,K)=SNI(J,K)*T3
                CSI(J,K)=CSI(J,K)*T3
          1163 CS(I,J,K)=CSI(I,J,K)-CSI(J,K)
275             NCRUSH(I,K)=2
                NCP=NCP+1
                GO TO 1164
          1032 DO 1033 J=1,3
          1033 CS(I,J,K)=VC(J,K)
280       1164 VA(1,K)=CS(I,1,K)-0.5*CS(I,2,K)
                VA(2,K)=CS(I,2,K)-0.5*CS(I,1,K)
                VA(3,K)=CS(I,3,K)*3.0
C       ELASTO-PLASTIC MATRIX
                T1=0.0
285             DO 1025 J=1,3
```

```
      T2=0.0
      DO 1026 KJ=1,3
 1026 T2=T2+DC(J,KJ,LEF)*VA(KJ,K)
 1025 T1=T1+VA(J,K)*T2
  290 DO 1027 J=1,3
      DO 1027 KJ=1,3
 1027 DEP(J,KJ)=VA(J,K)*VA(KJ,K)
      DO 1028 J=1,3
      DO 1028 KJ=1,3
  295 DA(J,KJ)=0.0
      IF(J.EQ.KJ) DA(J,KJ)=1.
      DO 1028 N=1,3
 1028 DA(J,KJ)=DA(J,KJ)-DEP(J,N)*DC(N,KJ,LEF)/T1
      DO 1029 J=1,3
  300 DO 1029 KJ=1,3
      DEP(J,KJ)=0.0
      DO 1029 N=1,3
 1029 DEP(J,KJ)=DEP(J,KJ)+DC(J,N,LEF)*DA(N,KJ)
      DO 1030 J=1,3
  305 VA(J,K)=0.0
      DO 1030 KJ=1,3
 1030 VA(J,K)=VA(J,K)+DEP(J,KJ)*SNI(KJ,K)
      DO 1031 J=1,3
      EXS(J,K)=CS(I,J,K)-VA(J,K)+EXS(J,K)
  310 1031 CS(I,J,K)=CS(I,J,K)+VA(J,K)
C     SCALE FINAL (ELASTO-PLASTIC) STRESSES TO THE YIELD SURFACE
      T3=CS(I,1,K)*CS(I,1,K)+CS(I,2,K)*CS(I,2,K)-CS(I,1,K)*CS(I,2,K)+3.0
     **CS(I,3,K)*CS(I,3,K)
      T3=SQRT(T3)/CCOMP
  315 DO 1034 J=1,3
      VA(J,K)=CS(I,J,K)
      CS(I,J,K)=CS(I,J,K)/T3
 1034 EXS(J,K)=VA(J,K)-CS(I,J,K)+EXS(J,K)
      GO TO 1180
  320 C     PLASTICITY OF CRACKED CONCRETE
 1170 IF(CS(I,1,K).GT.C1) GO TO 1180
      TB=SNI(1,K)*T1*T1+SNI(2,K)*T2*T2+SNI(3,K)*T1*T2
      IF(TB.GT.PELMAT(LEF,13)) GO TO 1175
      NCRUSH(I,K)=1
  325 CRS(I,K)=CRF(I,K)
      CRF(I,K)=CRF(I,K)+1.570796326?9
 1172 NCC=NCC+1
      S1=CS(I,1,K)
      GO TO 1177
  330 1175 S1=CS(I,1,K)-C1
      CS(I,1,K)=C1
      IF(NCRUSH(I,K).EQ.2) GO TO 1177
      NCRUSH(I,K)=2
      NCP=NCP+1
  335 1177 EXS(1,K)=S1*T1*T1+EXS(1,K)
      EXS(2,K)=S1*T2*T2+EXS(2,K)
      EXS(3,K)=S1*T1*T2+EXS(3,K)
      IF(NCPUSH(I,K).EQ.1) GO TO 1861
C     REINFORCEMENT
  340 1180 DO 1845 J=1,2
      KJ=2*J+4
      N=KJ-1
```

```
      IF(PELMAT(LEF,N).EQ.0.0) GO TO 1045
      LUK=J+18
345   YIELD1=PELMAT(LEF,LUK)
      S1=ABS(SS(I,J,K))
      IF(S1.GE.YIELD1) GO TO 1045
      SS(I,J,K)=SS(I,J,K)+SSI(J,K)
      IF(NCRACK(I,K).LT.5) GO TO 1035
350   IF(SS(I,J,K).GE.0.0) GO TO 1035
      IF(SS(I,J,K).LT.-YIELD1) GO TO 1036
      SS(I,J,K)=-YIELD1
      NSY=NSY+1
      GO TO 1045
355   1035 S1=ABS(SS(I,J,K))
      IF(S1.LE.YIELD1) GO TO 1045
      IF(SS(I,J,K).GT.0.0) GO TO 1038
      1036 S1=SS(I,J,K)+YIELD1
      SS(I,J,K)=-YIELD1
360   GO TO 1039
      1038 S1=SS(I,J,K)-YIELD1
      SS(I,J,K)=YIELD1
      1039 T1=COS(PELMAT(LEF,KJ))
      T2=SIN(PELMAT(LEF,KJ))
365   S1=S1*PELMAT(LEF,N)
      EXS(1,K)=EXS(1,K)+S1*T1*T1
      EXS(2,K)=EXS(2,K)+S1*T2*T2
      EXS(3,K)=EXS(3,K)+S1*T1*T2
      NSY=NSY+1
370   1045 CONTINUE
      1061 CONTINUE
      DO 1191 J=1,3
      DO 1191 K=1,4
      IF(EXS(J,K).NE.0.0) GO TO 1192
375   1191 CONTINUE
      GO TO 1060
C     EQUIVALENT NODAL FORCES - PR
      1192 CALL SHAPE(I,1)
      DO 1048 J=1,8
380   J2=2*J
      J1=J2-1
      PR(J1)=0.0
      PR(J2)=0.0
      DO 1048 K=1,4
385   PR(J1)=PR(J1)+V(J,K)*EXS(1,K)+Z(J,K)*EXS(3,K)
      1048 PR(J2)=PR(J2)+Z(J,K)*EXS(2,K)+V(J,K)*EXS(3,K)
      THICK=PELMAT(LEF,1)
      DO 1194 J=1,8
      J2=J*2
390   J1=J2-1
      K2=INODE(I,J)*2
      K1=K2-1
      FI(K1)=FI(K1)+PR(J1)*THICK
      1194 FI(K2)=FI(K2)+PR(J2)*THICK
395   1068 CONTINUE
      WRITE(NW,555) ICO,NCC
      IF(NSY.GT.0) WRITE(NW,557) NSY
      IF(NCP.GT.0) WRITE(NW,556) NCP
C     NODSUM=TOTAL NUMBER OF NODE CHANGES BETWEEN THE REASSEMBLAGES OF
```

```
C     THE STIFFNESS MATRIX
C     IF(MODSUM.GT.0) REASSEMBLE THE STIFFNESS MATRIX
      MODSUM=MODSUM+NCC+NST
C     MCIK=LOAD INCREMENT AFTER WHICH THE OUTPUT IS GIVEN FOR EACH ITERATION
      IF(MI.LE.MCIK) GO TO 2323
      CALL FORDIS(FORCE,DISP,IDIFOR,IPOINT)
      CALL XPRINT
 2323 IF(MODSUM.LE.0) GO TO 2324
C     REASSEMBLE THE GLOBAL STIFFNESS MATRIX
      CALL NEWSTF
      CALL MODIFY
      CALL CHOLE1(KOT)
      IF(KOT.EQ.1) GO TO 9995
      MODSUM=0
      GO TO 2020
 2324 DO 1063 I=1,NTOT
      IF(FI(I).EQ.0.0) GO TO 1063
      T1=ABS(FI(I))
      IF(T1.GT.TOLERA) GO TO 2020
 1063 CONTINUE
      GO TO 2025
 2020 KARA=1
      GO TO 1020
 2025 IF(MI.GT.MCIK) GO TO 2370
      CALL FORDIS(FORCE,DISP,IDIFOR,IPOINT)
      CALL XPRINT
 2378 IF(MI.LE.MLIMIT) GO TO 1010
      GO TO 11
 9991 WRITE(NW,9990)
      GO TO 9993
 9995 WRITE(NW,9994)
      GO TO 9993
 9997 WRITE(NW,9996)
 9993 CALL FORDIS(FORCE,DISP,IDIFOR,IPOINT)
      CALL XPRINT
      GO TO 11
 9999 WRITE(NW,9998) ND
   11 CONTINUE
   18 FORMAT(I5)
   16 FORMAT(I5/8A10)
   17 FORMAT(1H1,///,' PROBLEM',I2,//,' NOCH =',I2,/////,1X,8A10)
  555 FORMAT(//,' ITERATION NO.',I2,5X,' NUMBER OF CRACK MODE CHANGES ='
     ',I2)
  556 FORMAT(/,22X,'CONCRETE PLASTICITY CHANGES  =',I2)
  557 FORMAT(/,22X,'REINF.   PLASTICITY CHANGES  =',I2)
 1065 FORMAT(///,' INCREMENTAL LOADING NO.',I2)
 5000 FORMAT(2I5,3F10.0,2I5,/(8F10.0))
 5001 FORMAT(///,' CONTROL PARAMETERS',
     1        //,' IDIFOR (DISP. OUTPUT CONTROL)          =',I5,
     2         /,' IPOINT (LOC. OF LIMIT DISP. CONTROL)  =',I5,
     3         /,' DISPMX (LIMIT DISPLACEMENT)           =',F8.4,
     4         /,' TLR    (RESIDUAL FORCE TOLERANCE)     =',F8.4,
     5         /,' BETA   (SHEAR RETENTION FACTOR)       =',F8.4,
     6         /,' MCIK   (STRESS OUTPUT CONTROL)        =',I5,
     7         /,' MLIMIT (NUMBER OF LOAD INCREMENTS)    =',I5,
     8         /,' LOAD INCREMENT RATIOS                 =',10F8.5,/,(39X,
     810F8.5))
```

```
 9990 FORMAT(//,' NUMBER OF ITERATIONS FOR THIS LOAD INCREMENT EXCEEDS 1
     *5, EXECUTION TERMINATED')
 9994 FORMAT(//,' UNSTABLE STIFFNESS MATRIX, EXECUTION TERMINATED')
 9996 FORMAT(//,' LIMIT DEFORMATION REACHED, EXECUTION TERMINATED')
 9998 FORMAT(//,' HALF BAND WIDTH =',I3,' GREATER THAN 46 (MAX. ALLOWED)
     *, EXECUTION TERMINATED')
      STOP 123
      END
```

```
      SUBROUTINE BANDWD
      COMMON/DATA/KOD(149),X(149),Y(149),INODE(40,9),PELMAT(9,13),DC(3,3
     *,9)
      COMMON/LET/NUMNP,NUMEL,NELTYP,THICK,NTOT,NB,LEF
      NB=0
      DO 68 IQ=1,NUMEL
      MAX=0
      MIN=100000
      DO 69 JQ=1,8
      IF(MAX.LT.INODE(IQ,JQ)) MAX=INODE(IQ,JQ)
      IF(MIN.GT.INODE(IQ,JQ)) MIN=INODE(IQ,JQ)
   69 CONTINUE
      MAXMIN=MAX-MIN
      IF(NB.LT.MAXMIN) NB=MAXMIN
   68 CONTINUE
      NB=(NB+1)*2
      RETURN
      END
```

```
      SUBROUTINE CHOLE1(KOT)
      COMMON/VALU/DISP(298),FORCE(298),S(298,46)
      COMMON/LET/NUMNP,NUMEL,NELTYP,THICK,NTOT,NB,LEF
      KOT=0
      PSL=1.0E-10
      IF(S(1,1).LE.PSL) GO TO 11
      S(1,1)=SQRT(S(1,1))
      FCTR=1.0/S(1,1)
      DO 2 JJ=2,NB
    2 S(1,JJ)=S(1,JJ)*FCTR
      N1=NTOT-NB+1
      NT=NB
      DO 5 I=2,NTOT
      IF(I.GT.N1) NT=NTOT-I+1
      I2=I-1
      DO 5 J=1,NT
      SUM=0.0
      IF(J.EQ.NB) GO TO 6
      I1=I+J-NB
      IF(I1.LT.1) I1=1
      DO 10 K=I1,I2
      L=I-K+1
      N=L+J-1
   10 SUM=SUM+S(K,L)*S(K,N)
      IF(J.GT.1) GO TO 6
      TOL=S(I,1)-SUM
      IF(TOL.LE.PSL) GO TO 11
      S(I,1)=SQRT(TOL)
      GO TO 5
    6 IF(ABS(S(I,1)).LE.PSL) GO TO 11
      S(I,J)=(S(I,J)-SUM)/S(I,1)
    5 CONTINUE
      GO TO 12
   11 KOT=1
   12 RETURN
      END
```

```
      1         SUBROUTINE CHOLE2(FI,DI)
                DIMENSION FI(298),DI(298)
                COMMON/VALU/DISP(298),FORCE(298),S(298,46)
                COMMON/LET/NUMNP,NUMEL,NELTYP,THICK,NTOT,NB,LEF
      5         DI(1)=FI(1)/S(1,1)
                DO 15 I=2,NTOT
                I1=I-NB+1
                IF(I1.LT.1) I1=1
                I2=I-1
     10         SUM=0.0
                DO 20 K=I1,I2
                L=I-K+1
             20 SUM=SUM+S(K,L)*DI(K)
             15 DI(I)=(FI(I)-SUM)/S(I,1)
     15      C  BACK SUBSTITUTION
                DI(NTOT)=DI(NTOT)/S(NTOT,1)
                DO 25 L=2,NTOT
                I=NTOT-L+1
                SUM=0.0
     20         N1=L
                IF(L.GT.NB) N1=NB
                DO 27 J=2,N1
                K=I+J-1
             27 SUM=SUM+S(I,J)*DI(K)
     25      25 DI(I)=(DI(I)-SUM)/S(I,1)
                RETURN
                END
```

```
      SUBROUTINE ELASMX
      DIMENSION PR(3)
      COMMON/DATA/KOD(149),X(149),Y(149),INODE(40,9),PELMAT(9,13),DC(3,3
     *,9)
      COMMON/LET/NUMNP,NUMEL,NELTYP,THICK,NTOT,NB,LEF
      COMMON/IO/NR,NW
C     CONVERT ANGLES FROM DEGREES TO RADIANS - MULTIPLY BY CHANGE
      CHANGE=0.01745329
      DO 10 I=1,NELTYP
C     CONCRETE ELASTICITY MATRIX
      CNSTNT=PELMAT(I,3)/(1.0-PELMAT(I,4)*PELMAT(I,4))
      DC(1,1,I)=CNSTNT
      DC(1,2,I)=CNSTNT*PELMAT(I,4)
      DC(1,3,I)=0.0
      DC(2,1,I)=DC(1,2,I)
      DC(2,2,I)=DC(1,1,I)
      DC(2,3,I)=0.0
      DC(3,1,I)=0.0
      DC(3,2,I)=0.0
      DC(3,3,I)=CNSTNT*((1.0-PELMAT(I,4))/2.0)
C     STEEL ELASTICITY MATRIX
      DO 14 K=5,7,2
      IF(PELMAT(I,K).EQ.0.0) GO TO 14
      K1=K+1
      IF(PELMAT(I,K1).EQ.0.0) GO TO 11
      IF(PELMAT(I,K1).EQ.90.0) GO TO 12
      PELMAT(I,K1)=PELMAT(I,K1)*CHANGE
      C1=COS(PELMAT(I,K1))
      S1=SIN(PELMAT(I,K1))
      GO TO 13
   11 C1=1.0
      S1=0.0
      GO TO 13
   12 C1=0.0
      S1=1.0
   13 PR(1)=C1*C1
      PR(2)=S1*S1
      PR(3)=C1*S1
      CNST=PELMAT(I,2)*PELMAT(I,K)
      DO 16 LL=1,3
      DO 16 MM=1,3
   16 DC(LL,MM,I)=DC(LL,MM,I)+CNST*PR(LL)*PR(MM)
   14 CONTINUE
   10 CONTINUE
      RETURN
      END
```

```
      SUBROUTINE FORDIS(FI,DI,IDIFOR,IPOINT)
      DIMENSION FI(299),DI(299)
      COMMON/DATA/KOD(149),X(149),Y(149),INODE(48,9),PELMAT(9,13),DG(3,3
     *,9)
      COMMON/LET/NUMNP,NUMEL,NELTYP,THICK,NTOT,NB,LEF
      COMMON/IO/NR,NW
      WRITE(NW,37)
      DO 38 I=1,NTOT
      IF(FI(I).EQ.0.0) GO TO 38
      IYA=I/2
      IYA1=(I-1)/2
      IF(IYA.EQ.IYA1) GO TO 36
      KK=IYA
      IF(KOD(KK).GT.1) GO TO 38
      JDR=2
      GO TO 35
   36 KK=IYA+1
      JDR=1
      KALK=KOD(KK)+1
      GO TO (35,38,35,38) KALK
   35 WRITE(NW,34) KK,FI(I),JDR
   38 CONTINUE
      IF(IDIFOR.EQ.0) GO TO 42
      WRITE(NW,39)
      IF(IDIFOR.EQ.2) GO TO 45
      ILAC=(IPOINT+1)/2-IPOINT/2
      IF(ILAC.EQ.0) GO TO 43
      ILAC=(IPOINT+1)/2
      IL1=IPOINT
      IL2=IL1+1
      GO TO 44
   43 ILAC=IPOINT/2
      IL2=IPOINT
      IL1=IL2-1
   44 WRITE(NW,41) ILAC,DI(IL1),DI(IL2)
      GO TO 42
   45 DO 40 ILAC=1,NUMNP
      IL2=2*ILAC
      IL1=IL2-1
   40 WRITE(NW,41) ILAC,DI(IL1),DI(IL2)
   34 FORMAT(I4,F12.2,I7)
   37 FORMAT(///,' NODAL FORCES',///,' NODE    VALUE    DIRECTION (1 FOR X
     *,2 FOR Y)',/)
   39 FORMAT(///,6X,' NODAL DISPLACEMENTS',///,6X,' NODE       DISP. X'
     *       DISP. Y',//)
   41 FORMAT(I10,2E16.7)

   42 RETURN
      END
```

```
      SUBROUTINE FUNC(XXXX,YYYY,IMA,JMA)
      COMMON/ISOPAR/XX(8),YY(8),D(3,3,4),EST(16,16),OS(2,2),XI(14),F(14)
     *,XN(8),YN(8),V(8,4),Z(8,4),A(21,DET,KOUNT
      X1(X,Y)=0.25*(1.0-X)*(2.0*Y+Y)
      X2(X,Y)=-X*(1.0-Y)
      X3(X,Y)=0.25*(1.0-Y)*(2.0*X-Y)
      X4(X)=0.5*(1.0-X*X)
      X5(X,Y)=0.25*(1.0+Y)*(2.0*X+Y)
      X6(X,Y)=-X*(1.0+Y)
      X7(X,Y)=0.25*(1.0+Y)*(2.0*X-Y)
      XN(1)=X1(XXXX,YYYY)
      XN(2)=X2(XXXX,YYYY)
      XN(3)=X3(XXXX,YYYY)
      XN(4)=X4(YYYY)
      XN(5)=X5(XXXX,YYYY)
      XN(6)=X6(XXXX,YYYY)
      XN(7)=X7(XXXX,YYYY)
      XN(8)=-XN(4)
      YN(1)=X1(YYYY,XXXX)
      YN(2)=-X4(XXXX)
      YN(3)=X7(YYYY,XXXX)
      YN(4)=X6(YYYY,XXXX)
      YN(5)=X5(YYYY,XXXX)
      YN(6)=-YN(2)
      YN(7)=X3(YYYY,XXXX)
      YN(8)=X2(YYYY,XXXX)
      XS=0.0
      XT=0.0
      YS=0.0
      YT=0.0
      DO 60 I=1,8
      XS=XS+XN(I)*XX(I)
      YS=YS+XN(I)*YY(I)
      XT=XT+YN(I)*XX(I)
   60 YT=YT+YN(I)*YY(I)
      DET=XS*YT-XT*YS
      SX=YT/DET
      TX=-YS/DET
      SY=-XT/DET
      TY=XS/DET
C     V(I,4)=DNI/DX  Z(I,4)=DNI/DY  ALL EVALUATED AT THE INTEGRATION POINTS
      V(IMA,KOUNT)=SX*XN(IMA)+TX*YN(IMA)
      Z(IMA,KOUNT)=SY*XN(IMA)+TY*YN(IMA)
      IF(IMA.EQ.JMA) GO TO 100
      V(JMA,KOUNT)=SX*XN(JMA)+TX*YN(JMA)
      Z(JMA,KOUNT)=SY*XN(JMA)+TY*YN(JMA)
  100 RETURN
      END
```

```
      SUBROUTINE INTEG(IMA,JMA)
      COMMON/ISOPAR/XX(8),YY(8),D(3,3,4),EST(16,16),OS(2,2),XI(14),F(14)
     *,XN(8),YN(8),V(8,4),Z(8,4),A(2),DET,KOUNT
C     THE INTEGRALS ARE CALCULATED USING GAUSSIAN QUADRATURE
      DO 5 J=1,14
    5 XI(J)=0.0
      KOUNT=0
      DO 10 J=1,2
      DO 10 I=1,2
      KOUNT=KOUNT+1
      CALL FUNC(A(I),A(J),IMA,JMA)
      AREA=ABS(DET)
C     F(I) ARE THE FUNCTIONS TO BE INTEGRATED
      F(1)=V(IMA,KOUNT)*V(JMA,KOUNT)*D(1,1,KOUNT)
      F(2)=V(IMA,KOUNT)*V(JMA,KOUNT)*D(1,3,KOUNT)
      F(3)=V(IMA,KOUNT)*V(JMA,KOUNT)*D(3,3,KOUNT)
      F(4)=V(IMA,KOUNT)*Z(JMA,KOUNT)*D(1,2,KOUNT)
      F(5)=V(IMA,KOUNT)*Z(JMA,KOUNT)*D(1,3,KOUNT)
      F(6)=V(IMA,KOUNT)*Z(JMA,KOUNT)*D(2,3,KOUNT)
      F(7)=V(IMA,KOUNT)*Z(JMA,KOUNT)*D(3,3,KOUNT)
      F(8)=V(JMA,KOUNT)*Z(IMA,KOUNT)*D(1,2,KOUNT)
      F(9)=V(JMA,KOUNT)*Z(IMA,KOUNT)*D(1,3,KOUNT)
      F(10)=V(JMA,KOUNT)*Z(IMA,KOUNT)*D(2,3,KOUNT)
      F(11)=V(JMA,KOUNT)*Z(IMA,KOUNT)*D(3,3,KOUNT)
      F(12)=Z(IMA,KOUNT)*Z(JMA,KOUNT)*D(2,2,KOUNT)
      F(13)=Z(IMA,KOUNT)*Z(JMA,KOUNT)*D(2,3,KOUNT)
      F(14)=Z(IMA,KOUNT)*Z(JMA,KOUNT)*D(3,3,KOUNT)
      DO 20 K=1,14
   20 XI(K)=XI(K)+F(K)*AREA
   10 CONTINUE
      RETURN
      END
```

```
      SUBROUTINE LIMIT
      COMMON/DATA/MOD(1600),XI(1600),YI(1600),INODE(600,9),PELMAT(9,13),BC(3,3
     *,9)
      COMMON/VALU/DISP(2000),FORCE(2000),STRSS(600,6)
      COMMON/ISOPAR/XX(8),YY(8),DN(3,3,4),FST(24,16),QS(2,2),XI(16),F(16)
     *,XN(8),YN(8),V(3,3),Z(8,8),AREA,DET,KOUNT
      COMMON/LIT/NUMNP,NUMEL,NELTYP,THICK,NTOT,NN,LEF
      COMMON/IO/NR,NW
      COMMON/STRS/CS(600,3,4),SS(600,2,4),GSI(3,4),SSI(2,4),S1,S2,SNI(3,4)
     *,ALPHA,THETA,FE,CRF(600,4),CRS(600,4),MCRXG(600,4),MCRUSH(600,4)
      COMMON/NONLIN/NLINIT,DIV(25),MGIK,ILR,IOIFOR,IPOINT,DISPMX,BETA
      FT=10.2E+300
      FC=FT
      FS1=FT
      FS2=FT
      IFC=0
      IFT=0
      IFS1=0
      IFS2=0
      LFC=0
      LFT=0
      LFS1=0
      LFS2=0
      DO 18 I=1,NUMEL
      LEF=INODE(I,9)
      CCOMP=0.9*PELMAT(LEF,9)
      STENSN=PELMAT(LEF,10)
      FTC=STENSN/CCOMP
      CALL STRESS(I,DUSP,3)
      DO 11 K=1,4
      DO 16 J=1,3
      CS(I,J,K)=GSI(J,K)
      IF(J.EQ.3) GO TO 16
      SS(I,J,K)=SSI(J,K)
   16 CONTINUE
      CALL HUMRE(I,K)
C     CONCRETE STRESSES
C     CHECK BIAXIAL COMPRESSION
      IF(S1.GT.0.0) GO TO 20
      IF(S2.GT.0.0) GO TO 30
      COMP=S1*S1+S1*S2+S2*S2
      IF(COMP.EQ.0.0) GO TO 50
      COMP=CCOMP/COMP
      IF(FC.LE.COMP) GO TO 50
      FC=COMP
      IFC=1
      LFC=K
      GO TO 50
C     CHECK COMPRESSION-TENSION
   20 IF(S2.GT.0.0) GO TO 40
      TENSON=S1-FTC*S2
      GO TO 45
   30 TENSON=S2-FTC*S1
      GO TO 45
C     CHECK BIAXIAL TENSION
   40 TENSON=S1
      IF(S1.LT.S2) TENSON=S2
```

```
      IF(TENSON.EQ.0.0) GO TO 50
      TENSON=CTENSN/TENSON
      IF(FT.LE.TENSON) GO TO 50
      FT=TENSON
      IFT=I
      LFT=K
C     STEEL STRESSES
   50 IF(SS(I,1,K).EQ.0.0) GO TO 55
      STEEL1=ABS(SS(I,1,K))
      STEEL1=PELMAT(LEF,11)/STEEL1
      IF(FS1.LE.STEEL1) GO TO 55
      FS1=STEEL1
      IFS1=I
      LFS1=K
   55 IF(SS(I,2,K).EQ.0.0) GO TO 11
      STEEL2=ABS(SS(I,2,K))
      STEEL2=PELMAT(LEF,12)/STEEL2
      IF(FS2.LE.STEEL2) GO TO 11
      FS2=STEEL2
      IFS2=I
      LFS2=K
   11 CONTINUE
   10 CONTINUE
      WRITE(NW,300) IFC,LFC,IFT,LFT,IFS1,LFS1,IFS2,LFS2
C     SELECT THE SCALING FACTOR FS= ELASTIC LIMIT
      FACTOR=FT
      IF(FACTOR.GT.FC) FACTOR=FC
      IF(FACTOR.GT.FS1) FACTOR=FS1
      IF(FACTOR.GT.FS2) FACTOR=FS2
      IF(FACTOR.EQ.FT) WRITE(NW,111) LFT,IFT,FT
      IF(FACTOR.EQ.FC) WRITE(NW,111) LFC,IFC,FC
      IF(FACTOR.EQ.FS1) WRITE(NW,111) LFS1,IFS1,FS1
      IF(FACTOR.EQ.FS2) WRITE(NW,111) LFS2,IFS2,FS2
      DO 200 I=1,NTOT
      DISP(I)=DISP(I)*FACTOR
  200 FORCE(I)=FORCE(I)*FACTOR
      WRITE(NW,88)
      DO 210 I=1,NUMEL
      DO 203 K=1,4
      DO 205 J=1,3
      SN(J,K)=SN(J,K)*FACTOR
  205 CS(I,J,K)=CS(I,J,K)*FACTOR
      DO 206 J=1,2
  206 SS(I,J,K)=SS(I,J,K)*FACTOR
  203 CONTINUE
  210 CONTINUE
      CALL FORBIS(FORCE,DISP,IDIFD,IPOINT)
      CALL XPRINT
   88 FORMAT(//,' END OF ELASTIC ANALYSIS SCALED VALUES ARE GIVEN BELOW')
  300 FORMAT(//,' CRITICAL STRESS RATIOS   ELEM   LOC',//,
     1' CONCRETE COMPRESSION      ',I4,I6,/,
     2' CONCRETE TENSION          ',I4,I6,/,
     3' REINFORCEMENT (ORGN 1)    ',I4,I6,/,
     4' REINFORCEMENT (ORGN 2)    ',I4,I6)
  111 FORMAT(//,' AT LOCATION',I2,' ELEMENT',I3,' IS CRITICAL, MULTIPLIE
     1R TO REACH ELASTIC LIMIT ',F14.8)
      RETURN
```

END

```
      SUBROUTINE MASTER(N)
      COMMON/DATA/KOD(149),X(149),Y(149),INODE(40,8),PELMAT(9,13),DC(3,3
     *,9)
      COMMON/VALU/DISP(298),FORCE(298),S(298,46)
      COMMON/ISOPAR/XX(8),YY(9),D(3,3,9),EST(16,16),DS(2,2),XI(14),F(14)
     *,XN(8),YN(8),V(8,4),Z(8,4),A(2),DET,KOUNT
      DO 110 I=1,8
      DO 110 J=I,8
      IF(INODE(N,I).LT.INODE(N,J)) GO TO 111
      K2=2*INODE(N,J)
      L2=2*INODE(N,I)
      GO TO 112
  111 K2=2*INODE(N,I)
      L2=2*INODE(N,J)
  112 K1=K2-1
      L1=L2-1
      DO 110 K=K1,K2
      DO 110 L=L1,L2
      IF(L.LT.K) GO TO 110
      IF(INODE(N,I).LT.INODE(N,J)) GO TO 113
      II=K-K1+2*J-1
      JJ=L-L1+2*I-1
      GO TO 119
  113 II=K-K1+2*I-1
      JJ=L-L1+2*J-1
  119 M=L-K+1
      S(K,M)=S(K,M)+EST(II,JJ)
  110 CONTINUE
      RETURN
      END
```

```
      SUBROUTINE MODIFY
      COMMON/DATA/KOD(149),X(149),Y(149),INODE(40,9),PELMAT(9,13),DC(3,3
     *,9)
      COMMON/VALU/DISP(298),FORCE(298),S(298,46),
      COMMON/LET/NUMNP,NUMEL,NELTYP,THICK,NTOT,NB,LEF
      DO 750 I=1,NUMNP
      IF(KOD(I).EQ.0) GO TO 750
      NSAVI=1
      IF(KOD(I).EQ.2) GO TO 760
      KK=2*I-1
      GO TO 751
  760 IF(KOD(I).EQ.1) GO TO 750
      NSAVI=2
      KK=2*I
  751 FORCE(KK)=DISP(KK)
      S(KK,1)=1.0
      IF(KK-1) 727,727,728
  728 K2=KK-1
      K1=KK-NB+1
      IF(K1.LT.1) K1=1
      DO 777 IKK=K1,K2
      KM=KK-IKK+1
      FORCE(IKK)=FORCE(IKK)-S(IKK,KM)*DISP(KK)
  777 S(IKK,KM)=0.0
      IF(KK-NTOT) 727,750,750
  727 J1=KK+1
      J2=KK+NB-1
      IF(J2.GT.NTOT) J2=NTOT
      DO 773 JKJ=J1,J2
      LM=JKJ-KK+1
      FORCE(JKJ)=FORCE(JKJ)-S(KK,LM)*DISP(KK)
  778 S(KK,LM)=0.0
      IF(NSAVI.EQ.1) GO TO 760
  750 CONTINUE
      RETURN
      END
```

```
      SUBROUTINE MOHR(I,K)
      COMMON/STRS/CS(40,3,4),SS(40,2,4),CSI(3,4),SSI(2,4),S1,S2,SNI(3,4)
     *,ALPHA,THETA,FE,CRF(40,4),CRS(40,4),MCRACK(40,4),MCRUSH(40,4)
C     PRINCIPAL DIRECTION
      FARIK=CS(I,1,K)-CS(I,2,K)
      IF(ABS(FARIK).LT.1.0E-10) GO TO 5
      TANG2=CS(I,3,K)*2.0/FARIK
      THETA=0.5*ATAN(TANG2)
      GO TO 10
    5 THETA=1.5707963267
C     PRINCIPAL STRESSES
   10 T1=COS(THETA)
      T2=SIN(THETA)
      T3=T1*T2*2.0
      T1=T1*T1
      T2=T2*T2
      S1=CS(I,1,K)*T1+CS(I,2,K)*T2+CS(I,3,K)*T3
      S2=CS(I,1,K)*T2+CS(I,2,K)*T1-CS(I,3,K)*T3
      RETURN
      END
```

```
      SUBROUTINE MEMSTF
      DIMENSION VA(3,4)
      COMMON/NONLIN/MLIMIT,DIV(25),MCIK,TLR,IDIFOR,IPOINT,DISPMX,BETA
      COMMON/ISOPAR/XX(8),YY(8),D(3,3,4),EST(16,16),DS(2,2),XI(16),F(16)
     *,XN(8),YN(8),V(8,4),Z(8,4),A(2),DET,KOUNT
      COMMON/DATA/KOD(149),X(149),Y(149),INODE(40,9),PELMAT(9,13),DC(3,3
     *,9)
      COMMON/VALU/DISP(298),FORCE(298),S(298,46)
      COMMON/LET/NUMNP,NUMEL,NELTYP,THICK,NTOT,NB,LEF
      COMMON/STRS/CS(40,3,4),SS(40,2,4),CSI(3,4),SSI(2,4),S1,S2,SNI(3,4)
     *,ALPHA,THETA,FE,CRF(40,4),CRS(40,4),MCRACK(40,4),MCRUSH(40,4)
C     REASSEMBLE THE GLOBAL STIFFNESS MATRIX
      DO 2000 IKI=1,NTOT
      DO 2000 JKJ=1,ND
 2000 S(IKI,JKJ)=0.0
      DO 2050 I=1,NUMEL
      LEF=INODE(I,9)
      DO 2051 K=1,4
      IF(MCRUSH(I,K).EQ.1) GO TO 2059
      IF(MCRACK(I,K).LT.5) GO TO 2060
C     CONCRETE WITH TWO CRACKS OPEN OR CRUSHED (ZERO STIFFNESS)
 2059 DO 2061 J=1,3
      DO 2061 L=1,3
 2061 D(J,L,K)=0.0
      IF(MCRACK(I,K).EQ.5) GO TO 3020
      GO TO 2051
 2060 IF(MCRACK(I,K).EQ.1) GO TO 3000
C     UNCRACKED CONCRETE
      DO 2065 J=1,3
      DO 2065 L=1,3
 2065 D(J,L,K)=DC(J,L,LEF)
      GO TO 2051
C     CRACKED CONCRETE
 3000 CONTINUE
      CONC=PELMAT(LEF,3)
      T1=COS(CRF(I,K))
      T2=SIN(CRF(I,K))
      T3=T1*T2
      T1=T1*T1
      T2=T2*T2
      D(1,1,K)=T1*(T1+4.*T2*BETA)*CONC
      D(1,2,K)=T1*T2*(1.-4.*BETA)*CONC
      D(1,3,K)=(T1*T3+2.*(T2*T3-T1*T3)*BETA)*CONC
      D(2,1,K)=D(1,2,K)
      D(2,2,K)=T2*(T2+4.*T1*BETA)*CONC
      D(2,3,K)=(T2*T3+2.*(T1*T3-T2*T3)*BETA)*CONC
      D(3,1,K)=D(1,3,K)
      D(3,2,K)=D(2,3,K)
      D(3,3,K)=(T1*T2+(T1-T2)*(T1-T2)*BETA)*CONC
C     REINFORCEMENT
 3020 DO 3030 L=6,8,2
      J=L-1
      IF(PELMAT(LEF,J).EQ.0.0) GO TO 3030
      M=(L-4)/2
      LUK=M+10
      S1=ADSISS(I,M,K))
      IF(S1.EQ.PELMAT(LEF,LUK)) GO TO 3030
```

```
      VA(1,K)=COS(PELMAT(LEF,L))
      VA(2,K)=SIN(PELMAT(LEF,L))
60    VA(3,K)=VA(1,K)*VA(2,K)
      VA(1,K)=VA(1,K)*VA(1,K)
      VA(2,K)=VA(2,K)*VA(2,K)
      RATIO=PELMAT(LEF,2)*PELMAT(LEF,3)
      DO 3031 IK=1,3
65    DO 3031 JK=1,3
3031  D(IK,JK,K)=D(IK,JK,K)+RATIO*VA(IK,K)*VA(JK,K)
3030  CONTINUE
2051  CONTINUE
      DO 2066 IK=1,8
70    JL=INODE(I,IK)
      XX(IK)=X(JL)
2066  YY(IK)=Y(JL)
      THICK=PELMAT(LEF,1)
      CALL STIFF
75    CALL MASTER(I)
2050  CONTINUE
      RETURN
      END
```

```
      SUBROUTINE SHAPE(I,IYSA)
      COMMON/DATA/KOD(149),X(149),Y(149),INODE(48,9),PELMAT(9,13),DC(3,3
     *,9)
      COMMON/ISOPAR/XX(8),YY(8),D(3,3,4),EST(16,16),DS(2,2),XI(14),F(14)
     *,XN(8),YN(8),V(8,4),Z(8,4),A(2),DET,KOUNT
C     COMPUTE THE DERIVATIVES OF THE SHAPE FUNCTIONS
C     IYSA=0 DETERMINE DNI/DX AND DNI/DY (NO INTEGRATION)
C     IYSA=1 MULTIPLY DNI/DX AND DNI/DY BY THE JACOBIAN FOR PSEUDO LOADS
      DO 5 IK=1,8
      JL=INODE(I,IK)
      XX(IK)=X(JL)
    5 YY(IK)=Y(JL)
      DO 6 IK=1,8
      KOUNT=0
      DO 7 II=1,2
      DO 7 JJ=1,2
      KOUNT=KOUNT+1
      CALL FUNC(A(JJ),A(II),IK,IK)
      IF(IYSA.EQ.0) GO TO 7
      AREA=ABS(DET)
      V(IK,KOUNT)=V(IK,KOUNT)*AREA
      Z(IK,KOUNT)=Z(IK,KOUNT)*AREA
    7 CONTINUE
    6 CONTINUE
      RETURN
      END
```

```
      SUBROUTINE STIFF
      COMMON/ISOPAR/XX(8),YY(8),D(3,3,4),EST(16,16),OS(2,2),XI(14),F(14)
     *,XN(8),YN(8),V(9,4),Z(8,4),A(2),DET,KOUNT
      COMMON/LET/NUMNP,NUMEL,NELTYP,THICK,NTOP,NB
C     GENERATE THE STIFFNESS MATRIX FOR A
C     LINEAR EDGE STRAIN ISOPARAMETRIC RECTANGLE
      DO 30 IR=1,8
      DO 30 JP=IR,8
      CALL INTEG(IR,JP)
C     OS(IR,JP) IS THE 2*2 STIFFNESS MATRIX FOR A PARTICULAR IR,JP COMBINATION
      OS(1,1)=XI(1)+XI(5)+XI(9)+XI(14)
      OS(1,2)=XI(2)+XI(4)+XI(11)+XI(13)
      OS(2,2)=XI(3)+XI(6)+XI(10)+XI(12)
      IF(IR-JP) 70,71,70
   71 OS(2,1)=OS(1,2)
      GO TO 72
   70 OS(2,1)=XI(2)+XI(7)+XI(8)+XI(13)
   72 IT=2*IR
      IMINUS=IT-1
      JT=2*JP
      JMINUS=JT-1
C     GENERATE THE ELEMENT STIFFNESS MATRIX BY SUPERPOSING THE 2*2 MATRICES
      EST(IMINUS,JMINUS)=OS(1,1)*THICK
      EST(IMINUS,JT)=OS(1,2)*THICK
      EST(IT,JMINUS)=OS(2,1)*THICK
      EST(IT,JT)=OS(2,2)*THICK
   30 CONTINUE
      DO 90 KEL=1,15
      KPLUS=KEL+1
      DO 90 KELP=KPLUS,16
   90 EST(KELP,KEL)=EST(KEL,KELP)
      RETURN
      END
```

```
      SUBROUTINE STRESS(N,DISP,ISAVI)
      DIMENSION DISP(298),W(16)
      COMMON/DATA/KOD(149),X(149),Y(149),INODE(40,9),PELMAT(9,13),DC(3,3
     *,9)
      COMMON/STRS/CS(40,3,4),SS(40,2,4),CSI(3,4),SSI(2,4),S1,S2,SNI(3,4)
     *,ALPHA,THETA,FE,CRF(40,4),CRS(40,4),NCRACK(40,4),NCRUSH(40,4)
      COMMON/ISOPAR/XX(8),YY(8),DJ(3,3,4),EST(16,16),OS(2,2),XI(14),F(14)
     *,XN(8),YN(8),V(8,4),Z(8,4),A(2),DET,KOUNT
      COMMON/NONLIN/MLIMIT,DIV(25),NCIK,TLR,IDIFOR,IPOINT,DISPMX,BETA
C     ISAVI=0 STRAINS AND STRESSES
C     ISAVI=1 STRAINS ONLY
      LEF=INODE(N,9)
C     ELEMENT DISPLACEMENTS
      DO 10 I=1,8
      J=2*INODE(N,I)-1
      K=2*I-1
      W(K)=DISP(J)
      J=J+1
      K=K+1
   10 W(K)=DISP(J)
C     STRAINS
      CALL SHAPE(N,0)
      DO 11 K=1,4
      DO 12 I=1,3
   12 SNI(I,K)=0.0
      DO 11 J=1,8
      J2=2*J
      J1=J2-1
      SNI(1,K)=SNI(1,K)+V(J,K)*W(J1)
      SNI(2,K)=SNI(2,K)+Z(J,K)*W(J2)
   11 SNI(3,K)=SNI(3,K)+V(J,K)*W(J2)+Z(J,K)*W(J1)
      IF(ISAVI.EQ.1) GO TO 20
      DO 19 K=1,4
C     CONCRETE STRESSES
      DO 13 I=1,3
   13 CSI(I,K)=0.0
      IF(NCRACK(N,K).EQ.1) GO TO 17
      IF(NCRACK(N,K).EQ.5) GO TO 18
      DO 16 I=1,3
      DO 16 J=1,3
   16 CSI(I,K)=CSI(I,K)+DC(I,J,LEF)*SNI(J,K)
      GO TO 18
   17 T1=COS(CRF(N,K))
      T2=SIN(CRF(N,K))
      CSI(1,K)=PELMAT(LEF,3)*(SNI(1,K)*T1*T1+SNI(2,K)*T2*T2+SNI(3,K)*T1*
     *T2)
C     STEEL STRESSES
   18 DO 14 I=1,2
      SSI(I,K)=0.0
      J=(I-1)*2+5
      IF(PELMAT(LEF,J).EQ.0.0) GO TO 14
      J1=J+1
      T1=COS(PELMAT(LEF,J1))
      T2=SIN(PELMAT(LEF,J1))
      SSI(I,K)=PELMAT(LEF,2)*(SNI(1,K)*T1*T1+SNI(2,K)*T2*T2+SNI(3,K)*T1*
     *T2)
   14 CONTINUE
```

```
   19 CONTINUE
   20 RETURN
      END
```

```
      SUBROUTINE XDATA
      DIMENSION FI(1491),DI(149)
      COMMON/DATA/KOD(149),X(1491),Y(1491),INODE(40,9),PELMAT(9,13),DC(3,3
     *,9)
      COMMON/VALU/DISP(298),FORCE(298),S(298,46)
      COMMON/LET/NUMNP,NUMEL,NELTYP,THICK,NTOT,NB,LEF
      COMMON/IO/NR,NW
      COMMON/NONLIN/MLIMIT,DIV(25),MCIK,ILR,IDIFOR,IPOINT,DISPMX,BETA
C     READ HEADING, NUMBER OF NODES, NUMBER OF ELEMENTS, NUMBER OF DIFFERENT
C     TYPES OF MATERIAL PROPERTIES
      READ(NR,10) NUMNP,NUMEL,NELTYP
      WRITE(NW,11) NUMNP,NUMEL,NELTYP
C     READ AND GENERATE NODAL POINT DATA
      NESKI=0
C     KOD - BOUNDARY CONDITION INDICATOR
C       0 - FREE
C       1 - RESTRAINED IN X DIRECTION
C       2 - RESTRAINED IN Y DIRECTION
C       3 - FIXED
C     READ NODE, BOUNDARY CONDITION, COORDINATES, KNOWN FORCES AND DISPLACEMENTS,
C     AND INCREMENT FOR NODAL DATA GENERATION
   20 READ(NR,30) N,KOD(N),X(N),Y(N),DI(N),FI(N),INCR
      IF(NESKI.EQ.0) GO TO 100
      IF(INCR.EQ.0) GO TO 100
      NUM=(N-NESKI)/INCR
      NUM1=NUM-1
      IF(NUM1.LT.1) GO TO 100
      ZINCR=NUM
      DX=(X(N)-X(NESKI))/ZINCR
      DY=(Y(N)-Y(NESKI))/ZINCR
      K=NESKI
      DO 40 J=1,NUM1
      KK=K
      K=K+INCR
      X(K)=X(KK)+DX
      Y(K)=Y(KK)+DY
      KOD(K)=KOD(NESKI)
      DI(K)=0.0
   40 FI(K)=0.0
  100 NESKI=N
      IF(N.LT.NUMNP) GO TO 20
      WRITE(NW,70)
      WRITE(NW,80) (I,X(I),Y(I),KOD(I),I=1,NUMNP)
C     READ AND GENERATE ELEMENT MATERIAL PROPERTIES
      WRITE(NW,199)
      DO 200 I=1,NELTYP
      READ(NR,201) (PELMAT(I,J),J=1,13)
      IF(PELMAT(I,2).EQ.0.0) PELMAT(I,2)=29000000.
      IF(PELMAT(I,3).EQ.0.0) PELMAT(I,3)=60624.63*SQRT(PELMAT(I,9))
      IF(PELMAT(I,4).EQ.0.0) PELMAT(I,4)=0.17
      IF(PELMAT(I,10).EQ.0.0) PELMAT(I,10)=1.38*(PELMAT(I,9))**0.667
      IF(PELMAT(I,13).EQ.0.0) PELMAT(I,13)=-0.083
      WRITE(NW,202) (PELMAT(I,J),J=1,13)
  200 CONTINUE
C     READ AND GENERATE ELEMENT DATA
      NESKI=0
  241 READ(NR,206) N,(INODE(N,J),J=1,9),INCR
```

```
      IF(NESKI.EQ.0) GO TO 300
      IF(INODE(N,9).EQ.0) INODE(N,9)=INODE(NESKI,9)
      IF(INCR.EQ.0) GO TO 300
      INKR=N-NESKI-1
      DO 217 II=1,INKR
      K=NESKI+II
      K1=K-1
      DO 220 J=1,8
  220 INODE(K,J)=INODE(K1,J)+INCR
  217 INODE(K,9)=INODE(K1,9)
  300 NESKI=N
      IF(N.LT.NUMEL) GO TO 241
      WRITE(NW,270)
      DO 269 I=1,NUMEL
  269 WRITE(NW,271) I,(INODE(I,J),J=1,9)
      NTOT=2*NUMNP
      DO 310 I=1,NTOT
      DISP(I)=0.0
  310 FORCE(I)=0.0
C     NON-ZERO FORCES AND DISPLACEMENTS
      WRITE(NW,350)
      DO 311 I=1,NUMNP
      IF(DI(I).EQ.0.0) GO TO 314
      VALUE=DI(I)
      ILKI=2*I-1
      IDIRC=1
      KALK=KOD(I)+1
      GO TO (316,317,316,317) KALK
  314 IF(FI(I).EQ.0.0) GO TO 311
      VALUE=FI(I)
      ILKI=2*I
      IDIRC=2
      IF(KOD(I).GT.1) GO TO 317
  316 FORCE(ILKI)=VALUE
      WRITE(NW,351) I,VALUE,IDIRC
      GO TO 311
  317 DISP(ILKI)=VALUE
      WRITE(NW,352) I,VALUE,IDIRC
  311 IF(IDIRC.EQ.1) GO TO 314
  311 CONTINUE
      READ(NR,5008) IDIFOR,IPOINT,DISPMX,TLR,BETA,MOIK,MLIMIT,(DIV(I),I=
     *1,MLIMIT)
      WRITE(NW,5001) IDIFOR,IPOINT,DISPMX,TLR,BETA,MOIK,MLIMIT,(DIV(I),I
     *=1,MLIMIT)
   10 FORMAT(3I5)
   11 FORMAT(///
     ** NUMBER OF NODES          =',I5//
     ** NUMBER OF ELEMENTS       =',I5//
     ** DIFF. TYPES OF ELEMENTS =',I5//)
   30 FORMAT(2I5,4F10.0,I5)
   70 FORMAT(///,6X,'NODE',10X,'X(I)',11X,'Y(I)',8X,'KODE',/)
   80 FORMAT(I10,2F15.2,I8)
  100 FORMAT(//,' ELEMENT PROPERTIES',/,' THICK    E STEEL     E CONC.
     1    V     PI    ANG 1     PZ    ANG 2     FC      FT    FY 1    FY 2
     2S')
  201 FORMAT(8F10.0)
  202 FORMAT(/,F6.2,F12.0,F11.0,F6.2,2(F7.4,F7.2),4F7.0,F7.3)
```

```
      286 FORMAT(16I5)
      270 FORMAT(///,18X,'ELEMENT                    NODAL POINTS                  T
     'YPE',//)
      271 FORMAT(18X,I5,2X,8I5,I7)
      350 FORMAT(///,1X,'NON-ZERO FORCES AND DISPLACEMENTS',//,1X,'NODE    VA
     'LUE    DIRECTION (1 FOR X, 2 FOR Y)',/)
      351 FORMAT(1X,I3,F12.5,I7,'     FORCE')
      352 FORMAT(1X,I3,F12.5,I7,'     DISP.')
     5000 FORMAT(2I5,3F10.0,2I5,/(8F10.0))
     5001 FORMAT(///,' CONTROL PARAMETERS',
     1         ///,' IDIFOR (DISP. OUTPUT CONTROL)          =',I5,
     2          /,' IPOINT (LOC. OF LIMIT DISP. CONTROL)   =',I5,
     3          /,' DISPMX (LIMIT DISPLACEMENT)            =',F8.4,
     4          /,' TLR    (RESIDUAL FORCE TOLERANCE)      =',F8.4,
     5          /,' BETA   (SHEAR RETENTION FACTOR)        =',F8.4,
     6          /,' MCIK   (STRESS OUTPUT CONTROL)         =',
     7          /,' NLIMIT (NUMBER OF LOAD INCREMENTS)     =',I
     8          /,' LOAD INCREMENT RATIOS                  =',10F8.5,/,139X,
     810F8.5))
      RETURN
      END
```

```
      SUBROUTINE XPRINT
      COMMON/STRS/CS(40,3,4),SS(40,2,4),CSI(3,4),SSI(2,4),S1,S2,SNI(3,4)
     *,ALPHA,THETA,FE,CRF(40,4),CRS(40,4),MCRACK(40,4),MCRUSH(40,4)
      COMMON/IO/NR,NW
      COMMON/LET/NUMNP,NUMEL,NELTYP,THICK,NTOT,NS,LEF
      COMMON/ISOPAR/XX(8),YY(8),D(3,3,4),EST(16,16),DS(2,21,XI(14),F(14)
     *,XN(8),YN(8),V(9,4),Z(8,4),A(2),DET,KOUNT
     -COMMON/VALU/DISP(298),FORCE(298),S(298,46)
      COMMON/DATA/KOD(149),X(149),Y(149),INODE(49,9),PELMAT(9,13),DC(3,3
     *,9)
      WRITE(NW,89)
      DO 16 I=1,NUMEL
      WRITE(NW,92)
      DO 19 K=1,4
      IF(MCRACK(I,K).EQ.5) GO TO 11
      IF(MCRUSH(I,K).NE.1) GO TO 28
      SS(I,1,K)=0.0
      SS(I,2,K)=0.0
   11 S1=0.0
      GO TO 14
   28 IF(MCRACK(I,K).EQ.0) GO TO 17
      S1=CS(I,1,K)
   14 S2=0.0
      THETA=CRF(I,K)
C     GO TO 18
      GO TO 21
   17 CALL MOHR(I,K)
C  STRAIN COMPUTATIONS
C  18 CALL STRESS(I,DISP,1)
C     ALPHA=0.5*ATAN(SNI(3,K)/(SNI(1,K)-SNI(2,K)))
C     ALPHA=ALPHA*57.29577951
   21 MODE=MCRACK(I,K)
      THETA=THETA*57.29577951
      IF(MCRUSH(I,K).GT.0) MODE=-MCRUSH(I,K)
      WRITE(NW,80) I,K,MODE,S1,S2,THETA,SS(I,1,K),SS(I,2,K)
   19 CONTINUE
   16 CONTINUE
   89 FORMAT(//,6X,'ELEM LCTN MODE  SIGMA(1)  SIGMA(2)  ANGLE  STEEL(1)
     1 STEEL(2)',/)
   80 FORMAT(4X,3I5,2F10.1,F8.1,2F10.1)
   92 FORMAT(/1
      RETURN
      END
```